Functional morphology of the prosoma of *Baltoeurypterus tetragonophthalmus* (Fischer) (Chelicerata : Eurypterida)

Paul A. Selden

ABSTRACT: The prosomal morphology of *Baltoeurypterus tetragonophthalmus* (Fischer) from the Baltic Silurian is redescribed and reconstructed. The first eurypterid labrum and new secondary sexual characters of *Baltoeurypterus* are described. The radially-arranged coxae of *Baltoeurypterus* were capable of adduction and abduction for food mastication, but not promotor–remotor movements for locomotion. Joint diagrams are presented for the first time for an extinct arthropod. Promotion and remotion of the limbs occurred about subvertical trochanteral pivots, as in all other chelicerates except xiphosurans. *Baltoeurypterus* probably walked in a "slow" gait; a method of choosing possible gaits for extinct arthropods is outlined. Swimming in *Baltoeurypterus* was effected by means of a rowing action of the posterior limb pair, which is provided with complex joints for collapsing the paddle during the recovery stroke. The limb arrangement and joint mechanisms of *Baltoeurypterus* are intermediate between those of the xiphosurans and the arachnids. It is possible that a sister relationship exists between the eurypterids and some arachnid groups, which would render Merostomata and Arachnida unnatural assemblages.

KEY WORDS: Arthropoda, Estonia, feeding, Gotland, locomotion, Merostomata, Silurian, swimming, walking.

Baltoeurypterus tetragonophthalmus (Fischer) is exceptional amongst Palaeozoic arthropods in that minute details of limb podomere and joint morphology are preserved. Thus it is possible to make direct comparisons with Recent arthropod limb mechanisms, such as those revealed by the meticulous work of Manton (1952 to 1977). Such comparisons enhance the accuracy of reconstructions of the extinct animal and its mode of life. Essential new information is also provided for studies on the phylogeny of Chelicerata.

B. tetragonophthalmus was first described from Podolia as a species of *Eurypterus* by Fischer (1839) who coined the specific name in the belief that the animal had square eyes. Schrenk (1854) and Eichwald (1854) described specimens from Saaremaa (Ösel), Estonia, but both authors referred them to the American species *E. remipes* DeKay. Eichwald (1857) realised that the Saaremaa material was conspecific with that from Podolia, and also that the square eyes of *tetragonophthalmus* were a preservational artefact, so he renamed the animal *E. fischeri* (Eichw.). He later discovered this species on Gotland (Eichwald 1860). The genus *Baltoeurypterus* was defined by Størmer (1973) and contains another species, *serratus* (Jones & Woodward), from Gotland (Kjellesvig-Waering 1979). *B. tetragonophthalmus* has also been reported from Norway (Størmer 1938) and Romania (Văscăutanu 1932).

The Saaremaa specimens come from a locality at Viita farm, Rootsiküla village, parish of Kihelkonna. The eurypterid bed is 0·38–0·40 m below the top of the "Eurypterus Dolomite", which forms the upper half of the Viita Formation, the lowest formation of the Rootsiküla Stage (Kaljo 1970). Details of the sedimentological characteristics and associated fauna are published in Kaljo (1970). The rock is probably an early diagenetic dolomitic limestone. The Got-land material is from a coastal locality at Djupviksudden, Kräklingbo (Hede 1929) and the thin-bedded, marly lime-stone in which it occurs belongs to the lowermost part of the Hemse Beds (Manten 1971). The Saaremaa eurypterid bed is Wenlock (*nassa* zone) in age, and the Gotland bed is Ludlow (low *leintwardinensis* zone) in age (M. G. Bassett, pers. comm.).

Morphological descriptions of *B. tetragonophthalmus* were given by Nieszkowski (1858, 1859), Schmidt (1883) and Holm (1896, 1898, 1899). Holm's 1898 work was particu-larly detailed as he had been able to dissolve the limestone completely away from the fossils, leaving the specimens mounted dry or in Canada Balsam on microscope slides. Holm used only Saaremaa material for his 1898 study. His later work utilised material from both Saaremaa and Got-land, but this remained unpublished at his death in 1926. Parts of Holm's plates intended for publication have since appeared in Waterston (1964), Wills (1965) and Kjellesvig-Waering (1979). Wills's 1965 paper was a "supplement" to Holm's 1898 monograph, and dealt mainly with the bran-chial and genital organs of the mesosoma, about which Holm had discovered a great deal.

The present study concentrates on the morphology of the prosomal appendages and their functions, being the parts most able to provide new locomotory, feeding and homolog-ical data. Reference should be made to Holm (1898) for general descriptions and reconstructions, and to Wills (1965) for the morphology of the mesosomal structures. Specimens illustrated by Holm (1898) are not figured again herein. Regarding variation, Gotland specimens tend to have slightly smaller spines and other protuberances; there may also be a slight increase in the number of protuberances through ontogeny. Where marked deviation occurs this is

stated, but there are insufficient specimens of each podomere of every instar for statistical analysis.

1. Terminology and preservation

1.1. Terminology

The prosomal appendages are numbered from the anterior with Roman numerals. Individual podomeres are numbered from proximal to distal with Arabic numerals. Podomere 1 of limbs II to VI is termed the coxa, the terminology of the other podomeres is discussed in section 6. Orientations regarding limbs are given as if the limb were outstretched laterally at right angles to the body axis. The form with the Type A genital appendage (Størmer 1934) is here considered to be the female, and Type B the male, following Holm (1898) and Wills (1965) (although Størmer & Kjellesvig-Waering (1969) favoured the reverse interpretation). Important terms are defined below; new terms are denoted by an asterisk.

Adesmatic. Lacking tendons (Couzijn 1976); cf. eudesmatic.

Articulation. The close connection of podomeres at a joint, where the least amount of movement occurs. The articulation axis is an imaginary line passing through the articulation(s), about which movement occurs.

Bristle. Large, stiff seta.

Carapace. Dorsal prosomal plate, including narrow ventral doublure.

*Carina. Row of lunules or denticles, especially arranged longitudinally on a podomere.

*Coxal triangle On coxae II to V, the approximately triangular ventral surface, excluding the movable teeth of the gnathobase.

Denticle. Discrete, narrow, raised lunule of a carina.

Doublure. Narrow, recurved, ventral part of the carapace, separated from the ventral marginal plates of the prosoma by an ecdysial suture (cf. Størmer 1955, figs).

Eudesmatic. With tendons (Couzijn 1976); cf. adesmatic.

Follicle. Perforation in cuticle presumed to have been the site of attachment of a seta.

Joint. Mechanism by which podomeres are connected, and usually articulated; not a synonym of podomere as in Størmer (1955).

*Lappet. Semicircular flap of cuticle on anterior surface of coxa II.

*Lintel. Superior, commonly bulbous or lobed overhang of distal joint of coxa.

*Lunule. Cresent-, U-, V- or J-shaped cuticular structure, characteristic of eurypterids (Fig. 1).

Mucro. Squat, obtuse or right-angled cuticular projection, usually at distal edge of a podomere (pl. mucrones).

*Scaphoid process. Upturned-boat-shaped process adjacent and posterior to the infero-anterior articulation on the proximal border of podomere 2 of limbs IV, V and VI.

Seta. Hair-like cuticular process, basally set in membrane in a follicle.

Spine. Acutely pointed cuticular process, fixed or movable.

Tubercle. Squat cuticular process, neither pointed (mucro, spine) nor lunulate, and usually bearing follicles.

Specimen numbers prefixed Ar are deposited in the Palaeontology Department, Naturhistoriska Riksmuseum, Stockholm, Sweden; those numbered I3406 are from a box of 31 slides deposited in the British Museum (Natural History), London; those numbered ExE9 were prepared by Wills for his 1965 paper and are deposited in the Department of Geological Sciences, University of Birmingham, England.

1.2. Preservation

B. tetragonophthalmus is preserved as thin, golden-brown or tan coloured material covering moulds. Wills (1965, p. 96) considered the brown material to consist entirely of the original chitinous cuticle. Non-carbonised organic matter is almost certainly present in the cuticle, as evidenced by the brown colour, but most of the organic matrix has been replaced by silica (Dalingwater 1975). Siliceous replacement has also been recorded in *Pterygotus ludensis* Salter (Dalingwater 1973). Rosenheim (1905) found evidence for the presence of chitin in the cuticle of *Truncatiramus osiliensis* (Schmidt) from Saaremaa.

The *B. tetragonophthalmus* material retains its brown colour after etching from the rock matrix. Gotland specimens (Figs 24a, b, f–h, k; 27a, b, e, f, i–l, n–r, v, z; 28d, e, g–j, n, r, s; 31b, n, o, v, w, z, aa; 32 c–g, m, n, q, r) are distorted little and have a characteristic lustre. Those from Saaremaa, however, are more flattened, indicating sediment compaction after burial. Scanning electron microscopy (SEM) reveals angular pitting on the cuticle surface of Saaremaa specimens, caused by the growth of dolomite rhombs adjacent to the cuticle during diagenesis (Fig. 23a; see also Eisenack 1956, fig. 1). Consequently, the Saaremaa material lacks lustre. Many of the specimens are from weathered rock surfaces on which Recent fungi have grown. These fungi are occasionally revealed by the etching process (Fig. 23m). Similar sub-spherical bodies were described from *Truncatiramus serricaudatus* Kjellesvig-Waering by Waterston (1964, p. 18) as "problematica".

Nearly all eurypterid fossils are exuviae (Clarke & Ruedemann 1912, p. 25; Størmer 1934, p. 57, 1976, p. 124) although Andrews *et al.* (1974) have expressed views to the contrary. The *Baltoeurypterus* remains are almost certainly exuviae (Kjellesvig-Waering 1979; Wills 1965, p. 96) as all the tissues preserved (including tendons) are ectodermal in origin. No trace of internal organs, such as the tough, mesodermal endosternite which occurs in all chelicerates except Solifugae and a few mites (Firstman 1973), has been found in *Baltoeurypterus*.

The flattening of the Saaremaa specimens probably occurred in stages. Whilst lying on the sea bed, some decay of arthrodial membranes allowed collapse and movement of parts of the body. There is evidence of current action from the orientation and dismemberment of the fossils in the rock (Wills 1965, p. 96; Kaljo 1970, p. 272). After burial, some compaction took place, and further collapse and disruption occurred on etching the cuticle from the rock matrix. One effect of this collapse and compaction was to cause the large coxae VI to compress dorso-ventrally and push the anterior coxae forwards to lie like tiles on a roof (Holm 1898, p. 13) (Figs 32v, w). Holm believed that this was the arrangement of the coxae in life and he reconstructed the ventral side of the body in this way (Holm 1898, pl. 2, fig. 1). An intimate study of the coxae reveals no evidence for reconstructing them lying near the horizontal plane (cf. Waterston 1979, p. 304).

2. Description

2.1. Cuticular structures

The ultrastructure of the cuticle of *B. tetragonophthalmus* was studied by Dalingwater (1975) and was briefly discussed by Mutvei (1977) in comparison with the cuticles of other chelicerates (see also Dalingwater 1980). Laminae and pore canals (up to 1μ diameter) can be seen in Figure 23o, and this figure also shows canals of about $1–2\mu$ in diameter

traversing the cuticle of the gnathobasic teeth. Those canals which emerge in a plane perpendicular to the page appear as narrow, inverted V-shapes (an optical effect due to the narrow depth of field of the photograph) and could be what Eisenack (1956) mistook for fine teeth (Nebenzähnchen) that do not appear in silhouette. Both Eisenack (1956) and Dalingwater (1975) referred to fine (1–2μ across) canals. Eisenack (1956) suggested they formed part of the sense organs or were secretory ducts, and Dalingwater (1975) compared them to the ducts seen in *Carcinus* cuticle by Dennell (1960) who suggested they were related to the denser phenolic tanning at the tips of the teeth. These canals show a considerable resemblance to the chemoreceptors of the gnathobasic teeth of *Limulus* described by Patten (1894) and Barber (1956). The dendritic structures (Fig. 23n), which appear to be impressions on the inner surface of the cuticle, are similar to the nerves in the lumen of the tooth illustrated by Patten (1894). It is possible that, even after ecdysis, traces of sensory nerves may remain imprinted on the internal surface of the cuticle, and that the canals bore nerve fibrils of chemosensory organs in life. (Clarke & Ruedemann (1912, p. 54) appear to have misinterpreted Patten's findings in thinking that the anterior gnathobasic teeth of *Limulus* were themselves the gustatory organs, and inferred from this that the ventral movable teeth of coxae II to IV of *Baltoeurypterus* were comparable in function.) Another possibility is that these canal organs were "strain gauge" proprioceptors monitoring cuticular stress, as they are superficially similar to the funnel canal organs found in the dactyl of the walking legs of some Crustacea (Shelton & Laverack 1968).

Larger holes (follicles) occur in the cuticle (Fig. 27a). These have generally been ascribed a sensory function, but there is some debate regarding whether they housed setae or some other sensillum. Eisenack (1956) gave a lengthy description of the follicles which he termed Fenstern (windows), believing them not to have borne setae in life, but to have had a thin cuticular covering (campaniform sensilla). No evidence for a thin cuticular covering has been found in the present study. The follicles have also been described by Dalingwater (1975) as "goblet-shaped setal sockets".

Two types of follicular structure are revealed in SEM observations on limb-tip cuticle of *B. tetragonophthalmus*. One type (Fig. 23a), by comparison with *Limulus* cuticular structures (Fig. 23d), appears to be a follicle with a broken seta, whilst the other (Figs 23b, c) is either an indeterminate sensillum or a follicle with the seta absent, by comparison with *Limulus* (Fig. 23e).

Many types of setae occur on the *Baltoeurypterus* cuticle, but few are seen emerging from the larger follicles. During ecdysis a new seta is formed (Gnatzy & Tautz 1977; Haupt & Coineau 1978), so that the old one should remain in its socket. It is probable that the setae, loosely held in their sockets by membrane, are lost during burial, diagenesis and preparation, as in trilobites (Miller 1976; Størmer 1980). The setae vary from small, short ones as found on the scimitar lobe of limb III of the male, through slender setae (Figs 24o; 28o, t), to stiff bristles (Fig. 24c). The setae (see Eisenack 1956 for detailed description) have a bulbous base and a lumen throughout their length. Tobien (1937) distinguished four types of sensory setae in *Truncatiramus osiliensis* (Schmidt).

Wills (1965), Dalingwater (1975) and others described a roughly polygonal pattern on the surface of *B. tetragonophthalmus* cuticle. Polygonal reticulation occurs on crustacean cuticle as a result of calcification. As eurypterid cuticles are not thought to have been calcified in life, the pattern may be the result of the impression of dolomite rhombs together with a general wrinkling. The smoothest *Baltoeurypterus* cuticle occurs on the anterior and posterior surfaces of the coxae, and bears only fine setae and "stretch marks" (Fig. 27o).

The most characteristic cuticular structure is the lunule (Fig. 1; see also Depitout 1962). Lunules vary in shape from almost straight, transverse discontinuous lines (Fig. 23h), similar to the terrace lines of trilobites (Miller 1975), through broad lunules (Fig. 23h), to crescents, V-shapes (Fig. 31f) and narrow U-shapes. They may show no noticeable relief, or may be "raised", especially when narrow (Fig. 31f). Symmetric lunules grade into asymmetric lunules (Fig. 27x), and the extreme form of these is the stria (usually folliculated) which occurs on the movable spines of limbs II to IV (Fig. 28k). Lunule cusps are directed anteriorly or mesially on the body and proximally on limbs. All types of lunule may be folliculated, and this is usually accompanied by relief. Greater relief produces the narrow, raised lunules or denticles of the posterior carinae of limbs V and VI (Fig. 28d), the multifolliculated tubercles of the inferior surfaces of limbs II to IV (Fig. 24h), mucrones, which are commonly folliculated (especially when adjacent to an articulation), and spines, either small or very large (as the fixed spines of the penultimate podomeres of limbs II to V). Although the cuticle is thicker at a lunule, some of the dark colour is due to pigmentation.

Joints consist of thin, flexible, untanned cuticle (arthrodial membrane) between podomeres, with or without one or two articulations. Cuticular spines, mucrones and tubercles are commonly associated with a joint (Fig. 28d) and their setae may be proprioceptive in function. Most joints in the limbs of *Baltoeurypterus* are either hinges or pivots (Manton 1977, p. 192). Hinge joints consist of a single, or two adjacent, articulations, which are commonly superior in position, and an expanse of arthrodial membrane around the remainder of the joint. Pivot joints bear two articulations at opposite sides of the joint, with arthrodial membrane around the remaining sides. Specialised joints occur in places, for example the body–coxa joints bear no articulations, and the podomere 6–podomere 7 joint of limb VI is a rotatory joint modified from a hinge.

A simple articulation consists of a thickened boss of cuticle at the point of closest attachment of the two podomeres, and which opposes a similar boss on the adjacent podomere. Articulations may be greatly thickened areas of cuticle, for example the anterior of the two articulations at a pivot joint, or only weakly developed, in which case it may be difficult to discern whether or not a true articulation is present. The strong articulations of the basal pivots (coxa–podomere 2 joints) of limbs IV to VI have a characteristic arrangement which was described by Holm (1898, p. 20). Superior to the articulation the coxal edge is recurved,
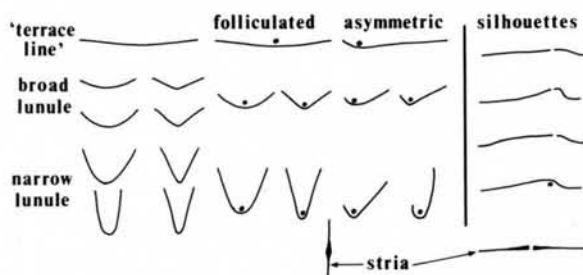

Figure 1 Diagrammatic representation of the shape variations and terminology of lunules from the cuticle of *Baltoeurypterus tetragonophthalmus*.

covering the proximal part of podomere 2. Inferior to the articulation, the arthrodial membrane increases in expanse so that in a short distance its width is considerable. On the coxal side of the articulation, a furrow extends at a right angle to the coxal distal edge, which corresponds to a thick ridge internally. Just inferior to this articulation, on the proximal edge of podomere 2, is an upturned-boat-shaped cuticular feature here termed the "scaphoid process" (Fig. 31g). This type of articulation is not only quite distinctive but also very strong.

Arthrodial membranes are preserved as thin, light coloured cuticle. The remains of tendons commonly occur as striae on the arthrodial membrane (Fig. 31a), or as long, lath-like strips of cuticle at the proximal borders of the terminal podomeres of the limbs (Figs 24f; 27a).

2.2. Carapace, ventral marginal plates and labrum
The prosoma consists of a dorsal carapace, internal and ventral structures, including appendages and a pair of ventral marginal plates (Fig. 2). The anterior and lateral carapace rim is bent under onto the ventral surface forming a doublure. The ventral marginal plates are not part of the doublure (cf. Størmer 1955) but are separated from it by an ecdysial suture.

Carapace. The carapace is usually preserved intact; it is thus well known and has been used in statistical studies (e.g. Andrews *et al.* 1974). The carapace is shown in Figure 23f, and reconstructed in Figure 2. By analogy with the xiphosurans, thicker and more elevated areas, such as the cardiac lobe (glabella of Clarke & Ruedemann 1912), are distinguished by darker cuticle. Pale cuticle characterises thinner or more depressed areas such as muscle attachment sites. Folds and splits indicate parts which have suffered compression and extension respectively, during flattening, and these

Figure 2 *Baltoeurypterus tetragonophthalmus.* Exploded reconstruction of the carapace, ventral marginal plates, right-hand coxae and chelicera, labrum, endostoma and metastoma, left superoantero-lateral aspect.

are also useful in reconstructing the original shape. Nieszkowski (1859) thought that some of these folds were present in life. The cardiac lobe is a postero-median triangular area of dark cuticle and raised lunules. The lobe is bounded laterally by pale patches which may reflect internal muscle apophyses. A pair of pale spots on the frontal raised areas may aslo reflect muscle scars, possibly of anterior plastrotergals as in *Limulus* (Lankester *et al.* 1885). At the anterior tip of the postero-median lobe lies a patch of small lunules in a dark field, where the dark patches bounding the lobe converge and meet dark areas from the anterior. Immediately anterior lie the two ocelli. A dark triangle in front of the ocelli is interpreted as a slight node by analogy with *Limulus* (Fig. 2). The lateral parts of the carapace are inclined, as evidenced by the longitudinal compression folds, but at the front there are two elevated areas, running from behind the ocelli to the anterior margin. These tubercled areas, which coalesce in the female (see Wills 1965 for carapace sexual dimorphism), bound a median depression.

Eyes. Wills (1965, p. 101 and ppl. 1, fig. 1) showed that Holm (unpublished plates) had discovered the compound nature of the lateral eyes, and it can be seen that the lens-packing system is of the logarithmically decreasing type (Clarkson 1975, p. 20 & fig. 5K), similar to that found in the trilobite *Scutellum (Paralejurus) campaniferum* (Beyrich) (see Levi-Setti 1975, pl. 15). The visual fields of the compound eyes were wide and overlapped a great deal in front. This anterior overlap implies stereoscopic vision in this direction, a prerequisite for an active predator (Stockton & Cowen 1976).

Compound vision would however have been poor posterodorsally. The paired median ocelli, which appear to have been situated postero-laterally on a small raised node, may have been photosensitive. The cuticle thins over the ocelli, as it does over the median glabellar tubercle of the trilobite *Nileus*, which Fortey and Clarkson (1976) suggested was sensitive to light in the dorsal blind spot of the compound eyes. The paired median ocelli of *Baltoeurypterus*, with overlapping visual fields, could have sensed changes in light intensity caused by the movement of an approaching predator, in the otherwise blind postero-dorsal direction. On the basis of morphology and position of the eyes, *Baltoeurypterus* appears to have been both hunter and hunted.

Ventral marginal plates. Holm (1898, p. 9) described the marginal plates in detail. *Baltoeurypterus* has a simple ventral plate system (Fig. 2), consisting of two marginal plates which broaden anteriorly to where they join at a median suture (Fig. 23j). The mesial edge is distinct, and passes into thin ventral cuticle surrounding the coxae. The coxae are commonly found attached to the marginal plate at the lintel (Figs 23g, h, j). One feature not reported by previous writers is a dark spot on the marginal plate situated just anterior to the lintel lobe of coxa V (Figs 23g, i). The function of these spots is unknown.

The suture of the marginal plates with the carapace runs just inside the ventral surface, gradually nearing the edge posteriorly until a short distance from the postero-lateral corner of the carapace where it turns outwards and runs along the carapace edge. It continues round the posterolateral corner and ends a short distance along the posterior edge of the carapace (Fig. 23h). By comparison with *Limulus*, it is probably no longer functional as an ecdysial suture from the point where it leaves the ventral surface.

Labrum. The labrum has not hitherto been described in any eurypterid. Wills (1965, p. 104) mentioned some "labral skin" which he encountered on one of his specimens (not figured). This labral skin does not appear to be equivalent to
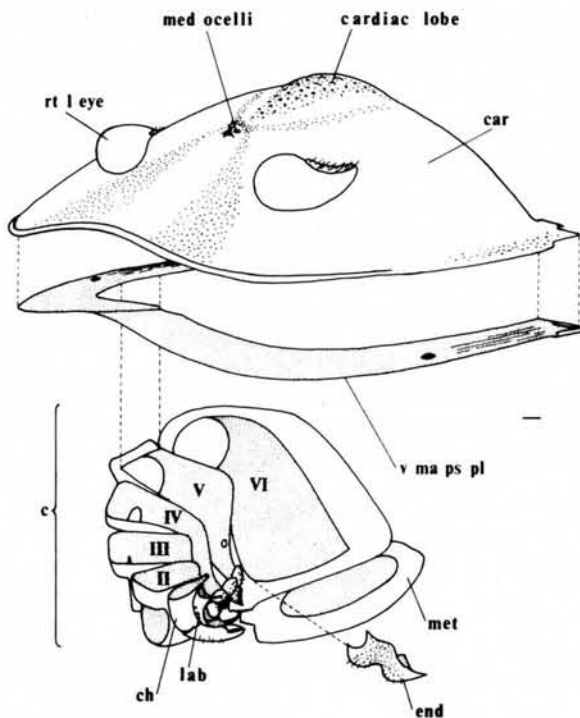
the labrum described here. Holm (1898, p. 11) could find no structure in *Baltoeurypterus* comparable to the "lancet-like plate" (the labrum) of *Limulus*.

Figures 2; 23l; 24m, n, r show the labrum and its relation to the surrounding podomeres. It takes the form of a curved lath, the edges of which are attached to the anterior lappet of coxa II. Ventrally it thins into the cuticle of the mouth cavity. Dorsally the edge is bowed and there are supero-posterior lateral extensions which follow projections at the bases of the chelicerae. A strip of cuticle extends forwards from the dorsal edge of the labrum and merges into the thin ventral prosomal cuticle. The anterior surface bears a row of raised lunules. The *Limulus* labrum also bears a line of thickened nodes on this surface.

2.3. Chelicerae

Hall (1859) anticipated the form of the chelicerae in *Baltoeurypterus*, but they were not adequately described until 1898 (Holm, p. 11). The chelicera is sitiated between the labrum and coxa II, and consists of three podomeres (Fig. 11).

Podomere 1. The basal podomere was not well known to Holm, but he figured a specimen which shows the distal joint (1898, pl. 3, fig. 4). This podomere has a "streamlined" cross-section, the sharp inferior edge fitting into the crevice behind the lappet of coxa II. The superior surface, which pointed forwards in life, bears a row of lunules with cusps proximal (Fig. 24c). The other surfaces are smooth. The proximal edge shows no apparent articulation, but the inferior corner is extended into a gutter-like projection, which may have housed a muscle running to the endosternite. Strong anterior and weaker posterior articulations are present on the widest part of the distal joint. Inferior to the articulations the distal border is thickly fringed with setae and bristles, especially on the anterior side. A large, serrated spine lies at the extreme infero-distal corner (Figs 24c, m).

Podomeres 2 and 3. Podomeres 2 and 3 form the pincer. Holm figured some examples (1898, pl. 3, figs 1, 2, 4 & 5) but did not describe them in detail (1898, p. 12). The form of podomere 2 is seen in Figures 24f, g, j, k, m. The plane of the proximal joint is not at right angles to the long axis of the podomere, but is bevelled, and the superior side is extended whilst the inferior side is emarginated. Articulations may be seen at this joint in Figure 24k. Follicles are present on the surfaces of podomere 2 and are most dense on the superior and distal sides, and especially on the outer surfaces of the fixed finger of the pincer. The anterior surface of podomere 2 is flatter than the other sides (Figs 24f, g) and this helped the two chelicerae to work more closely together. The distal joint plane is at right angles to the long axis of the podomere and there are two articulations, one supero-anterior and one infero-posterior. The fixed finger of the chela has a fairly straight inferior surface and the tip is slightly hooked.

Podomere 3, the movable finger of the chela, is more markedly curved. A tendon for the closer muscle can be seen at the proximal joint in Figure 24f. *Limulus* chelicerae bear a row of stiff bristles along the lines of contact of the chela fingers. No evidence of bristles is found on the *Baltoeurypterus* chela, instead a straight, stiffened ridge is present on the supero-anterior (concave) surface of podomere 3 (Fig. 24f). The fixed finger also has a ridged infero-posterior surface. The tip of podomere 3 is slightly hooked so that when the chela is closed it slides superior to the tip of podomere 2, ensuring correct alignment of the fingers (Fig. 24p). Note that, as in *Limulus*, the movable finger is to the outside (Fig. 24e).

2.4. Prosomal appendage II

Figure 3 shows the major differences between limbs II, III and IV. Individual podomeres may be identified by reference to the text, the reconstructions (Figs 4, 5, 6) and the summary Figure 20. Limbs II and III of the male are readily identified by their sexual modifications. Holm (1898, p. 12) and Schmidt (1883) described the gross morphology of these limbs.

Coxa. Excluding the lintel, the shape of the coxa approximates a rectangular prism which narrows slightly towards the mouth cavity (Fig. 4). The coxal anterior surface (Fig. 24a) is setose, and bears a semicircular flap of cuticle, the lappet, which is connected to the labrum (Figs 2; 24r). The posterior surface is more rounded at the dorsal edge than the anterior, and the posterior dorsal edge bears a row of prominent
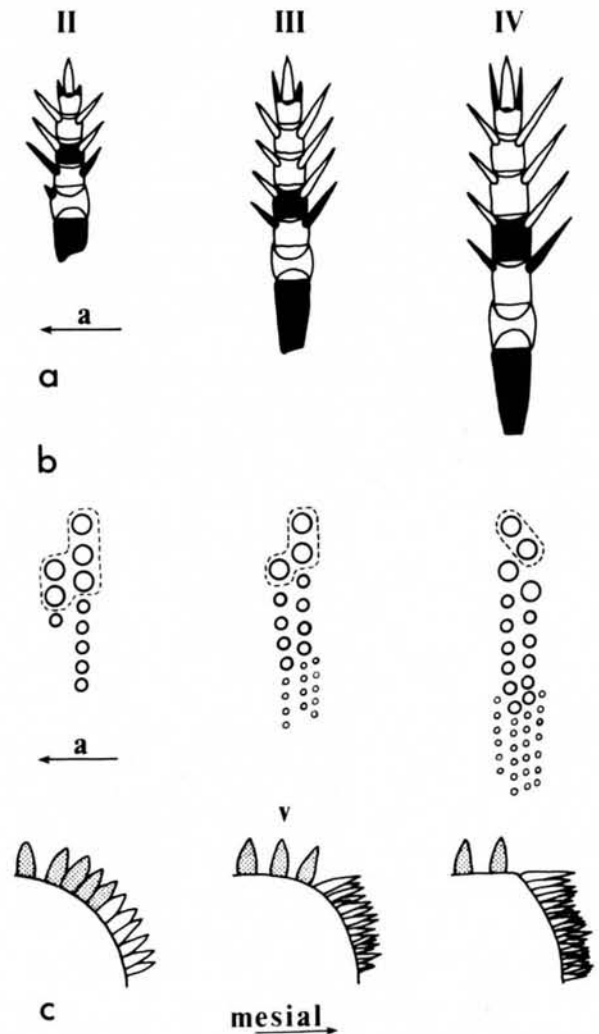
Figure 3 Some criteria used to distinguish limbs II, III and IV of *Baltoeurypterus tetragonophthalmus*.

a. Inferior aspect, distinguishing features shown in black. (i) Relative lengths of limbs (governed by number and length of podomeres). (ii) Podomere number: limb II, 7; Limbs III and IV, 8. (iii) Podomere proportions (illustrated by podomere 4): limb II, shorter than broad; limb III, as short as broad; Limb IV, longer than broad. (iv) Increase in length of coxal triangles from limb II to limb IV. (v) Presence of anterior movable spine on podomere II2. (vi) Anterior movable spine on podomeres 3 to 5 of limb II at least as long as posterior; anterior movable spine on podomeres 3 to 6 of limbs III and IV shorter than posterior.

b. Dental formulae of gnathobasic teeth; dashed lines enclose ventral movable teeth.

c. Lateral aspect of gnathobases showing relative positions of movable (shaded) to fixed teeth.

muscle scars (Figs 24b, l). The ventral surface consists of a roughly trapezoidal area (the coxal triangle) and the gnathobase. The coxal triangle (Figs 24i, q) bears raised lunules, many with follicles, which are most prominent at the anterior, mesial and distal sides.

Holm (1898, p. 15) counted 8 teeth on the gnathobase and described them as short, thick, stumpy and conical, lacking any regular arrangement. Eleven teeth in a posterior row of 8 and an anterior row of 3 can be seen in Figures 24b, i. This dental formula (Fig. 3) is consistent in all specimens. The 5 most ventral teeth are the largest, most obtuse and are commonly missing (Figs 24i, o), as they are set in membrane and were therefore movable in life. The mesial teeth are smaller, pointed and more firmly attached to the gnathobase. There is, however, a gradual transition from ventral to mesial teeth (cf. coxae III and IV, Fig. 3). The surfaces of the teeth are smooth (Figs 24a, b; 31w) but the larger, movable teeth bear setal follicles. Long bristles and setae surround the teeth (Fig. 24o). A movable endite (the epicoxa of Holm) is attached to the gnathobase (Figs 24j, m, n, q, r). This consists of a setose sac with bristles on the mesial surface.

The lintel (Figs 24a, b, l) is a lateral extension of the coxa which overhangs the distal joint. The lintel is slightly bilobed and small lunules occur on its ventral surface. The coxal distal joint is slightly elliptical and articulations occur in infero-anterior and supero-posterior positions (Fig. 24l). The anterior articulation is the most prominent. Large expanses of membrane occur at the dorsal and, especially, ventral edges of the joint.

Podomere 2. The second podomere takes the form of a bent cylinder, the ends of which are at right angles to each other (Figs 24q, r; 27q, r). The superior surface is about six times the length of the inferior, and partly by this means, the

ramus is incurved under the carapace. The proximal edge of the podomere bears infero-anterior and supero-posterior articulations (Fig. 24d) corresponding to those on the distal edge of the coxa. The cuticle is smooth apart from a few faint lunules and some setae (Figs 27q, r). The distal edge bears superior and inferior articulations (Fig. 24d). A spine lies in an infero-anterior position on the distal border, and this spine commonly has a minor apex at the side (Fig. 24d). The spine may be missing (Figs 24q; 27q) as it was set in thin cuticle and hence was movable. A row of small spines occurs around the anterior distal edge, and the posterior distal edge bears a row of setae (Figs 24q, r; 27q, r).

Podomeres 3 to 5. Podomeres 3, 4 and 5 of limb II (Figs 24d, m, n; 27t) are similar in many respects, but podomeres 3 and 4 are sexually dimorphic. All three podomeres are broader than long, but there is a tendency to increase in length relative to breadth from podomere 3 to podomere 5. The distal part of the inferior surface of each podomere is composed of thinner cuticle which gives the impression of a shorter inferior length (Fig. 24d). On all three podomeres the circumference of the proximal edge is greater than that of the distal. The ratio of proximal to distal circumference increases from podomere 3 to podomere 5.

Follicles are most numerous on the anterior surfaces of the podomeres, particularly near the distal border, where there are large mucrones. On podomere 3 the mucrones are quite small and their derivation from raised lunules is obvious (Fig. 24h). Podomeres 4 and 5 bear four large mucrones antero-distally, the largest being adjacent to the anterior movable spine. The two largest are almost equal in size on podomere 4 (Figs 27i, j), whereas on podomere 5 the most anterior is much larger than the rest (Fig. 27z).

Proximal to the mucrones lie some broad, raised lunules. The mucrones grade into this type of lunule around the socket of the anterior movable spine. On podomere 3 these broad lunules are symmetrical, they are less so on podomere 4 and are distinctly L-shaped on podomere 5. These lunules extend in a roughly proximo-posterior–antero-distal direction on the inferior surface, and become narrower and smaller as they grade into raised follicles (Fig. 24h). The raised follicles increase in size and culminate in a large multifolliculated tubercle at the base of the posterior movable spine. This tubercle (Fig. 27t) increases in size from podomere 3 to podomere 5 and becomes a major feature on podomere 6. The band of follicles on the inferior surface is weak on podomere 5, but another tubercle is present on this podomere adjacent to the anterior movable spine (Fig. 27z). The posterior distal edge is smooth and bears about four broad raised lunules; these are weak on podomere 3 and are most prominent on podomere 5.

Podomere 3 bears superior and inferior articulations proximally. The distal edge of this podomere bears an antero-superior articulation which extends along the superior hinge line. Podomere 4 (Figs 27i, j) bears a superior articulation distally and adjacent posteriorly to this is a small multifolliculated mucro. This mucro occurs at all superior hinge articulations. Podomere 5 bears an antero-superior articulation distally with a superior extension along the hinge line.

The large anterior and posterior spines are set in thin cuticle and thus were movable, as concluded by Schmidt (1883) and Holm (1898, p. 14). The general shape of the spines is that of an elongate cone, gently curved on the inferior side. The spine surface bears follicles set in spindle-shaped cuticular thickenings (striae). The posterior movable spine shown in Figure 24h is very small and may be the result of regeneration after injury. The anterior movable spines of podomeres 3 and 4 are modified in the male (Figs
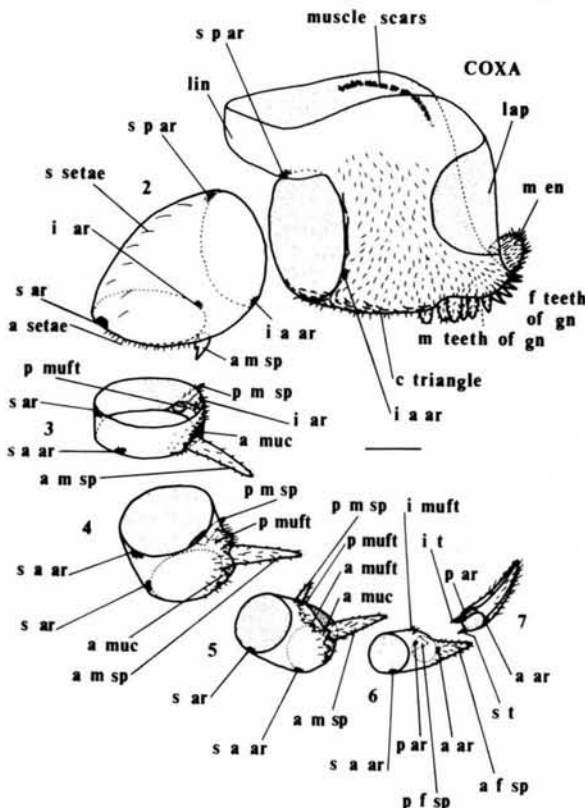
Figure 4 *Baltoeurypterus tetragonophthalmus.* Exploded reconstruction of right limb II, female, antero-lateral aspect.

24d, m; 27j, w). That of podomere 3 is squat and leaf-like in outline, and that of podomere 4 is strawberry-shaped with a pointed apex. Both modified spines bear knobs and asymmetric lunules on the proximal and distal sides. Holm (in Wills 1965, ppl. 1, fig. 6) had discovered these modified spines, but Wills (1965, p. 102, footnote) was of the opinion that Holm had figured limb III of the female, or alternatively that they were merely crumpled spines. Figure 27w shows limbs II and III (which is also modified in the male) together on the same animal which bears a type B genital appendage.

Podomeres 6 and 7. Podomere 6 (Figs 27a, b, k, l) takes the form of an isometric cylinder with a large, fixed spine on the anterior side and a much smaller fixed spine on the posterior side; both are directed distally. On the inferior surface, close to the distal edge, lies a large multifolliculated tubercle. The proximal border bears an antero-superior articulation and inferiorly some tendon remnants may be seen. The surfaces of the podomere, especially the distal parts and the spines, bear follicles. The distal joint bears anterior and posterior articulations situated at the bases of the spines.

Podomere 7 (Figs 27a, b, k, l) is a curved spine with longitudinal cuticular thickenings on the inferior, infero-anterior and infero-posterior sides. Inferiorly, a raised boss marks the attachment of a wide tendon, and superiorly a narrow tendon may be seen in Figures 27a, b, displaced to the outside of podomere 6. Follicles occur over the whole surface of the podomere, and especially towards the apex.

2.5. Prosomal appendage III

This limb (Figs 5; 27g, y), like the foregoing, occurs in male and female forms. Holm (1898, p. 15) described the general morphology of both forms.

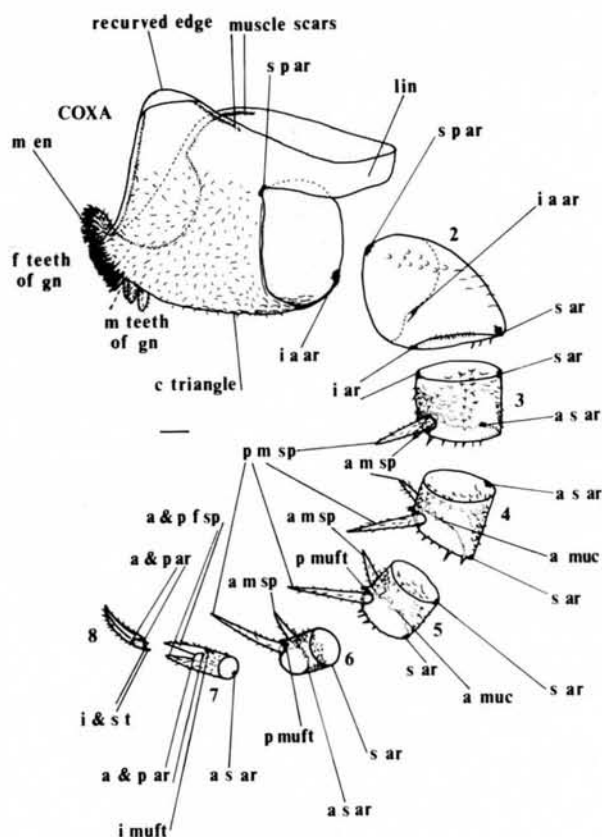**Coxa.** The anterior surface of coxa III (Fig. 27o) is similar

in shape to that of coxa II but there is no lappet. The submarginal muscle scar follows the dorsal edge of the anterior surface but mesially describes a semicircle away from the mesial edge. The posterior surface (Fig. 27n) is acutely angled dorsally, where the edge is recurved externally, and there was probably an attachment here for muscles to the endosternite. Coxa IV (Fig. 28c) has a rounded dorsal edge to the anterior surface, which would fit the shape taken by the dorsal posterior margin of coxa III. Both the anterior and posterior surfaces of coxa III bear setae, and "stretch-marks" (Fig. 27o) occur on the mesial edge of the anterior surface, similar to those seen on the *Limulus* coxa in this position.

The coxal triangle (Fig. 24q) is longer transversely than that of coxa II, but the cuticular features are similar. Holm (1898, p. 16) described two movable ventral teeth on the gnathobase, and two rows of fixed teeth which decrease in size mesially. The largest fixed tooth described by Holm is set in fairly thin cuticle (Fig. 27s) and was therefore probably movable. There are two main rows of fixed teeth, and also a short row of small teeth on the posterior edge of the gnathobase. The teeth generally number less than thirty. Holm (1898, p. 16) also mentioned the bristles surrounding the teeth (Figs 27o, s) and the movable endite (Fig. 24n).

The distal joint (Figs 24q; 27n, o) bears strong infero-anterior and slightly weaker supero-posterior articulations. The posterior edge of the joint is fairly straight, which may reflect the proximity of the larger coxa IV behind, the transverse abduction of which might otherwise be hindered by the protruding edge. The lintel of coxa III is more extensive but shallower than that of coxa II.

Podomere 2. Podomere III2 (Figs 27d, e) differs in shape from podomere II2 in that both the proximal and distal joints deviate from circles. Both the infero-anterior and supero-posterior articulations occur on salients of the proximal margin. These are separated by emarginations bearing tendon remnants. The infero-anterior articulation is the stronger of the two and resembles the scaphoid process of podomere V2 to some degree.

The distal edge bears superior and inferior articulations. The former occurs at the tip of a superior salient. The posterior distal edge is more emarginated than the anterior, thus permitting a slightly greater amount of flexure in this direction at the joint. There is a prominent row of spines, about 5 in number, just anterior to the superior articulation. Adjacent posteriorly to the superior articulation, the distal edge bears two tiny spines, but otherwise the edge is smooth until the start of a row of spines and setae along the posterior margin. The surface of podomere 2 bears only faint lunules running obliquely across the proximal part of the supero-posterior surface. This is followed on the distal part of the superior surface by a line of large setae running towards the superior distal articulation (Fig. 27e).

Podomeres 3 to 6. Podomeres 3, 4 and 5 are sexually dimorphic, podomere 6 is not. Figure 5 gives a reconstruction of the female form. Figure 27y shows the male. All four podomeres are approximately equant. The distal podomeres are generally smaller than the proximal, except that the superior surface of podomere 4 is markedly extended distally, particularly in the male (Fig. 27m) but also in the female (Figs 27c, x).

In the female, the cuticle sculpture most readily distinguishes the podomeres of limb III from those of other limbs. In particular, the superior surfaces bear narrow lunules which, except on podomere 3, when distal bear follicles, and when proximal are broader. They grade into broader lunules anteriorly. The superior surfaces of the podomeres of limb II

Figure 5 *Baltoeurypterus tetragonophthalmus.* Exploded reconstruction of right limb III, female, postero-lateral aspect.

are devoid of raised sculpture, those of limb IV bear more prominent raised lunules.

The anterior surfaces bear broad, folliculated lunules, the long axes of which trend more proximal–distal towards the inferior surface, where follicles may be absent. Distally, the broad lunules become large distal anterior mucrones, which, as on limb II, may help in distinguishing the podomeres. On the more distal podomeres, the follicles on the anterior surface are more densely arranged and, especially in the male, their lunules are less raised. Polomere 3 bears a row of small mucrones in the female (Figs 27c, p, aa). The male podomere 3 bears a row of small mucrones antero-distally, but the anterior movable spine is removed to the inferior surface, and an enormous mucro, which is probably derived from the anterior mucro series, lies in a postero-inferior position (Figs 27m, y). Although Holm made no mention of this mucro, it may be seen in his figures (1898, pl. 3, figs 5, 8 & 9; pl. 4, figs 8 & 9; pl. 6, fig. 9). Podomere 4 (Figs 27c, m, x, y, aa) bears 3 large mucrones antero-distally, the middle one being the largest, and the inferior one is adjacent to the anterior movable spine. The distal anterior mucrones on podomere 5 (Figs 27u, y, aa) are very similar to those of podomere 4, although the small mucrones running superior to the main series are slightly more prominent on podomere 5. On podomere 6, the middle mucro is very large, and the rest are quite small (Figs 27h, u, v, aa).

The inferior surfaces of podomeres 3 to 6 are similar to those of podomeres 3 to 5 of limb II. Narrow, raised follicles occur here, and there is a single, large, multifolliculated tubercle adjacent to each posterior movable spine. This tubercle increases in size from podomere 3 to podomere 6. In the male, the multifolliculated tubercle is absent from podomere 3 (which bears the enlarged mucro), but the other podomeres resemble the female in this feature. Podomere 4, male, bears a slight raised boss (Figs 27m, y) adjacent to the multifolliculated tubercle.

The posterior surfaces of podomeres 3 to 6 bear only weakly developed lunules in both sexes, except around the bases of the posterior movable spines. In the female, the distal edges bear a row of sharp spines posteriorly, whose number and size vary, apparently ontogenetically. Small mucrones are present on podomere 6 in place of the spines (Figs 27h, u). The spines are absent from the mature male, but an immature male (Fig. 28aa) shows spines present on podomeres 5 and 6.

Antero-superior articulations with superior extensions occur at the distal joints of podomeres 3 and 6 (Fig. 5). Superior articulations occur at the distal joints of podomeres 4 and 5 (Fig. 5).

The posterior movable spines are longer than the anterior in the female, and both increase in length from podomere 3 to podomere 6 (Fig. 27g). In the male, the posterior movable spine is absent from podomeres 3 and 4, but the anterior movable spine is present, and of similar dimensions to that of the female, on podomeres 3 to 6. On podomere 3 the anterior movable spine is inferior in position in the male. The posterior movable spine is present on the male podomere 5 (Fig. 27f) even though this podomere bears the large "scimitar lobe". Wills (1965, p. 102) considered that the spine arose from the base of the scimitar lobe. Although it is very close to the base of the scimitar lobe, it is not on the lobe, as the present figures (Figs 27f; 28aa) and Holm's published (1898, pl. 3, fig. 8, pl. 6, fig. 9) and unpublished plates (Wills 1965, ppl. 1, fig. 5) indicate. Its common absence indicates that it was movable.

The scimitar lobe (Figs 27f, w, y; 28m, aa) was described by Holm (1898, p. 16) who figured three specimens (1898,

pl. 3, figs 8 & 9; pl. 6, figs 9 & 10). He is correct in saying that it is neither formed from a modified spine, nor is articulated at its base, but is incorrect in stating that it is composed of thin cuticle and is devoid of sculpture. The cuticle appears to be as thick as that of the inferior surface of the podomere and bears minute setae (Fig. 28m).

Podomeres 7 and 8. Podomeres 7 and 8 (Figs 27h, u, y) resemble podomeres 6 and 7 of limb II but differ in that the anterior and posterior fixed spines of the penultimate podomere are longer on limb III (Fig. 3).

2.6. Prosomal appendage IV

Limb IV (Fig. 6) is the largest in the series of three spinose limbs, but differs from limbs II and III in many respects (Fig. 3), and also exhibits features in common with limb V. Eight podomeres are present, and the limb, like V and VI, is not sexually dimorphic.

Coxa. Coxa IV is the largest of the three spinose limb coxae. Like coxa III it bears similar muscle scars on the anterior and posterior surfaces (Fig. 28c). The coxal triangle is larger and more triangular than on coxae II and III, but the cuticular features are similar. The gnathobase bears two movable ventral teeth (Fig. 28o), two rows of mesial fixed teeth, and subsidiary rows of smaller fixed teeth (Fig. 28y). The largest fixed tooth has a characteristic shape. The number of fixed teeth is variable but is greater than on coxa III. Bristles and setae surround the teeth and a movable endite is present (Fig. 24n). The distal joint and lintel (Fig. 28c) are similar to those of coxa III.

Podomere 2. Podomere 2 of limb IV (Figs 28p, q, t) resembles podomere 2 of limb III but there are several distinguishing features. The broad lunules on the infero-anterior surface and the smaller lunules on the infero-posterior surface are more prominent on podomere IV2 than on podomere III2. Podomere IV2 bears more spines
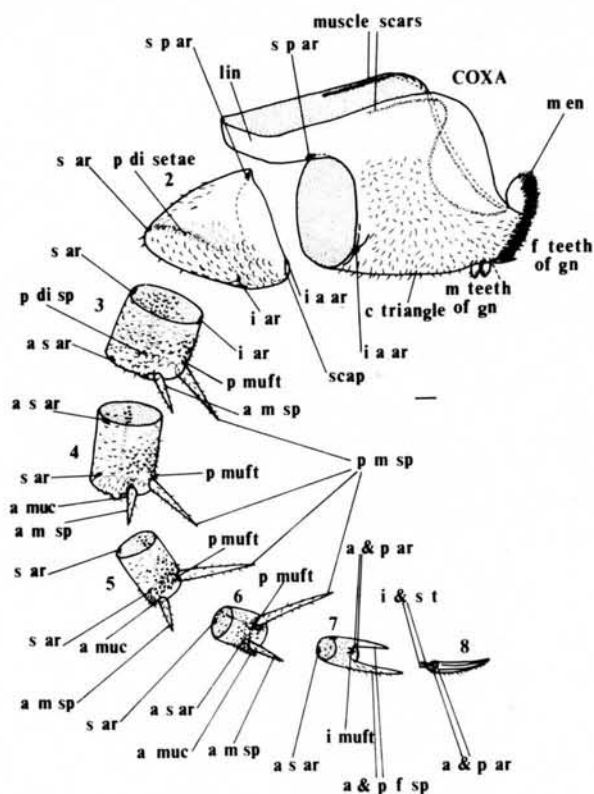

Figure 6 *Baltoeurypterus tetragonophthalmus.* Exploded reconstruction of right limb IV, antero-lateral aspect.

and setae in numerous rows on the posterior distal edge than does podomere III2. The superior convexity is more anterior in position than on podomere III2, and thus is tending towards the condition in podomere V2. The proximal edge bears infero-anterior and supero-posterior articulations. A lobe at the infero-anterior articulation (Fig. 6) is approaching the shape of the scaphoid process of podomeres V2 and VI2. Distally, there are superior and inferior articulations.

Podomeres 3 to 6. In general, these podomeres are longer than their cross-sectional diameters, but when compressed this may not be apparent. The ratio of proximal circumference to distal circumference increases from podomere 3 to podomere 6. Podomere IV3 resembles podomere III3, but may be distinguished by its smaller anterior distal mucrones and the larger posterior movable spine. Similar cuticular features are present on podomere IV3 as on podomere III3, but are more strongly developed (Figs 28k, l). The three succeeding podomeres (4, 5 and 6) can be readily distinguished from all other podomeres on limbs II, III and IV by their supero-posterior carinae. These carinae, which attain their strongest development on limbs V and VI, are composed of narrow lunules which are commonly folliculated (Figs 28k, p).

Apart from the carina, the surface sculpture of podomeres 4, 5 and 6 of limb IV resembles that of podomeres 4, 5 and 6 of limb III. Due to the decrease in size of the podomeres relative to the constant size of the follicles, there appears to be a greater number of follicles on the anterior surfaces of the more distal podomeres. The multifolliculated tubercle adjacent to the posterior movable spine increases in size on the more distal podomeres. The anterior distal mucrones,

which are small on podomere 3, are larger on podomere 4; on podomere 5 the middle one is the largest, and on podomere 6 this mucro is very large and the others are small. A row of spines occurs on the posterior distal edge of podomeres 3, 4 and 5, (Figs 28j, l, r) but is absent from podomere 6 (Fig. 28v). The articulation points (Fig. 6) are in similar positions to those on limb III. The movable spines (Figs 28k, p, q, z) increase in length from podomere 3 to podomere 6. The anterior movable spines are never more than half the length of the posterior.

Podomeres 7 and 8. These (Figs 28u, v, z) differ from podomeres 7 and 8 of limb III only in the greater length of their spines.

2.7. Prosomal appendage V

Limb V contrasts to the foregoing three limbs in that it bears no movable spines and has nine podomeres. Continuing the trend of an increase in limb length posteriorly, podomeres 4 to 7 in the main part of the ramus are much longer than their cross-sectional diameters. Probably related to the increased length of podomeres 4 to 7 are the prominent carinae which provide strength. The podomere count is increased by the presence of two trochanters (podomeres 2 and 3) following the coxa. Complete rami of this limb are shown in Figures 28cc–ee and a reconstruction is given in Figure 7.

Coxa. Nieszkowski (1859), Schmidt (1883) and Holm (1898, p. 17) recognised that coxa V is larger than coxae II, III and IV, but disagreed on how far coxa V extended to the carapace edge. The lintel is smaller relative to the rest of the
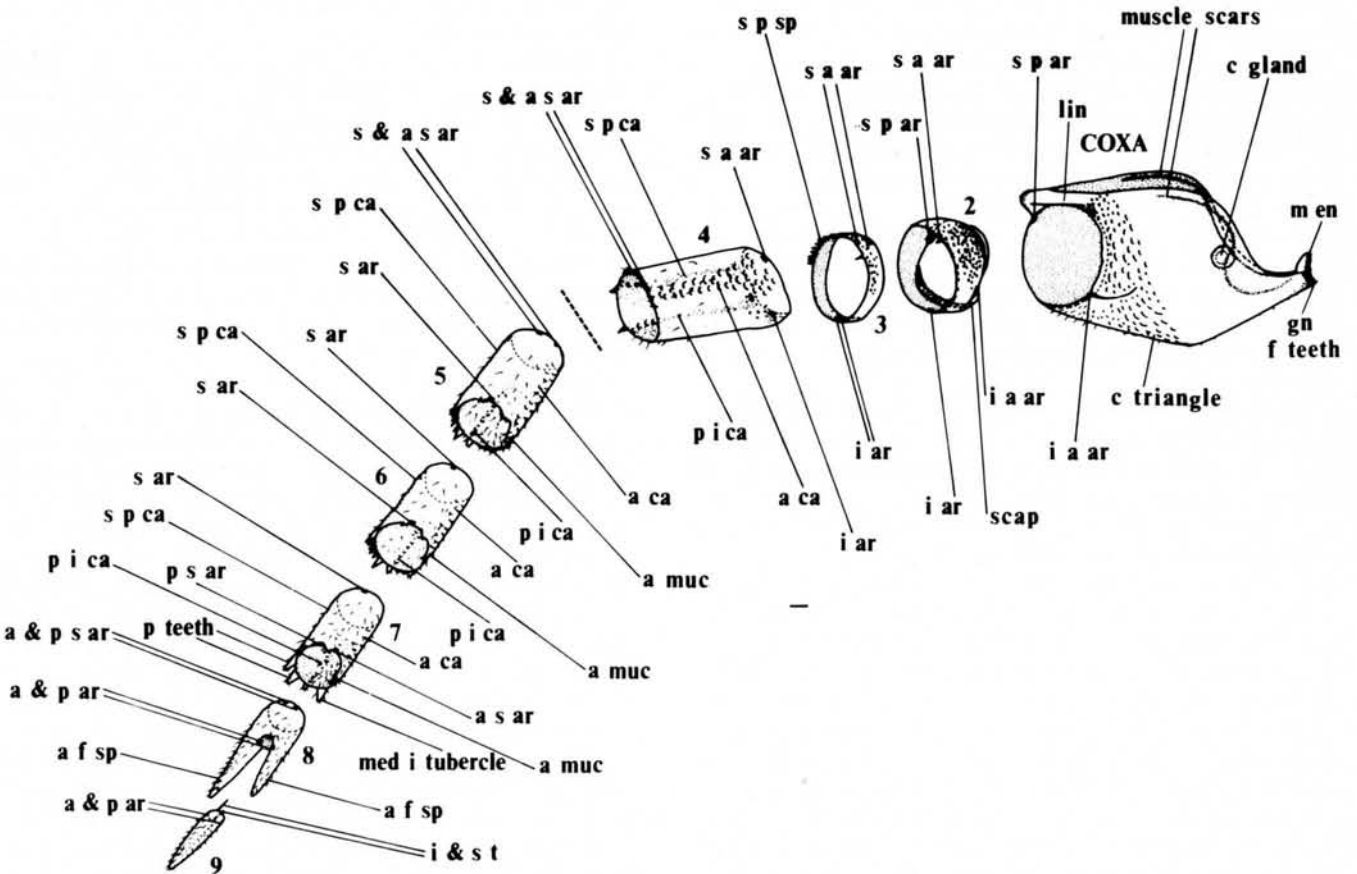
Figure 7 *Baltoeurypterus tetragonophthalmus*. Exploded reconstruction of right limb V, anterior (podomeres 1 to 4) and supero-anterior (podomeres 5 to 9) aspects; the break between podomeres 4 and 5 is artificial and allows features to be seen more clearly.

coxa in limb V (Fig. 7) and hence the distal joint is closer to the carapace edge and is situated directly beneath the mesial edge of the ventral marginal plate. A coxal extension carries the gnathobase into the oral cavity.

The anterior and posterior surfaces were called inner and outer lamellae respectively by Holm (1898, p. 17). Both surfaces bear setae. The submarginal muscle scars (Fig. 28bb) are comparable to those of coxae III and IV, with the exception of a deviation around the coxal gland opening. The distal part of the anterior surface bears broad lunules which grade into narrower lunules on the anterior lintel lobe, the coxal triangle, and around a dark streak which extends from the distal infero-anterior articulation mesially in a broad curve towards the dorsal edge (Fig. 28w).

Of all the coxal triangles, that of coxa V is the most triangular in shape. The posterior edge is a thickened ridge bearing raised follicles. The follicles are most numerous at the postero-distal corner of the triangle, and extend more thinly over its surface. There is a row of small, broad lunules along the distal border of the coxal triangle. A thickened ridge extends from the apex of the coxal triangle to the largest tooth of the gnathobase (Fig. 28b). This ridge is approximately the same length as the posterior border of the coxal triangle. It bears prominent bristles adjacent to the gnathobase.

The gnathobase lacks ventral movable teeth; only stout, fixed teeth are present (Figs 28n, o), surrounded by bristles. The teeth number about 40 (Holm (1898, p. 19) reckoned at least 15; Schmidt (1883) counted only 6), arranged in two rows of large teeth with subsidiary rows of smaller teeth. A movable endite is present (Figs 32h, z, cc).

The distal joint (Figs 28w, x) bears prominent infero-anterior and weaker supero-posterior articulations. The infero-anterior articulation is slightly more superior in position than the similar articulations on coxae II, III and IV. A ridge formed of broad lunules runs superior to the anterior articulation up to, and merging with, the anterior lintel lobe; the distal edge is recurved along this border (Figs 28x; 31z). The infero-posterior border is not so strongly sculptured and bears a large expanse of arthrodial membrane.

The lintel of coxa V (Figs 28c, w, x, z, aa) differs from those of coxae II, III and IV in that it is longer, the two lobes (anterior and posterior) are prominent and the inter-lobe region is narrow and comparatively deflated. The anterior lintel lobe bears small, slightly raised lunules and the posterior lobe and part of the interlobe region bear minute raised lunules.

Coxal gland opening. A subcircular hole is present half-way along the mesial edge of the posterior surface of coxa V and is bounded by a dark ring which is contiguous with the submarginal muscle scar (Figs 28a–c, w, x, bb). Holm (1898, p. 18) believed that in life the hole was covered by thin cuticle which is subsequently lost. None of the specimens examined showed any trace of a cuticular covering, but commonly the anterior surface showing through the hole gives the impression of a membrane. Holm (1898, p. 18) found a subcircular patch of thin cuticle on the anterior surface of the coxae of limbs III to V of *Limulus*, and believed these were homologues of the structure in *Baltoeurypterus* with an auditory function. There is no mention in the literature of the function of these coxal structures in *Limulus*, which are readily seen in *Limulus* material and in Holm's pl. 9, figs 3 to 5 of *Carcinoscorpius* and pl. 9, figs 12 to 14 of *Limulus*. If these structures had a sensory function, it would be expected that neurophysiologists would have discovered their innervations in this much-studied experimental animal.

Wills (1965, p. 102) suggested that the structure is the opening of the coxal gland, an excretory organ. Coxal glands occur in nearly all chelicerates, normally opening on the posterior surface of coxae III or V (Kaestner 1968). The coxal gland opening of *Limulus* occurs between coxae V and VI, but in fact is much closer to coxa V; in scorpions the gland opens on the posterior surface of coxa V. In most other arachnids the gland opens in a more anterior position. With present knowledge of this structure, Wills's (1965, p. 102) explanation seems the most plausible.

Podomere 2. Between the coxa and the first long podomere of the ramus of limbs V and VI lie two short, subannular podomeres. Podomere 2 is the longer of the two and partly resembles podomere 2 of limb IV, differing mainly in that the supero-anterior surface is only three times as long as the infero-posterior surface (compare Figs 6 and 7). Podomere 3 is very short and annular. Podomere 2 is shown in isolation in Figures 28f; 31b and podomere 3 in Figures 28g; 31j. Both podomeres are shown together in Figures 28a, b, cc–ee; 31p.

The supero-anterior surface of podomere 2 (Fig. 7) is bulbous and bears numerous narrow, raised lunules (Fig. 31b). The other surfaces of the podomere are narrower, the infero-posterior being the shortest. Scattered minute lunules only are found on the surfaces other than anterior and posterior. Broad lunules occur on the anterior and superior distal border, and adjacent to the supero-anterior articulation these are large and mucronate (Fig. 31b). The proximal infero-anterior articulation is strong and bears a scaphoid process. The proximal supero-posterior articulation is weaker. The proximal inferior edge is characterised by a large expanse of striated arthrodial membrane, the striae representing tendon bases arising from the podomere edge. The distal edge bears strong supero-anterior and weaker inferior articulations.

Podomere 3. Podomere 3 is annular and only slightly longer superiorly than inferiorly (Fig. 31j). A few narrow lunules occur distally on the superior surface, but otherwise this podomere is fairly smooth. The supero-posterior distal border bears a row of about 10 sharp fixed spines. A sharp mucro is present adjacent to the supero-anterior distal articulation, and another prominent mucro occurs on the anterior distal edge, in a similar position to the largest mucro on the anterior distal border of podomere 2. Inferior and supero-anterior articulations occur on both the proximal and distal edges (Fig. 7).

Podomeres 4 to 7. Podomeres 4 to 7 resemble one another in all being about twice as long as their cross-sectional diameters and all possessing three prominent longitudinal carinae. The supero-posterior carina is comparable to that of podomeres 4 to 6 of limb IV. The other two carinae are postero-inferior and anterior in position. Although these four podomeres are basically the same shape, each has a slightly greater circumference than the podomere distal to it. Holm (1898, p. 21) suggested that the area enclosed by the two posterior carinae of podomeres 4 to 7 may correspond to the inferior surfaces of limbs II to IV, and also that the cross-sections of podomeres V4 to V7 may have been triangular. They are reconstructed as circular herein (Fig. 7) in the absence of evidence to the contrary.

Podomere 4 differs from the succeeding three podomeres in its possession of a proximal postero-inferior convexity. The proximal and distal joint planes are slightly angled, giving this podomere a profile of an asymmetric parallelogram (Figs 28cc–ee; 31p). The proximal postero-inferior convexity is formed of two inflated areas at the bases of the two posterior carinae; the most superior inflated area bears small

lunules (Fig. 28i). The distal joint of podomere 4 is emarginated on the postero-inferior side (Fig. 28dd). A weak articulation occurs in a superior position on the distal edge (Fig. 28ee) and the close connection of podomeres 4 and 5 continues to the point where the anterior carina meets the distal edge where there is another weak articulation, thus forming a bicondylar hinge joint.

The supero-posterior and postero-inferior carinae are each composed of a single line of narrow raised lunules, except at the proximal end where a cluster of lunules is present. The postero-inferior carina is less prominent than the supero-posterior carina on podomeres 5 to 7, but carries more follicles (Fig. 28d). The supero-posterior carina (Figs 28s; 31o) terminates at the distal edge in a large mucro or fixed spine, the size of which increases from podomere 4 to 7 (Figs 28dd; 31l, o). There is also a spine at the distal end of the postero-inferior carina, but the carina actually terminates just inferior to this, in a large folliculated tubercle, on podomere 4. On the more distal podomeres, the fixed spine appears to be more removed from this terminal folliculated tubercle (Figs 28dd, ee) as the carina becomes more inferior in position. Four spines occur between the two posterior fixed teeth of podomeres 5 and 6 (Figs 28d; 31o).

The anterior carina consists of broad lunules, two or three abreast, many of which bear follicles. This carina is most prominent on podomere 4 but becomes less so on the more distal podomeres (Fig. 28ee). The carina terminates on the distal edge of podomere 4 in two broad, folliculated mucrones. These mucrones are present on the more distal podomeres but enlarged into fixed, folliculated teeth. The anterior carina terminates distally at the more anterior of these teeth on podomeres 5 and 6; the superior tooth is absent from podomere 7 (Fig. 28ee).

The intercarinal surfaces of podomeres 4 to 7 bear follicles. These are concentrated at the distal end of the inferior surface and on the anterior surface, especially adjacent to the anterior carina. The more distal podomeres exhibit a greater density of follicles (Fig. 31n).

A median inferior tubercle occurs on the distal border of podomere 4, flanked by small lunules. This tubercle becomes much larger and folliculated on the more distal podomeres (Fig. 28dd), as do the flanking lunules, and is largest on podomere 7 (Fig. 31l), which, however, lacks the flanking features. The superior distal edge bears an articulation on podomeres 4 to 6, with a multifolliculated mucro adjacent posteriorly to it. Podomere 7 bears two articulation points on the superior distal edge, one at either side of the multifolliculated mucro (Fig. 28ee).

Podomeres 8 and 9. Podomeres 8 and 9 of limb V (Figs 31e, l) resemble the two terminal podomeres of limb IV, but differ in that the anterior and posterior fixed spines of podomere V8 are longer than those of podomere IV7. Also, the anterior fixed spine of podomere V8 is shorter than the posterior, whereas the posterior fixed spine of podomere IV7 is the shorter. The posterior fixed spine of podomere V8 is as long as podomere V9. The fixed spines of podomere V8 and of V9 are less curved than the fixed spines of podomere IV7 and podomere IV8. An inferior multifolliculated tubercle is present on podomere V8. A small carina of narrow lunules runs along the proximal half of the posterior surface of the posterior fixed spine of podomere V8. Anterior and posterior articulations are present at the bases of the fixed spines on the distal border of podomere V8. The fixed spines of podomere V8 and podomere V9 bear numerous follicles.

The tips of the fixed spines of podomere 8 and podomere 9 show a dark, conical structure internally, which is exposed by wear on the tips (Fig. 31i, t). This dark body may be a strengthening structure to prevent excessive abrasion to the tips of the spines.

2.8. Prosomal appendage VI

Limb VI (Fig. 8) is the largest appendage and is characterised by its enormous coxa, the flattened, paddle-shaped distal part of the ramus, and some highly modified joints for twisting the distal part of the ramus about the limb axis
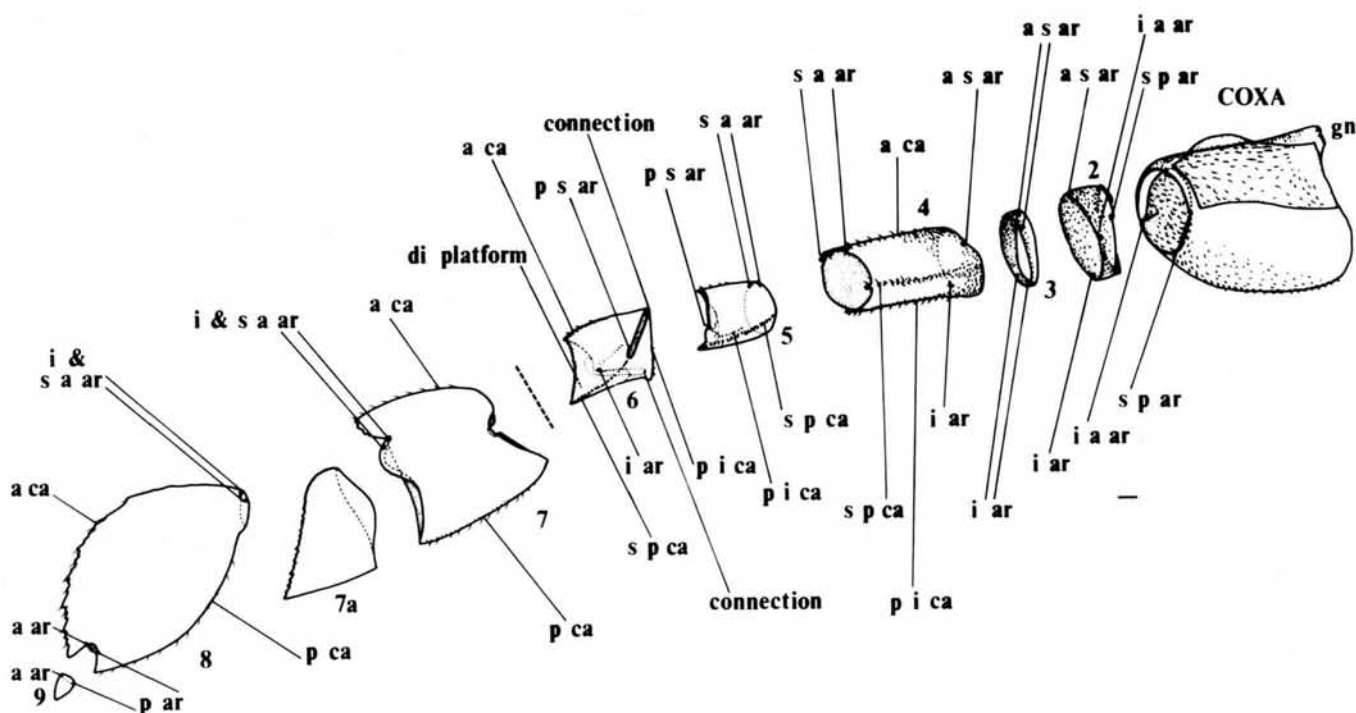

Figure 8 *Baltoeurypterus tetragonophthalmus*. Exploded reconstruction of left limb VI, supero-posterior (podomeres 1 to 6) and posterior (podomeres 7 to 9) aspects.

during swimming (section 5). Limb VI was described and figured by Nieszkowski (1859) and Schmidt (1883), and by Holm (1898, p. 22 *et seq.*) in detail.

Coxa. The coxa of limb VI differs in shape from the coxae of limbs II to V in being more expanded posteriorly and relatively shallow dorso-ventrally. In ventral aspect, coxa VI is roughly trapezoidal (Figs 31y, aa). The great posterior expansion has resulted in the loss of the coxal triangle, the ventral surface forming the greater part of the coxal surface.

The anterior surface is bounded ventrally by an acute edge running from the gnathobase, where it is well developed, to the anterior side of the distal joint, where it has become less acute, rounded and covered with broad lunules. The dorsal edge of the anterior surface (Fig. 31k) follows the dorsal edge of the posterior surface of coxa V, with which it is in close association. The anterior surface of coxa VI is setose but bears no raised sculpture.

The dorsal edge of the posterior surface runs in a much shallower S-curve than that of the dorsal edge of the anterior surface, from the supero-posterior part of the distal joint to the mesial edge of the coxa, joining it about $\frac{2}{3}$ of the way from the gnathobase to the rear. Instead of being vertical, as in coxae II to V, the posterior surface of coxa VI was inclined at a low angle to the horizontal in life. The postero-lateral $\frac{1}{3}$ of the posterior surface bears faint lunules but is otherwise devoid of sculpture. The posterior edge of coxa VI is an acute edge formed of discrete, thickened denticles (Fig. 31y), some of which bear follicles. The ventral surface of the coxa bears a characteristic pattern of lunules (Figs 31y, aa). The mesial area, covered by the metastoma in life, is devoid of sculpture, although some stretch marks are present on this area near the gnathobase.

The gnathobase of coxa VI is characteristic and quite distinct from the gnathobases of coxae II to V. No movable endite is present (but see endostoma, section 2.9). The large anterior tooth is black in colour as it is composed of extremely thick cuticle (Figs 31r, u–w, z, aa). Holm (1898, p. 23) described this tooth as chisel-shaped, and he also mentioned that it appears to be formed from the fusion of many smaller teeth, some specimens presenting a papulose appearance (Fig. 31r). The posterior part of the gnathobase consists of a row of seven (usually) teeth as a single, black, serrated ridge (Figs 31u, v, y–aa; 32z). In plan, this line of teeth subtends an angle of about 130° with the bevelled edge of the large anterior tooth, and in side view (Fig. 31v), an angle of about 30° is subtended by these lines. This angle is occupied by the anterior margin of the metastoma in life (Fig. 31p). The amount of wear on the teeth varies, some specimens showing extreme abrasion.

The distal joint of coxa VI is similar to that of coxa V but the lintel is narrower and more rounded (Fig. 23r). The articulations differ from those of coxa V in that the dark streak extending from the infero-anterior articulation of coxa VI runs at right angles to the edge and for a shorter distance than that of coxa V, the stretch marks on either side of the furrow (Figs 31y, aa) are more prominent and the supero-posterior articulation is less prominent on coxa VI.

Podomere 2. Podomere 2 of limb VI (Figs 31a, c, d, f, g, x) bears a considerable resemblance to podomere 2 of limb V. The major differences lie in: the general shape, podomere VI2 is shorter and less bulbous on the supero-anterior surface than podomere V2 (Fig. 31g); podomere VI2 is more strongly sculptured with small lunules than podomere V2; podomere VI2 bears a stronger proximal supero-posterior articulation than podomere V2, as well as some proximal superior striated membrane (Figs 31c, f) which is not apparent on specimens of podomere V2. As in podo-

mere V2, the proximal joint bears a strong infero-anterior articulation with a scaphoid process and a weaker supero-posterior articulation. Striated membrane occurs on the inferior and superior proximal edges. The distal joint bears supero-anterior and infero-posterior articulations.

Podomere 3. The lack of supero-posterior distal spines on podomere 3 of limb VI (Figs 31a, c, d, f, g, x; 32f, g) readily distinguishes it from podomere 3 of limb V which it otherwise resembles. It is annular, with supero-anterior and infero-posterior proximal articulations, and similar distal articulations to podomere V2 but more superior and inferior respectively (Fig. 8). A prominent row of broad mucrones occurs on the supero-anterior distal edge. The surfaces of the podomere bear small lunules which are more prolific on the posterior and inferior surfaces.

Podomere 4. Podomere 4 of limb VI (Figs 31d, q, x; 32i, q, r) resembles podomere 4 of limb V, the chief differentiating criterion being the more rounded terminal spines and mucrones of the carinae of podomere VI4. The inflated, lunulated areas at the bases of the posterior carinae are more prominent on podomere VI4, and the podomere itself is generally larger than podomere V4.

The proximal joint of podomere 4 bears antero-superior and postero-inferior articulations. The distal edge of podomere 4 bears a superior articulation surrounded by three multifolliculated mucrones, which continues anteriorly to the anterior carinal mucrones where there is a further weak articulation. The distal edge is emarginated on the infero-posterior side where much membrane occurs (Fig. 31x).

Podomere 5. Podomere 5 (Figs 31x; 32i, s, t, x, aa) is short, but the distal diameter is greater than the proximal diameter, hence it appears to taper proximally. The superior surface is roughly trapezoidal and appears quite smooth apart from an elongate patch of faint lunules in the anterior half of this surface, which terminates distally in two folliculated lunules. There is another short row of about three lunules running obliquely antero-proximal–postero-distally adjacent to the postero-superior articulation, which terminates in a folliculated lunule. Posterior to this folliculated lunule, on the distal edge, is another, and posterior to this is the large, pointed terminal multifolliculated mucro of the supero-posterior carina.

The supero-posterior carina consists of narrow, discrete, raised denticles without follicles (Figs 32s, x, aa). In side view this carina curves very gently over most of its length, but trends more steeply inwards proximally. The anterior carina consists of broad lunules, many with follicles, two or three abreast but increasing to four or five abreast proximally. Distally, it terminates in a very large, multifolliculated mucro (Fig. 32s).

The antero-inferior surface is smooth, and shorter than the superior surface. Distally, its edge runs in a broad S-shape, starting anteriorly as part of the terminal anterior carinal mucro, it is lunulated along the middle section, and terminates inferiorly in three large, triangular mucrones (Figs 32s, t, x). The middle mucro is the largest of the triplet. In some specimens (Fig. 31x) subsidiary mucrones occur between the major three.

A short carina of narrow, raised, folliculated lunules runs in a curve antero-proximal–postero-distally. It starts at a point infero-subproximally as a patch of small, faint lunules, and terminates distally in a folliculated tubercle (Figs 32x, aa) just posterior to the triplet of mucrones. This carina may represent the postero-inferior carina of other podomeres.

The postero-inferior surface is smooth. The distal edge of this surface bears strong denticles which appear almost to be a continuation of the postero-inferior carina, as this edge

runs obliquely infero-proximal–postero-distally up to the terminal supero-posterior carinal mucro (Figs 31x; 32x).

The distal joint bears a postero-superior articulation, and articulated specimens (Figs 32i, k, l, aa) show another connection at the antero-inferior distal edge with podomere 6. The superior edge anterior to the postero-superior articulation is recurved, forming a bar (Figs 32s, t, x), but much arthrodial membrane is present here (Fig. 31x). Posterior to the postero-superior articulation, the distal edge is not recurved but bows outwards and distally, connecting directly with podomere 6 (Figs 31x; 32i, s, t).

Podomere 6. Holm (1898, p. 25) described podomere 6 (Figs 32n, o) as bell-shaped. It is largely due to the shape of this podomere and the orientations of its joints that the flattened distal podomeres of limb VI were able to be used in rowing (section 5). The terminology of the surfaces is based mainly on the relationships of the surfaces to the identified carinae.

The inferior surface, between the anterior and postero-inferior carinae, is approximately kite-shaped. The anterior and postero-inferior carinae subtend an angle of just under 90° where they meet antero-inferiorly at the anterior end of the elliptical proximal joint (Figs 32i, n, y). The inferior surface is fairly smooth but bears a few follicles anteriorly. The inferior distal border consists of two gently curved embayments, on either side of a markedly prominent articulation (Fig. 32l). The more posterior half of this edge is fairly straight adjacent to the articulation and runs roughly parallel to the anterior carina, but curves more strongly up to the terminal postero-inferior carinal mucro, causing this edge to be J-shaped. The anterior half of the inferior distal edge forms the inferior border of a distal platform or "col" between the large terminal mucrones of the posterior carinae and the inferior articulation (Figs 32n, y). The posterior half of the inferior distal edge forms part of the distal joint.

The anterior carina (Figs 32n, y) consists of folliculated lunules, three or four abreast, and terminates in a large folliculated mucro or fixed tooth composed of many small denticles.

The superior surface is rhomboidal and bounded proximally by the proximal joint, anteriorly by the anterior carina, posteriorly by the supero-posterior carina, and the distal edge consists of a gently curved, serrated embayment. The superior surface bears a patch of small lunules in the central area. The distal edge, which is strongly serrated (Figs 32n, y), forms the superior edge of the distal platform.

The supero-posterior carina (Figs 32n, y, aa) consists of a single, curved line of discrete, raised, narrow lunules or denticles, a few of which bear follicles. It runs from the posterior end of the elliptical, proximal joint, to terminate distally in a large, multifolliculated mucro or tooth. This tooth is flanked (Fig. 32n) by denticles, and it overlooks the distal platform.

The posterior surface is approximately triangular. Superiorly it is bounded by the proximal joint and the supero-posterior carina, inferiorly it is bounded by the postero-inferior carina. The distal edge is fairly straight, except near the terminal postero-inferior carinal tooth, and lunulated. A cluster of lunules occurs near the distal edge adjacent to this tooth.

The postero-inferior carina consists of low, crescentic lunules, two abreast, in a straight line. It runs from the posterior end of the proximal joint, and terminates in a large, folliculated mucro or tooth.

The proximal joint is elliptical, and bears an articulation postero-superiorly, near the posterior end; the anterior end

is closely attached to the antero-inferior distal edge of podomere 5.

The distal joint lies in two planes. The elongate elliptical part runs almost parallel to the long axis of limb VI, and parallel to the anterior carina (Figs 32i, k, l, n, y). The more circular part lies in a plane almost at right angles to the elliptical part and is bounded by the distal platform. A strong articulation occurs on the inferior side of the joint, at the junction of the two parts of the joint, and projects towards the joint axis. A close connection with podomere 7 occurs on the superior side of the elongate part of the joint.

Podomere 7. Podomere 7 is flattened, the superior and inferior surfaces are greatly expanded and are almost mirror-images of each other. Both surfaces are smooth, apart from two or three follicles. The main criteria for distinguishing the inferior and superior surfaces are the shapes of their proximal and distal borders (Figs 8; 32m). The cross-sectional profile appears not to have been hydrofoil-shaped in life.

The anterior carina is curved, and consists of folliculated lunules proximally, which distally are raised into small folliculated denticles. The terminal feature is a large, flattened, serrated and multifolliculated tooth (Fig. 32m). The posterior carina consists of folliculated lunules along the whole of its length, two or three abreast. This carina is greatly curved and only minor denticles, no major mucro, are developed distally. Due to its position in articulated specimens (Figs 32i, k), this carina may represent the postero-inferior carina.

The superior edge of the proximal joint is J-shaped, with a strongly curved anterior part. The inferior edge is gently curved, apart from a rhomboidal notch which occurs where this edge attaches to the large articulation of the distal edge of podomere 6 (Figs 32e, m).

The distal border of the inferior surface is fairly straight, and bears an articulation almost at the anterior end. The distal edge of the superior surface runs in a gentle S-shape, the salient anterior part is a little more strongly curved and is also incurved. An articulation occurs close to the anterior end of this edge. Between the apex of the salient part of the superior distal edge and the most proximal part of the re-entrant distal edge, the edge is finely dentate, and may represent the vestige of a supero-posterior carina. These features may be seen in Figure 32m.

A large, flat, approximately triangular lobe (7a) is attached to the distal edge of podomere 7 (Figs 32e, i, k, u). This lobe may represent a flattened distal movable spine of podomere 7. The inferior and superior sides can be distinguished by the shape of the proximal joint.

Podomere 8. Podomere 8 (Figs 32e, k) forms the distal part of the paddle. It is approximately elliptical in outline, flattened in the same plane as podomere 7 and has a similar cross-section. The superior and inferior surfaces are mirror-images of each other. Both are smooth apart from a few scattered follicles near the anterior and posterior edges.

The posterior edge or carina is composed of discrete, folliculated denticles which increase in size distally, and the edge terminates in a large, flat mucro. The anterior edge is composed of smooth denticles proximally, and becomes serrated distally, terminating in a large flattened tooth.

The proximal joint is elliptical in cross-section and bears antero-superior and antero-inferior articulations. The distal joint is very short, elliptical, and bears anterior and posterior articulations.

Podomere 9. Podomere 9 (Figs 32j, k) is leaf-shaped, being flattened and obtusely pointed, but with a wide, elliptical proximal joint bearing anterior and posterior articula-

tions. Podomere 9 bears no follicles, but has the internal conical pigmented tissue (as do the terminal teeth of podomere 8) characteristic of terminal limb podomeres and spines. When articulated, the anterior edge lies partly inferior to the anterior terminal tooth of podomere 8, and the posterior edge lies partly superior to the posterior terminal tooth of podomere 8.

2.9. Endostoma and metastoma

Endostoma. The endostoma was well known to Holm (1898, p. 29), and its bilobate form is illustrated here in Figures 2; 32 b–d, bb. Wills (1965, p. 104 & pl. 2, figs 1–3) described a posterior fold or doublure along the posterior border of the endostoma. This doublure has not been seen on any other specimens, and is therefore probably an artefact. The posterior border of the endostoma has a definite shape and this edge is connected to thin cuticle. The anterior part of the endostoma merges more indistinctly into the setose cuticle of the mouth.

The endostoma is situated supero-anterior to the foremost part of the metastoma, in the rear part of the oral cavity (Figs 32z, cc) and, in life, would have been superior to the posterior tooth row of the gnathobase of limb VI (Figs 2; 32v, w, z, cc). It may have functioned in separating the chewing actions of coxa VI from those of the more anterior coxae, and perhaps also helped in pushing food forward towards the mouth (section 3).

The endostoma of *Baltoeurypterus* is almost certainly homologous with that of *Limulus* (Holm 1898, p. 31). Størmer (1934) considered that the endostoma probably developed from a posterior sternite of the prosoma. Probably the organ most comparable in function to the endostoma is a coxal movable endite. Possibly coxa VI once bore a movable endite, and the coxa VI endites have migrated dorsally and fused to become the endostoma, retaining their original function in part. This would also follow the trend suggested in section 2.8, that the gnathobase of coxa VI developed, by fusion of teeth, from one resembling the gnathobases of more anterior coxae. An isolated movable endite (of coxa V?) is illustrated in Figure 32h. The setae on the endostoma are less densely packed than on the movable endite, and the endostoma also lacks the bristles.

Metastoma. The metastoma (Figs 31r, 32o, p) was described by Holm (1898, p. 28). It almost certainly aided in food mastication by (a) forming the rear part of the oral cavity (Fig. 2) and thus preventing food from being lost during chewing, and (b) supporting food whilst the teeth of gnathobase VI broke it up, whilst also acting as a base about which coxae VI could possibly rotate (see section 3). In the latter function the metastoma is an analogue of the chilaria of *Limulus* (see Manton 1964). The great number of follicles on the surface of the metastoma suggests many setae were present in life, and in this respect an analogy with the sensory pectines of the scorpion may also be made.

3. Feeding

3.1. Coxa

The feeding method of *Limulus* has been known for many decades (e.g. Patten 1894) but, surprisingly, there has been little mention of the possible feeding mechanism of eurypterids. Patten (1894) briefly outlined the chewing movements of *Limulus* coxae, before describing his elegantly simple but effective experiments to determine the gustatory organs. The coxae of *Limulus* and *Tachypleus* are able to perform two distinct actions (Manton 1964). Promotor–

remotor movements of the coxa are caused primarily by alternate contraction of tergocoxal muscles which arise on the anterior and posterior proximal margins of the coxa adjacent to the pleurocoxal articulation and which insert on the carapace. During promotor–remotor movements, the body–coxa joint acts as a pivot, the articulation axis passing through the pleurocoxal articulation and the ventro-medial end of the joint (Fig. 9).

Transverse adduction is produced by contraction of plastrocoxal muscles which arise from the anterior and posterior proximal margins of the coxa and insert on the endosternite (Fig. 9). During adduction, the basal joint of the coxa acts as a hinge as the coxa articulates dorsally by means of a Y-shaped pleurite set in the leathery cuticle of the ventral body wall. Wyse and Dwyer (1973) studied the neuromuscular rhythms involved in the coxal movements of *Limulus*. They noticed that the Y-shaped pleurite, being set in fairly pliable ventral cuticle, is free to move dorsolaterally and observed this movement during transverse adduction–abduction but not during the promotor–remotor swing. Muscles 27 and 29 (Fig. 9) act as "pivot shifters", rotating the gnathobase during chewing. It appears, therefore, that a strong pleurocoxal articulation is not a requirement for transverse coxal movements, but is necessary if promotor–remotor movements occur at the same joint.

Manton (1964) considered abduction to be caused by contraction (with a low mechanical advantage) of a tergocoxal muscle (No. 25 of Lankester et al. 1885) which arises on the other side of the pleurocoxal articulation and inserts on the carapace. Wyse and Dwyer (1973) showed that muscle 25 is not active during abduction, and muscle 26 (Fig. 9), which is the main promotor, is recruited as an abductor only during strong chewing cycles. Without an abductor muscle, abduction must be passive, perhaps under hydrostatic pressure. Since successive coxal pairs adduct alternately (Manton 1964), whilst two pairs are adducting, fluid pressure will be increased and the other pairs may abduct under this pressure. Scorpion coxae III and IV move during feeding without any apparent basal articulation or specialised musculature (Couzijn 1976).
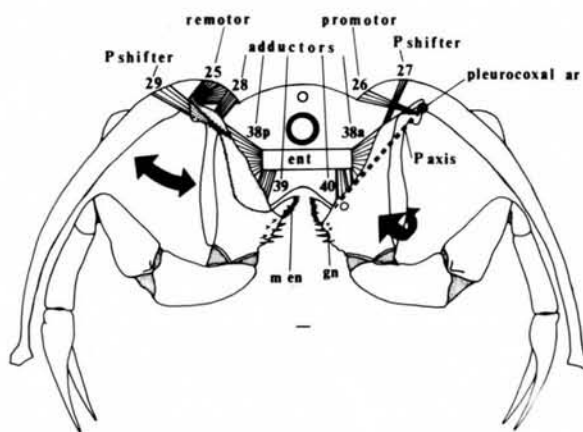
Figure 9 *Limulus polyphemus.* Diagrammatic transverse section, showing limbs V, viewed from the anterior, right coxa cut away to show posterior muscles, anterior muscles shown on left coxa (i.e. on right-hand side of diagram); muscles numbered after Lankester et al. (1885). Muscles 25–29 are tergocoxals, 38–40 are plastrocoxals; plastrotergals (suspensory muscles for endosternite) not shown. Black arrow on left-hand side of diagram indicates coxal movement during adduction–abduction, that on right shows promotor–remotor movements around coxal pivot. (Outline based on Wyse & Dwyer 1973.)

Table 1 Comparison of the coxae of *Limulus* and *Baltoeurypterus*, as used in feeding

	Limulus	*Baltoeurypterus*
For trituration of food.	Toothed gnathobase on limbs II to VI.	Toothed gnathobase on limbs II to VI.
To aid in directing food to mouth.	Movable endite dorsal to gnathobase.	Movable endite dorsal to gnathobase.
To increase mechanical advantage during adduction.	Extended (bilobed) dorso-lateral flange articulating with pleural wall.	Dorso-lateral lintel (bilobed) connected to ventral marginal prosomal plate.
To increase number of coxae around mouth	Antero-posterior flattening of coxae.	Antero-posterior flattening of coxae.
Muscle attachments.	Supero-posterior recurved edge with muscle attachment.	Supero-posterior recurved edge with muscle scars.

Table 2 Contrast between the coxae of *Limulus* and *Baltoeurypterus*, as used in walking

	Limulus	*Baltoeurypterus*
Body–coxa joint.	Relatively straight.	S-shaped.
Pleurocoxal articulation.	Present.	Absent, and wide lintel connection to ventral prosomal cuticle.
Mechanical advantage.	High; coxa–trochanter joint far from pivot axis of body–coxa joint to increase angle of swing.	Low; coxa–podomere 2 joint close to lintel.

In a direct comparison of the *Baltoeurypterus* coxa with that of the xiphosurans (Table 1) many morphological features correlated with feeding are common to both.

However, features of the *Limulus* coxa which are related to the provision of a promotor–remotor swing during walking are not shared by the *Baltoeurypterus* coxa (Table 2).

It is thus apparent that the *Baltoeurypterus* coxa could perform adduction–abduction chewing movements, but that promotor-remotor movements were strictly limited, and could not have provided the main promotor–remotor movements of the whole limb. The coxa also provided insertions

for the muscles which arose on the proximal podomeres of the ramus. Thus the second function of the *Baltoeurypterus* coxa was to provide a fairly firm base to the limb on which the ramus articulated during walking, swimming and food-gathering. In this respect, the *Baltoeurypterus* coxa is analogous to that of the arachnids, which is immobile during walking and has precisely this function (Manton 1977, chapter 10.5.E).

Figure 10 shows a reconstructed transverse section through *Baltoeurypterus* to give an indication of the arrangement of muscles that might have been present to provide
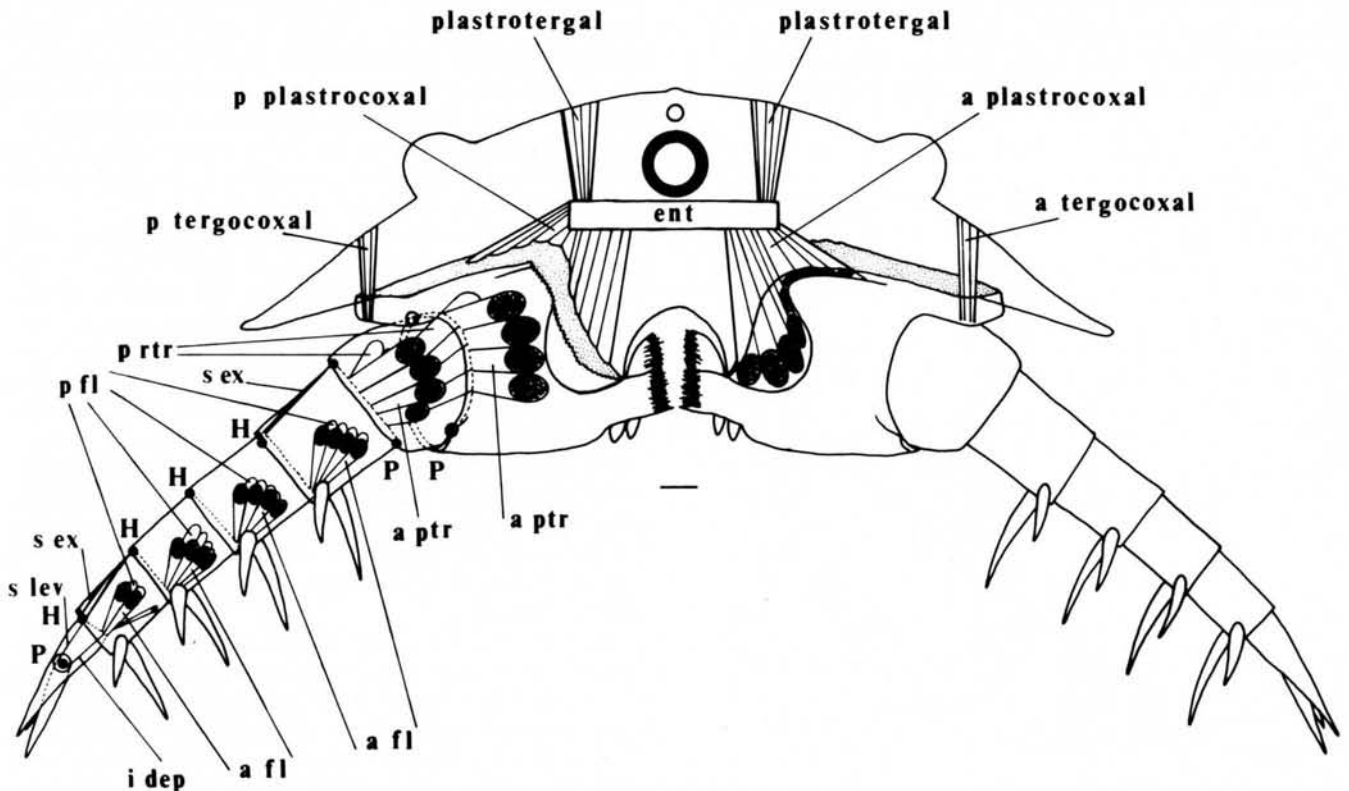
Figure 10 *Baltoeurypterus tetragonophthalmus*. Diagrammatic transverse section, showing limbs IV, viewed from the anterior, right coxa cut away to show posterior muscles, anterior muscles shown on left coxa (right-hand side of diagram); coxae and right limb ramus shown as if transparent to show possible musculature.

coxal movements. The reconstruction was produced from comparisons with *Limulus* (Fig. 9), evidence from coxal muscle scars, and the presumption of an endosternite (which occurs in nearly all chelicerates (section 1.2) and is necessary for efficient adductor muscle operation). Contraction of the anterior and posterior plastrocoxals would have provided the main adductor movements. The tergocoxals would have provided stabilisation and any tilting of the coxa during adduction. Abduction may have been caused by internal body fluid pressure during adduction of adjacent coxae.

Food caught by the food-gathering appendages of *Baltoeurypterus* would have been pushed into the oral cavity by the limb tips, aided by the chelicerae. Soft food could have been comminuted by the gnathobases of limbs II to V and pushed towards the mouth by the movable endites, in much the same manner as in *Limulus*. Hard carapaces and shells would first have had to be cracked open by the powerful teeth of gnathobase VI. Although coxa VI is a different shape to the other coxae, the musculature and mode of operation were probably similar. The coxae of limb VI probably performed slight rotational movements (the anterior plastrocoxals contracting more strongly than the posterior) during adduction due to the metastoma being positioned between them. Abduction was aided by the movement of the metastoma. The metastoma probably acted in much the same way as the chilaria of *Limulus* do, that is, in helping to hold food being crushed by the posterior gnathobases, and aiding in passing this forward to the more anterior gnathobases for further mastication. The endostoma separated the large coxa VI gnathobases from the more anterior gnathobases, and would have thus helped to prevent food that was being crushed by gnathobases VI from slipping forwards.

3.2. Chelicerae

The basal joint of the chelicera in *Limulus* is highly mobile, podomere 1 rotating about an enlarged anterior condyle. In *Baltoeurypterus* (Fig. 11) there appears to be no articulation at this joint and maximum flexibility of the chelicera would
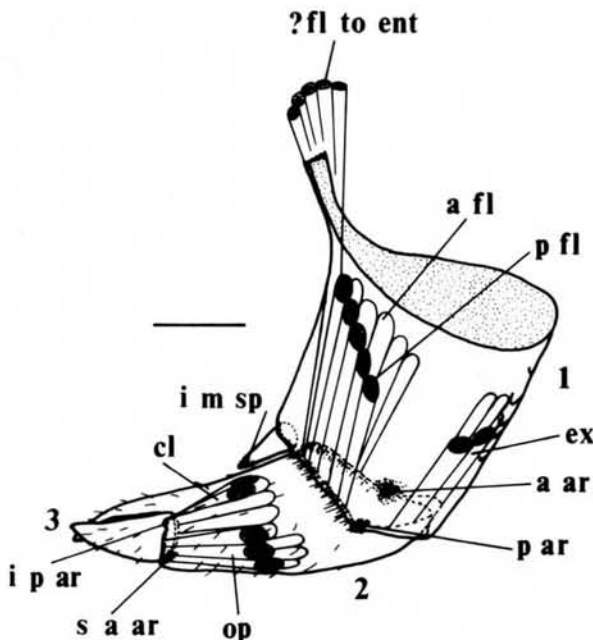

Figure 11 *Baltoeurypterus tetragonophthalmus.* Reconstruction of right chelicera, posterior aspect, shown as if transparent, with suggested musculature.

have occurred at the podomere 1–podomere 2 joint. Although constrained by its position between the labrum and coxa II, antero-superior movement of podomere 1 was probably possible. A possible mechanism is flexure by a muscle to the endosternite (Fig. 11, fl to ent) (acting against haemocoelic pressure) which, on relaxation, would restore podomere 1 to its original position. The musculature at the podomere 1–podomere 2 joint would have consisted of a simple flexor and extensor system. A simple opener and closer muscle system (Fig. 11) would have operated podomere 3, as suggested by Størmer (1936, fig. 1) for the chela of *Jaekelopterus rhenaniae*. These muscles probably arose on podomere 2 and inserted on the proximal margin of podomere 3. As the articulations at the podomere 2–podomere 3 joint are situated at opposite sides of the joint, rather than close together and distant from the insertion of the closer muscle, the mechanical advantage of the system is low. It is most probable that, as in *Limulus*, the chelicerae were chiefly employed in helping to pass food to the oral cavity, and catching pieces dropped by the gnathobases.

3.3. Food-gathering limbs

Limbs V and VI of *Baltoeurypterus* functioned as locomotory organs (sections 4 and 5) and the chelicerae are too small to have been effective in prey capture (cf. pterygotine eurypterids). The spinose limbs II to IV were the primary food-gathering appendages (although at least the posterior pair was also ambulatory, section 4).

Figure 10 shows the probable musculature of a food-gathering appendage, limb IV, deduced from a consideration of the joint morphology. The two most proximal joints of the ramus are pivots and would have been operated by anterior protractor muscles and posterior retractors. All these muscles are shown as intrinsic, extrinsic muscles are more commonly associated with promotor–remotor movements during walking. The inferior–superior or antero-inferior–supero-posterior pivot axes allowed some promotor–remotor movements, all other joints distally simply allowed flexion and extension in the plane of the long axis of the limb. Flexion was produced by flexor muscles. Extension was partly passive due to gravity on relaxation of the flexors (see Ward 1969), and partly under haemocoelic pressure, where no extensors are present.

The succession of superior hinges allowed the limb to be flexed, bringing food into the oral cavity where it was masticated by the coxal gnathobases. The distal pivot was operated by superior levator and depressor muscles. The evidence for these muscles is good, as long tendons are preserved. Long tendons suggest long muscles extending across two joints (Manton 1977, p. 196). The terminal podomere was probably nimble in its actions.

The movable spines were set in rings of arthrodial membrane. Some small muscles were probably present at the bases of the movable spines, but there is no evidence for any articulation points. The directions of movement of the spines were most likely to have been controlled by the directions of muscle contraction.

Many arthropods have specialised anterior limbs for prey capture, but multiple pairs of food-gathering limbs also with a locomotory function, as in *Baltoeurypterus*, *Limulus*, trilobites (*Olenoides*, Whittington 1975) and *Sidneyia* (Bruton 1981), may be considered generalised. Some authors have therefore concluded that "*Eurypterus* . . . was on the whole a sluggish animal. As it is not provided with strong organs of offense, it probably lived on worms or carrion." (Clarke & Ruedemann 1912, p. 79) and "*Eurypterus* may have been rather sluggish, content perhaps with grovelling." (Barbour

1914). *Baltoeurypterus* was well adapted for swimming (section 5) and was therefore not bound to a benthonic existence. It may have grubbed in the sediment for food, but was also able to catch swimming animals, and may itself have fallen prey to larger eurypterids.

4. Walking

With the realisation that the work of Manton (1952 to 1977) in elucidating Recent arthropod mechanisms could be used to reconstruct fossil arthropod walking patterns, a number of studies in this field have appeared recently. Hanken and Størmer (1975) and Briggs *et al.* (1979) used data from trace fossils to produce gait patterns, whilst Hughes (1975), Whittington (1975, 1980), Waterston (1979) and Bruton (1981) produced gaits from body fossil reconstructions. Hanken and Størmer (1975) demonstrated that a trail from the Silurian of Ringerike, Norway had probably been produced by the eurypterid *Mixopterus kiaeri* walking slowly. Waterston (1979) gave a most detailed and elegant account of the posture, stepping and gait pattern of *Parastylonurus ornatus* deduced from the morphology. A comparison of the walking modes of these two eurypterids with that of *Baltoeurypterus* is given in section 4.4.

4.1. Walking limb design

The mechanics of locomotory limbs are subject to certain physical constraints.

$$F_1L_1 = F_2L_2$$

where F_1 is the force applied to the system (by muscles) and F_2 is the force produced by the system, L_1 is the length between the articulation and the muscle origin and L_2 is the length of the leg being moved, measured from the articulation to the line of action of force F_2. Hence, for the force, F_2, to be large, L_2 or the leg length, must be short, and conversely, for a large angle of swing of the leg, less force is produced by the system. Furthermore, as Manton (1977, p. 204) pointed out, the power of a muscle is equal to the force it puts out multiplied by the distance through which the leg moves divided by the time taken, power = force × distance/time. Therefore for the force to be large, the distance must be small (as shown above) and the time long. For fast movements, the distance must be long and the force small.

So limbs designed for a strong, pushing action are short, their muscles are short but thick, and the system works slowly. The podomeres in such a limb are strongly constructed and the joints must also be strong (preferably pivots). Limbs designed for speedy movement are long, with a wide angle of swing and with long, thin, tendinous muscles, commonly traversing more than one joint. The podomeres of such a limb should be lightly constructed and the joints are normally weak hinges providing much flexure. Intermediate types of leg are rare. Animals which walk slowly but do not need pushing strength (e.g. many arachnids) tend to have longish legs for mechanical efficiency but use gait patterns (see later) which provide good stability. If faster running is required in arachnids, a quickening of pace with a large energy input, whilst retaining the fairly "slow" gait pattern, normally suffices (Manton 1952, table 1).

Muscles producing the main limb movement, whether strong pushing or fast propulsion, have their origins as far as possible from the articulation axis at a joint to produce maximum leverage. Extensor muscles, if present at a hinge joint, commonly work at poor mechanical advantage in order to allow the flexor muscles the greatest amount of leverage (Fig. 12).

4.2. Mechanics of limb V

Limb V of *Baltoeurypterus* appears to be the limb best adapted for walking, although it also aided in swimming (section 5), and limbs IV and VI, at least, were also used in walking (see later). Hardly any coxal promotor–remotor swing was possible (section 3) and the main swing of the ramus took place at the proximal pivot joints, as in the arachnids. Limbs V and VI of *Baltoeurypterus* bear a double trochanter arrangement at the base of the ramus (Fig. 21). This provided a wide angle of swing to the ramus during promotor–remotor movements. The coxa–podomere 2 joint of limb V was probably operated by protractor/levator and retractor/depressor sets of muscles. The following two joints were probably operated by protractor/depressor and retractor/levator sets of muscles. All these muscles, whether originating on podomere 2, 3 or 4, would have inserted on the coxa, and some may also have been extrinsic. There may also have been some short muscles extending across one joint only, to provide some stability to this complex mechanical arrangement.

The main locomotory muscles would have been the coxa–podomere 2 protractor/levator and retractor/depressor sets and the coxa–podomere 4 protractor/depressor and retractor/levator sets. The shape of podomere 2, with an expanded antero-superior surface and emarginated proximal infero-posterior edge with abundant arthrodial membrane, suggests that the limb ramus could flex backwards and downwards more than in any other direction. This would have provided the main propulsive thrust during walking, and also helped in a launch off the bottom for swimming. The oblique orientation of the articulation axis at the coxa–podomere 2 joint in limb V is more advantageous in walking than the nearer horizontal axes of limb VI used mainly for swimming.

The superior hinges of limb V allowed the limb to flex during the propulsive remotor phase, a necessity if the limb tip is to remain on the same spot and the body is to travel in a straight line during walking. The flexor muscles (Fig. 12) would have operated during the first part of the remotor swing, pulling the body forward until the limb base was as far forward as the limb tip, at which point progressive extension occurred up to the end of the remotor phase. During this extension the more distal flexors would have been more active in keeping the ramus rigid, most extension occurring at the podomere 4–podomere 5 joint, propulsion being given by contraction of the coxa–podomere 4 retractor/depressor muscles which would also have aided both the extension of the hinges and in keeping the limb tip on the substrate. The antero-superior position of the hinge between podomeres 4 and 5 would have assisted in the leg extension during the remotor propulsive stroke as in lithobiomorph Chilopoda (Manton 1965, p. 307). Extension plays a large part in the remotor propulsion of the scorpion (Manton 1958) in which two hinges with much flexure are present.

At the end of the remotor phase, the retractor/levators would have come into operation, lifting the limb off the substrate. Promotion was effected at first by contraction of the protractor/levators and later the protractor/depressors could cause the limb tip to make contact with the substrate again. During this latter part of the promotor stroke, the hinge extensors would have been brought into play to place the limb tip as far forward as possible.
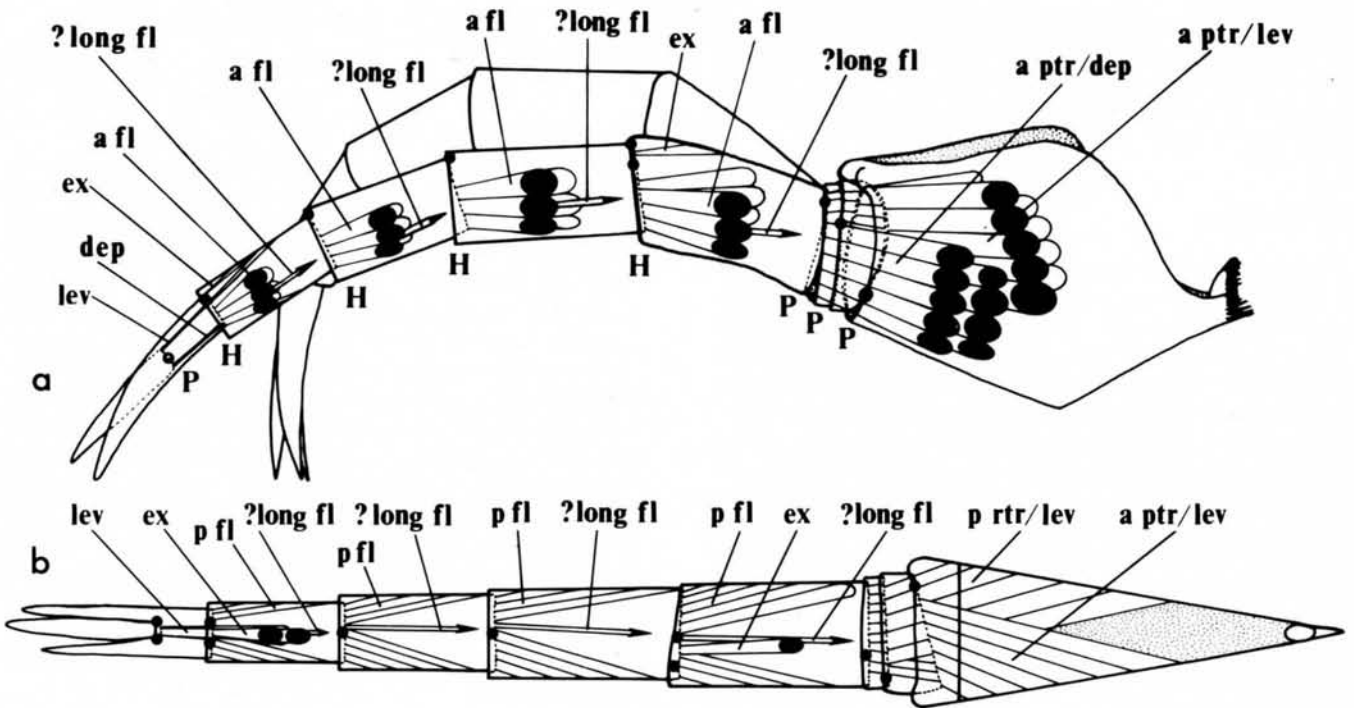
Figure 12 *Baltoeurypterus tetragonophthalmus*. Reconstructions of right limb V.
    a. Anterior aspect, two positions of ramus shown, the more outstretched is drawn as if transparent to reveal suggested musculature.
    b. Superior aspect, shown as if transparent to reveal suggested musculature.

4.3. Stepping

Stepping concerns the action of the whole limb during walking and has been analysed for arthropods in general by Manton (1952 to 1977), and in relation to nervous coordination by many authors (see Hoyle 1976 for review). A pertinent precis of Manton's conclusions concerning stepping was given by Waterston (1979, p. 302).

The positions of the main promotor–remotor axis of swing of the limb has a marked effect on the suitability of the limb for strong, slow movements or fast movements. Diplopods utilise a horizontal swing axis at the coxa–body joint (Manton 1977, fig. 5.3(a)) and the coxa–body joint of *Limulus* (Fig. 9), although oblique, is also set close to the main axis of the body. In both cases a strong pushing action is produced. In contrast, a limb best suited for faster walking usually arises from a lateral position on the body, away from the main body axis and has a near vertical axis of swing (Manton 1977, p. 209 and fig. 5.3(b)). Limbs V and VI of *Baltoeurypterus* have near vertical swing axes, set close to the lateral edge of the body, which provide large angles of swing for long strides in walking and wide rowing sweeps (section 5).

The relative length of successive limbs is important for a variety of reasons. In arthropods with few pairs of walking limbs (e.g. the Chelicerata), a difference in length between them is advantageous as it prevents interference of successive limbs during walking (Manton 1952), as does a radial coxal arrangement (Manton 1977, p. 453). However since all walking limbs normally execute similar strides (stride = pace = length between two successive footfalls of the same limb), if there is a great difference in limb length either the longer limbs must take shorter strides or there is a difference in the relative durations of promotor and remotor strokes between the limbs (see 4.4). The latter occurs in the scorpion gait (Manton 1952).

A suggestion of the fields of movement of the main walking limbs of *Baltoeurypterus* is given in Figure 13a (cf.

Manton 1952, text-figs 2 & 3; Waterston 1979, text-fig. 15). The thicker lines on this diagram denote the span of the limb, that is the distance travelled by the limb tip relative to the body during the propulsive remotor swing. The stride or pace would include the span and the extra distance which the body moves before the next footfall of the same limb (see Gray 1968, p. 304). The fields of movement shown are able to overlap because the limbs are different lengths.
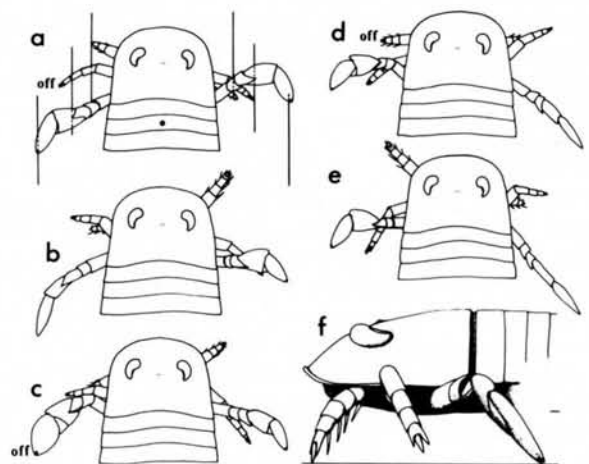
Figure 13 *Baltoeurypterus tetragonophthalmus*.
    a–e. Diagrammatic reconstruction of the anterior part of the body, superior aspect, walking with the gait shown in Figure 15d (gait pattern 2·0 : 8·0, phase difference (opposite) 0·5, phase difference (successive) 0·4); sequence consists of points ⅕ of a cycle apart (labelled with arrowheads on Fig. 15d); a has suggested centre of gravity (black spot), and span of each limb (straight black lines).
    f. Reconstruction sketch of the anterior part, left side of the animal as it might have appeared walking with the gait shown in Figure 15d at point a.

An important consideration is the number of limbs employed during walking. Theoretically, *Baltoeurypterus* has five pairs of limbs capable of walking. If all these limbs (II to VI) were used at the same time, the problems of differential limb length outlined above would ensue. Limb VI, for example, is five times the length of limb II. It is most likely therefore, that as in most arachnids, the anterior limbs were either not used in walking or contributed to ambulation only with an irregular step.

Further clues to the probable number of limbs employed in walking are gained from consideration of the stability of the animal. The factors governing stability during walking have been summarised by Gray (1968) for tetrapod vertebrates and Hughes and Mill (1974) for insects. In both cases, minimal stability is achieved only when the animal is in contact with the substrate at three points (usually three limb tips) and the centre of gravity of the animal lies within the triangle formed by these three *points d'appui* when viewed from above. Thus a minimum of four limbs is required for walking (unless a plantigrade stance is used) if three limbs are always to be in contact with the ground. As limbs are moved, so the weight of the animal shifts to one side or the other. This latter phenomenon enables tetrapod vertebrates and some Hexapoda (e.g. *Campodea*, Manton 1972) to be momentarily supported by only two limbs, whilst the centre of gravity shifts towards the next limb to be placed on the ground, during running. Arthropods which habitually walk on four legs are few, but include some Protura (Manton 1972) and Lepidoptera (e.g. Nymphalidae). Quadrupedal walking by these insects is slow.

Figure 13a shows a likely mean position of the centre of gravity of *Baltoeurypterus*. Owing to the greater bulk of the prosoma, including appendages, in relation to the narrow metasoma, the centre of gravity will have lain towards the anterior of the mesosoma. It can be seen that in order to maintain this point within a triangle formed by the minimum of three limb tips on the substrate for most of the time, limb VI must have been used in walking. It is possible that the opisthosoma or telson was in contact with the substrate at times of instability. Limb IV was most probably also used, as quadrupedal walking in arthropods is specialised, slow and less stable than hexapody. More anterior limbs may have contributed to ambulation but, being short, their stepping would have been fairly irregular and out of phase with the other limbs. The main limbs used in walking would therefore have been limbs IV, V and VI, and these are the ones considered in the analysis of the probable gait. The trail of *Mixopterus* (Hanken & Størmer 1975) shows hexapodous stepping by these limbs also. A digitigrade stance is suggested, there is no evidence for a plantigrade foot which is of greater benefit to terrestrial arthropods (Manton 1952, p. 102).

4.4. Gait pattern

When a walking limb moves, it does so forwards (promotor swing) and backwards (remotor swing). The time taken for one complete cycle of promotor–remotor movements is called the pace duration, and the distance travelled by the body during one cycle (conveniently measured by the distance between two successive footfalls) is termed the pace or stride. The relative durations of promotor (limb off the substrate) and remotor (limb on the substrate) strokes gives the gait pattern. This is usually given as a proportion out of ten, hence a limb off the substrate for $\frac{1}{4}$ of the pace duration, and on for $\frac{3}{4}$, will have a gait pattern of 2·5:7·5, the promotor duration being given first. Gait diagrams express the gait pattern graphically (Fig. 15) and gait "stills" (Fig.

13) attempt to portray the animal executing the gait (Manton 1977, fig. 7.1). The proportion of a pace by which an opposite or successive limb is out of phase from the limb opposite or in front is termed the phase difference. The phase differences of opposite and successive limbs may differ.

The speed of progression (Manton 1977, p. 298 *et seq.*) is governed by the length and angle of swing of the limb, the pace duration and the gait pattern. It is not possible to determine the pace duration of body fossils but when enough is known about the other factors this can be estimated. It has already been stated that a long limb and large angle of swing are advantageous for speedy locomotion. During fast walking the limb can only be in contact with the substrate for short periods of time, and "fast" gaits of 8·0:2·0 are employed by some runners. Slow walking requires stability and hence many limbs on the substrate at the same time, thus "slow gaits" are those around 2·0:8·0. This does not mean that an animal cannot run fast in a "slow" gait, a decrease in the pace duration would achieve this. Manton (1952, table 2) provided a list of gait patterns recorded for selected arthropods.

The phase difference between successive and opposite limbs (Manton, 1977, p. 308 *et seq.*) has no effect on the speed of walking, but affects the stability. For example, for pushing, swimming and jumping it is advantageous for paired limbs to act simultaneously, but would not be so for an insect walking when there would be a moment at which the body was supported by a single pair of mesothoracic legs. Stability is gained by ensuring that at least three limbs (not on the same side) are always in contact with the substrate, and this is favoured by the choice of a gait with a time interval k (Fig. 15, and Manton 1977, p. 311) during which the remotor strokes of the two successive limbs overlap. k can be calculated by subtracting the phase difference of successive limbs from the duration of the promotor stroke, hence an increase in the latter or a decrease in the former will increase k.

It is possible to construct a three-dimensional graph or matrix (Fig. 14a) with the two phase differences as the x and y axes, and the gait pattern on the z axis, and to outline regions in which certain requirements are met. Figure 14b is a horizontal slice from such a graph (Fig. 14a), and is the two-dimensional matrix of the variations in the number of limbs (out of six) on the substrate (enclosed areas) for all values of phase difference at a gait pattern of 2·0:8·0. The matrix is symmetrical about the phase differences of 0·5, but the enclosed areas would change in shape if slices were to be taken at other z values. It is hoped that this technique, introduced here for the first time, may be of use in choosing possible gaits for other extinct arthropods.

Baltoeurypterus could not have been an expert walker using precisely co-ordinated stepping and rigid adherence to a specialised series of gaits as shown by Uniramia (Manton 1973b), as it does not have a precise number of specialised walking limbs. *Limulus* (Manton 1964) walks slowly and burrows with a gait of 2·0:8·0, increasing to 5·0:5·0 when walking fast, but opposite limbs are in phase as befits an animal requiring strong pushing. A comparison with the Arachnida seems to be the most profitable. Arachnids (Manton 1973b) use slow gait patterns, irregular stepping and normally increase speed by decreasing the pace duration. The slow gait patterns provide long time intervals k and hence confer stability. Opposite limbs have a phase difference of about 0·5 and the phase difference of successive limbs lies around this value also.

A typical slow gait for *Baltoeurypterus* might well have

been 2·0:8·0. It will be seen from Figure 14b that high or low phase differences produce unstable gaits in which less than three limbs are on the substrate at one time (margins and corners of the diagram). High or low successive phase differences (areas of 6543 on left and right of diagram) are also unstable because they produce moments when three limbs on the same side are in contact with the substrate but no opposite limbs. Even if eight limbs were used, these gaits would still be fairly unstable. Phase differences of 0·5 opposite, 0·5 successive produce a suitable gait, but any slight irregularity would change the pattern from 63 to 6543. Gaits around the centre of the matrix appear to be the most suitable, bearing in mind that the lower the successive phase difference the greater k will be. Some gaits within the 654 area (most of the diagram) are a little unstable, for example any with a successive phase difference of 0·5 will produce moments when three limbs are on the substrate on one side and only one on the other, this places some strain on the lone limb.

Figure 15 shows gait diagrams of four possible slow gaits for *Baltoeurypterus*. The gaits differ principally in the se-

quence in which the limbs are placed on, or removed from, the substrate, they all have a long time interval k, and by having an opposite phase difference close to 0·5, one or other of the most posterior limbs is more than $\frac{1}{3}$ of the way through the remotor stroke, and therefore behind the centre of gravity (Fig. 13) at any moment. Figure 13 portrays a sequence of one cycle of limb movements of *Baltoeurypterus* walking with the gait shown in Figure 15d.

4.5. Comparison with *Mixopterus* and stylonuroids

Hanken and Størmer (1975) described a trail from the upper Silurian of Ringerike, Norway, which they showed was probably made by the eurypterid *Mixopterus kiaeri*. Their analysis was concerned mainly with the shape of the limbs which produced the observed tracks and, in particular, they showed that the outermost "A-tracks" were probably produced by a flattened swimming paddle. The size of the trail pointed to *Mixopterus* as the producer.

Hanken and Størmer (1975, fig. 8) gave a sequence of sketches to show *Mixopterus* performing a slow gait of 1·66:8·33, 0·833 phase differences (successive and opposite). This gait enables five limbs to be on the substrate at all times. However, like the gait shown in Figure 15a (2·0:8·0, 0·5 phase differences), any slight irregularity in stepping would produce a gait in which four or six limbs would be propulsive at times. Other possible drawbacks in the gait suggested for *Mixopterus* are: that there is no time interval k in which two successive limbs are in contact with the substrate at the same time, and that at certain points in the cycle (e.g. Hanken & Størmer 1975, fig. 8B) there are no propulsive limbs behind the centre of gravity (presumably at the third mesosomal tergite, although the enlarged anterior limbs may affect this).

Baltoeurypterus executing a gait of 2·0:8·0, 0·5 phase difference (opposite), 0·4 phase difference (successive) would produce a trail which resembles that of *Mixopterus* in arrangement of tracks, but the stride would be a little longer (perhaps because *Mixopterus* is supposed to have made the trail whilst only partially submerged and strode against greater resistance). A median groove might be produced by dragging the telson in slow crawling, but probably not by dangling genitalia (cf. Hanken & Størmer 1975, p. 264, and cf. their figs 9B & C which show no dragging of genital appendage).
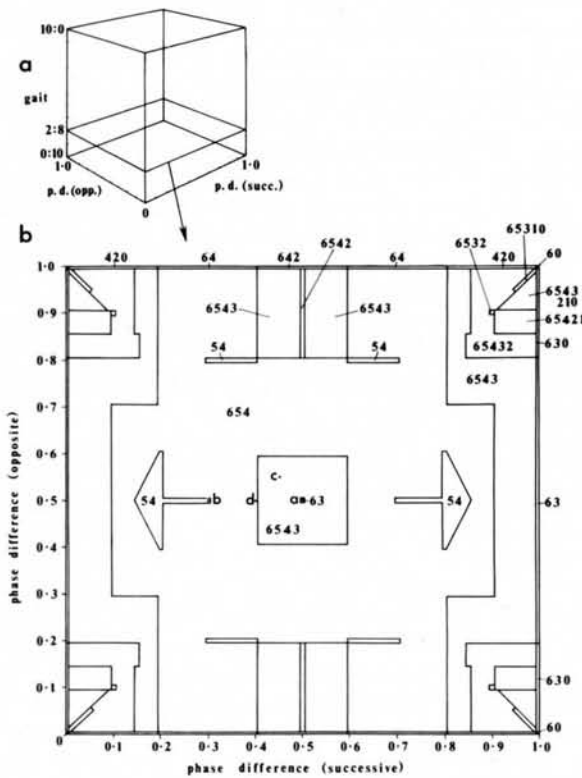
Figure 14 a. Three-dimensional graph of phase difference (opposite) (x axis), phase difference (successive) (y axis) and gait pattern (z axis), showing position of two-dimensional slice at gait 2·0:8·0 shown in b.
b. Matrix of the number of propulsive limbs during hexapodous walking in the gait pattern 2·0:8·0 as related to the phase differences of opposite and successive limbs. The numbers (654, 63, etc.) refer to the number of propulsive limbs at all points in the cycle of that gait; e.g. in Figure 15a, the number of propulsive limbs covering all points in the cycle would be referred to as 63, for Figure 15b, 54. a, b, c and d are the gaits shown in Figure 15. Thus, for minimum stability, no gait with a number less than 3 is possible, nor those (such as 6543 on left and right sides of the matrix) in which at one point in the cycle 3 limbs of one side only are in contact with the ground. Also, gaits above 0·8 phase difference (successive) have no time interval k, between successive footfalls. Note that the matrix is symmetrical, but that the shapes of the enclosed areas would be different at different gait patterns (z values). The matrix for 8·0:2·0 gait pattern would look the same but have different numbers in the enclosed areas.
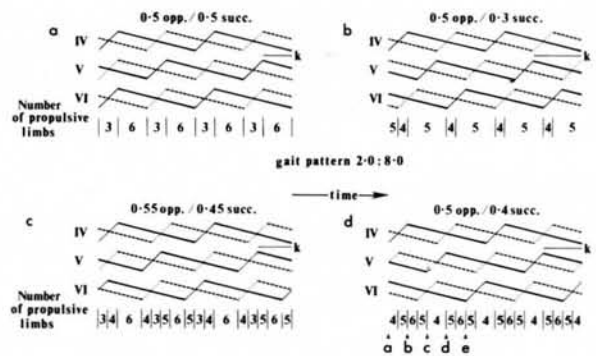
Figure 15 Gait diagrams in the style of Manton (e.g. 1977, fig. 7.3), for four possible *Baltoeurypterus* gaits. The thin lines denote right limbs in the promotor (recovery) phase and the thick lines the same limbs in the remotor (propulsive) phase; dotted lines are for left limbs in the promotor phase and dashed lines for the remotor phase. Two cycles are shown in each diagram. The time interval k is shown only for the footfalls of right limbs IV and V of the second cycle. The position of each gait in Figure 14b is marked. Gait d is illustrated in Figure 13.

Waterston (1979) demonstrated the probable mode of stepping and gait pattern performed by *Parastylonurus ornatus*, deduced from morphology. Waterston's conclusions compare well with those for *Baltoeurypterus* herein, but as it was not possible to reconstruct joint morphology in *Parastylonurus*, there are some differences, discussed below. The promotor–remotor movement of the walking limbs of *Parastylonurus* (Waterston 1979, p. 304) most probably occurred at the trochanteral joints, as in *Baltoeurypterus*. The lack of a coxal promotor–remotor swing is more likely to be due to the nature of the coxa–body connection (section 3) than to the coxae having been horizontal in life (section 1.3). Comparison with *Baltoeurypterus* suggests the three trochanteral joints would be pivots in *Parastylonurus*, and the following four joints on the ramus would be superior hinges providing flexion during contraction of the limb halfway through the remotor swing. Text-figure 14B in Waterston (1979) shows walking legs of *Parastylonurus* as they might have appeared when extended, and contracted during the remotor stroke. The joint between podomeres 4 and 5 is shown undergoing extension whilst the other hinges are flexing during contraction. In all extant chelicerates the upward bend of the leg during contraction occurs at the trochanteral pivots, and this was probably also the case in *Baltoeurypterus* and stylonuroids. Also, flexure of the limb in a plane other than near vertical, as suggested for stylonuroids by Waterston (1979, text-fig. 15), is an adaptation to particular habits, such as crevice-dwelling in Amblypygi and burrowing in scorpions. A suitable range of pivot and hinge axes in stylonuroid legs would probably, as in *Baltoeurypterus*, provide sufficient flexure of the limbs in a vertical plane to give the fields of movement shown in Waterston (1979, text-fig. 15, left).

The gait pattern suggested for *Parastylonurus* by Waterston (1979, p. 307) is $3 \cdot 33 : 6 \cdot 66$, $0 \cdot 333$ phase difference (opposite), $0 \cdot 366$ phase difference (successive). This gait is fairly "slow", but faster than that suggested herein for *Baltoeurypterus*. The $0 \cdot 366$ phase difference of successive legs provides only a small time interval k between placing one limb on the substrate and removing the next anterior. Thus fairly precise stepping is required to prevent instability.

In conclusion, the suggested walking patterns of eurypterids compare most favourably with those of arachnids (Manton 1973b), with a range of slow gait patterns, stepping probably a little irregular, and changes in speed due to changes in pace duration. The gait of *Limulus* is specialised and not directly comparable to eurypterid gaits.

5. Swimming

Ever since the first discovery of a fossil eurypterid (Mitchill 1818; DeKay 1825), the swimming function of limb VI was recognised. The similarity of this limb in *Baltoeurypterus*, and other eurypterids, to the fifth pereiopod of portunid crabs was noted by Holm (1898, p. 28) and Clarke and Ruedemann (1912, p. 51). The fifth pereiopod in swimming crabs is the main natatory organ, but Laurie (1893) noted that the crabs also use this limb for digging and therefore suggested a similar function for the eurypterid paddle, a view later supported by Størmer (1934). Holm (1898, p. 26–28) was aware of the general directions of movement at the joints of limb VI of *Baltoeurypterus* but gave no detailed account of the swimming action. Størmer (1934, pp. 35–37, 61–66, 1936, pp. 12–14) described the possible movements of some distal podomeres of the eurypterid paddle, and concluded (with other considerations) that eurypterids swam upside-down, and that the paddles were held oblique to the

direction of motion of the body during rowing (in the horizontal plane), or provided lift if propulsion was effected by rapid closure of the mesosomal gill flaps. *Mixopterus* was supposed to have swum mostly by use of the paddles moving up and down, and with the body not inverted (Hanken & Størmer 1975).

The body of *Baltoeurypterus* is elongate and tapers caudally (see Holm 1898, pl. 1) and is thus fairly streamlined. The prosoma and mesosoma are somewhat flattened dorsoventrally. The telson is styliform, and despite small epimera on the pretelson, it is unlikely that the caudal region was capable of providing thrust. Therefore swimming must have been effected by limbs VI primarily. It is useful to consider the possible modes of swimming available to an animal with paired appendages. An excellent review of these swimming methods was provided by Robinson (1975).

5.1. Swimming methods

For an animal with paired limbs, swimming underwater, the choice is between rowing and "subaqueous flying" using a hydrofoil. Rowing involves the movement of an oar anteroposteriorly parallel to the direction of motion of the body. During the propulsive backward stroke, the oarblade (a flat plate with high drag) acts as a lever to push the more streamlined body forwards. As the oarblade actually moves in an arc, except at the midpoint of the propulsive stroke, some force is expended sideways, and the amount increases anteriorly and posteriorly. Hence a small arc, or angle of swing, is efficient. Furthermore, as the oar acts as a lever, it is desirable to increase both the velocity ratio and the force (and mechanical advantage) of the system (Robinson 1975, p. 296). The best compromise solution for an arthropod is to increase the length of the arm of the oar whilst also increasing the amount of propulsive musculature. During the recovery phase, the oarblade must be collapsed, folded or rotated so that it presents much less resistance to the water.

Rowing is a means of aquatic propulsion most commonly used by small animals with low body drag. The larger water beetles such as *Dytiscus* (Hughes 1958), *Hydrophilus* (Hughes 1958) and *Acilius* (Nachtigall 1960, 1974) and the aquatic bugs, e.g. *Corixa* (Schenke 1963, 1965a, b, c), *Notonecta* (Schenke 1965d) and *Lethocerus* (Lauck 1959), use flattened podomeres with collapsible hairs as oar blades. The whirligig beetle, *Gyrinus* (Nachtigall 1962), has greatly flattened podomeres and a fringe of collapsible blades, whilst in portunid crabs (Kühl 1933; Lochhead 1961; Hartnoll 1971; Spirito 1972) the propodus and dactyl of the swimming leg are flattened and bear only fringes of short hairs (Fig. 32a). Rowing vertebrates are few but include otters (Tarasoff *et al.* 1972) and trionychid turtles (Zug 1971).

It is efficient for larger animals, such as penguins (Clark & Bemis 1979), sea turtles (Walker 1971) and plesiosaurs (Robinson 1975), and sea lions (English 1976) and the humpback whale *Megaptera* (Edel & Winn 1978) at times, to swim by means of hydrofoils. In this form of locomotion, the appendage is moved up and down at right angles to the direction of body motion. The thrust is produced as the lift component of the force produced by the hydrofoil, the angle of attack of which is varied during both up and down strokes in order to provide propulsion throughout the whole cycle (Robinson 1975, figs. 5, 6). It is advantageous for the flipper to be flexible in order to present a hydrofoil section in both the up and down strokes and the greater part of the limb should have a hydrofoil section. A high aspect ratio (long flipper) and wide angle of sweep are both beneficial but in practice are compromised to lessen drag and prevent overloading.

5.2. Functional morphology of *Baltoeurypterus* limb VI

Limbs VI of *Baltoeurypterus* are situated close to the centre of buoyancy (assumed centre of gravity) of the animal as in the swimming insects mentioned above. The coxae are greatly enlarged to house the powerful musculature required for swimming. The great enlargement of the coxae of Dytiscidae was facilitated by their immobility (Evans 1977); the lack of a promotor–remotor swing of *Baltoeurypterus* coxae VI is probably correlated with their enlargement also.

The general shape of the ramus of limb VI is much more akin to that of an oar than a flipper. Podomere 4 is long and not flattened, thus acting as the oar shaft, whilst the oar blade is provided by podomeres 7 and 8.

The promotor–remotor swing was effected at the trochanteral pivots, as in limb V. However, the axes of these pivots are arranged (Fig. 21) so as to provide mainly anteroposterior motion and little levation and depression. The musculature in this region, although greatly enlarged, would have been similar to that suggested for limb V.

The distal joint of podomere VI4 is a bicondylar hinge, as in limb V, and hence worked by flexor and extensor muscles. Flexion may have aided in the remotor stroke, but was most useful in the promotor stroke when the swimming blade was trailing to lessen drag (see 5.3). At the end of the promotor stroke, the extensor muscle would have aided in straightening the limb prior to the next propulsive stroke.

The proximal joint of podomere VI6 is a pivot with a strong postero-superior articulation. This pivot joint is arranged so that, during swimming, not only translation of the swimming blade occurs, but also some rotation. This is accomplished by the joint plane being oblique to the long axis of the limb (Fig. 16). The translation of the swimming blade in *Baltoeurypterus* is advantageous in that it enables the blade to be folded back during promotion, thus presenting less resistance to the water (Fig. 17). The distal joint of podomere 6 provides the further rotation needed in order to turn the blade from vertical to horizontal on the limb axis.

The pivot joint between podomeres 5 and 6 would have been operated by levator and depressor muscles (Fig. 16). There may also have been a small levator postero-superiorly to aid in holding podomere 6 steady during the remotor stroke. The podomere 6–podomere 7 joint would have been operated by a pair of rotator muscles and small muscles at
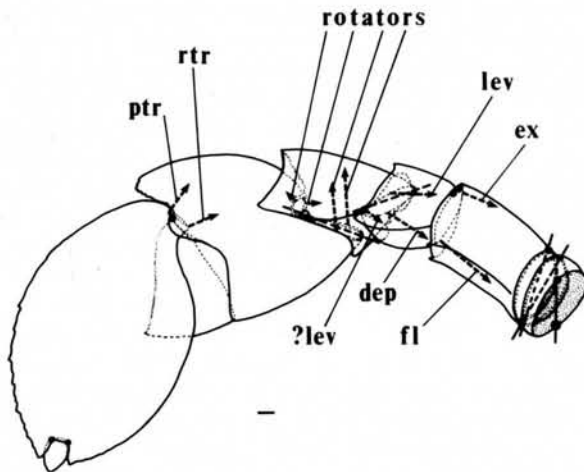
the distal end of the joint would aid in these movements. The joint between podomeres 7 and 8 of limb VI was provided with protractor and retractor muscles to fold podomere 8 back during promotion to decrease water resistance, and to extend podomere 8 during the power stroke. The function of lobe 7a was to increase the surface area of the swimming blade to increase the water resistance for propulsion.

The convergence between limb VI of *Baltoeurypterus* and the swimming limbs of extant arthropods such as portunid crabs (Warner 1977, p. 72) is striking. The oblique pivot between podomeres 5 and 6 of limb VI of *Baltoeurypterus* is comparable with the merus–carpus joint of *Macropipus* (Figs 32a; 33a, b). The rotatory joint between podomeres VI6 and VI7 of *Baltoeurypterus* parallels the carpus–propodus joint of *Macropipus* (Figs 33a, c) and *Portunus* (Kühl 1933), and the femur–tibia joint of *Gyrinus* (Nachtigall 1962, 1974). The distal platform of podomere VI6 of *Baltoeurypterus* is paralleled by a similar feature on the carpus of *Macropipus* fifth pereiopod (Figs 33b, c) and the expanded lobe on the propodus of this limb (Fig. 33a) is comparable to lobe 7a of *Baltoeurypterus* limb VI (Fig. 16).

5.3. Rowing and manoeuvrability

Figure 18 illustrates the swimming sequence in *Baltoeurypterus* diagrammatically. If limbs VI of *Baltoeurypterus* were used in the same phase, better thrust would be produced during the propulsive stroke, but there would then be deceleration during recovery. An advantage in having swimming limbs moving in phase is that the tendency to yaw is reduced. The water bugs *Corixa* and *Notonecta* move their limbs in phase during swimming, and many arthropods which are not well adapted to swimming will move their legs in phase when in water, for example mantids (Miller 1972) and locusts (Kennedy 1945). Fast-swimming water beetles such as *Acilius* (Nachtigall 1960, 1974) and *Dytiscus* (Hughes 1958) move their metapodia approximately in phase, whereas those aquatic Coleoptera which require more manoeuvrability use their limbs in an alternate fashion, for example *Gyrinus* (Nachtigall 1962, 1974) and *Hydrophilus* (Hughes 1958). In the case of *Hydrophilus*, however, it could be, as Hughes (1958) pointed out, that as this animal is herbivorous and does not require fast, efficient swimming, it has not changed to the in-phase swimming adaptation from its ancestral walking condition with legs moving in opposite phase. As limb V in *Baltoeurypterus* is not adapted for

Figure 16 *Baltoeurypterus tetragonophthalmus*. Reconstruction of ramus of left limb VI, posterior aspect, shown as if transparent to illustrate possible directions (arrows) of muscle action; articulations (black or open circles) and articulation axes shown.
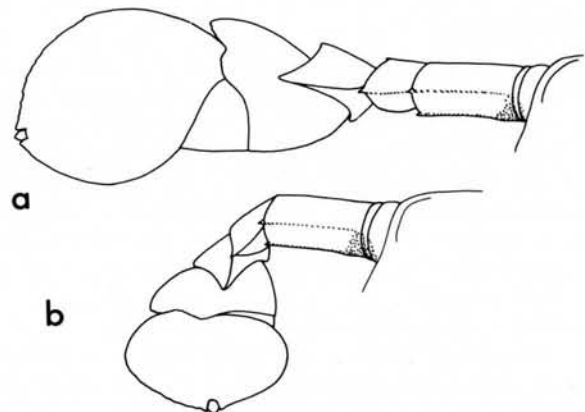
Figure 17 *Baltoeurypterus tetragonophthalmus*. Reconstructions of left limb VI, supero-posterior aspect.
   a. Outstretched halfway through propulsive stroke.
   b. Collapsed halfway through recovery stroke.

swimming, it could not have been used efficiently to counter yawing if limbs VI rowed alternately. Therefore it seems likely that limbs VI moved in phase and limbs V were used for steering.

The elongate body of *Baltoeurypterus* was not very manoeuvrable. (*Gyrinus*, which is a highly manoeuvrable swimmer, has an almost spherical body.) Pitching and rolling in *Baltoeurypterus* were prevented by the dorso-ventrally flattened body, the outstretched limbs and tergal epimera. If the swimming limbs were moved in phase, then uncontrolled yawing was prevented, but controlled yawing, i.e. steering, could have been achieved by the use of limb V, in a similar manner to the mesopodia of *Hydrophilus* (Hughes 1958) and *Corixa* (Schenke 1965b). Braking may have occurred by promotion of limb VI whilst still extended, and/or with an upward tilt of the prosoma which, together with the epimera, would have increased the frontal area presented to the water and thus effectively "stalled" the body, as in *Dytiscus* and *Acilius* (Nachtigall 1974).

5.4. Conclusions

Although the similarities between the swimming limbs of *Baltoeurypterus* and those of some Recent Crustacea and Hexapoda are remarkable, they are of no phylogenetic significance. The Arachnida are principally a terrestrial group whose aquatic members are secondarily so and poor swimmers, e.g. the water spider, *Argyroneta* (Bristowe 1958) and the water mites such as *Limnochares* (Smith & Barr 1977; Barr & Smith 1979). The Merostomata, on the other hand, are primarily aquatic, although some may have been able to crawl onto land for short periods (Størmer 1976; Fisher 1979). *Limulus* swims in a peculiar manner (see Milne & Milne 1967; Fisher 1975 for descriptions),
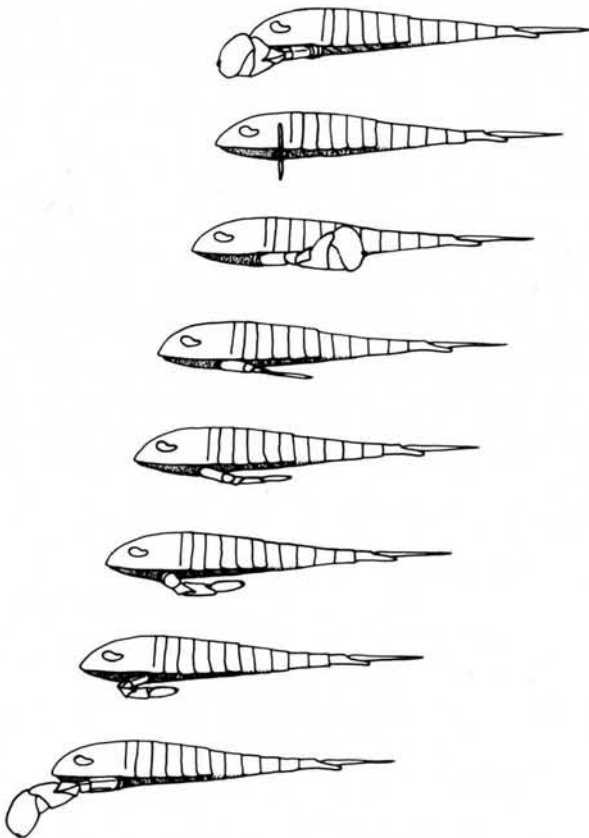
Figure 18 *Baltoeurypterus tetragonophthalmus.* Diagrammatic reconstruction of animal swimming to the left, left lateral aspect, left limb VI only shown through 1 cycle of swimming movements.

upside-down and using not only the prosomal limbs but also a metachronal beating of the gill covers for propulsion. *Diploaspis* was reconstructed (Størmer 1972) with a swimming paddle (based on one poorly preserved specimen). The swimming of *Baltoeurypterus* was entirely different from that of the Xiphosura, and no meaningful comparison can be made.

Most eurypterids have a natatory limb VI, although pterygotoids may also have used an expanded telson for propulsion. Størmer (1974) has discussed the origins of eurypterid swimming limbs and has distinguished a number of different types. The *Baltoeurypterus* limb VI is of the "Eurypterus type" (Størmer 1974), and other types, particularly the flipper-like swimming limbs of pterygotoid and hughmillerioid eurypterids, are probably not functionally comparable with it.

6. Podomere terminology

6.1. Serial homology

Størmer (1974, p. 362) showed that the primitive eurypterid limb was probably one which bore a pair of spines inferodistally on each podomere following the trochanter(s), apart from the terminal podomere which consisted of a single spine. He showed that all other types of eurypterid limb (excluding chelicerae) could be derived from this "spiniferous leg" (Størmer 1974, text-figs 1–10). The spiniferous leg is typified by limbs II to V of the Hughmilleriidae, and the anterior limbs (II to IV) of nearly all other eurypterids are also of this type. Further evolution of this limb involved the loss of these spines to produce a limb more suitable for walking, on somite V, and loss of all but one spine (lobe 7a), as well as other modifications, to form a swimming appendage (VI). It is probable that the swimming limb passed through a stage resembling limb V, during its evolution. Evidence for this includes the presence of two trochanters, of similar design, in both limbs, and retention (with modifications) of carinae on limb VI, which originated on limb V to provide strength in long podomeres. Thus there is an approximate evolutionary progression in the limbs of eurypterids from anterior to posterior upon which a serial homology may be based (Fig. 20).

6.2. Comparative podomere terminology

Notwithstanding the continuing confusion concerning chelicerate podomere terminology (e.g. Savory 1964, p. 18; remarks in Couzijn 1976) and the lack of some useful characters (e.g. muscles) in fossil material, for comparative purposes it is worthwhile to consider eurypterid podomere terminology. Note that in extant chelicerates, podomere terminology rests on functional considerations (see below), and may not, therefore, represent true homology.

Hansen (1930, p. 331), using information from Clarke and Ruedemann (1912) and Versluys and Demoll (1923), suggested posterior stylonuroid limbs to be composed of: praecoxa, transcoxa 1, transcoxa 2, praefemur, femur, patella, tibia, tarsus and transtarsus. Evidence was thus provided for his "praecoxa theory" (Hansen 1925). Størmer (1934) used Hansen's (1930) scheme, but Størmer (1936) substituted the now more usual terms coxa and trochanters for praecoxa and transcoxae. Later, Størmer (1944, 1955) substituted pretarsus for transtarsus. In his study of *Gigantoscorpio*, Størmer (1963) followed the scheme suggested by Vachon (1945) for *Limulus*, and this has since been used for eurypterid limbs (Størmer 1974; Waterston 1979). It is:

coxa, trochanter(s), prefemur, femur, tibia, basitarsus, tarsus, posttarsus.

In any comparison of the appendages of chelicerates, it is usual to use the walking legs. The simplest arthropod walking leg is one with many, short, undifferentiated podomeres, separated by simple joints, each permitting only little flexure (Manton 1973b, p. 273). As differentiation of this leg proceeded for increased mechanical efficiency, distinct topological and functional "landmarks" appeared which can be used for comparative purposes. In arachnids and eurypterids (section 4; Waterston 1979) the trochanteral pivots provide for wide angles of movement of the ramus (thus corresponding to the hip joint of vertebrates — Petrunkevitch (1955)). Proximal to the trochanter(s) is the coxa, which is commonly immovable in arachnids, and distal lies a long femur which terminates in the characteristic "knee", a strong superior hinge. Podomeres connecting the knee to the "foot" (tarsus) are the patella (or genu) and tibia. In arachnids the tarsus is usually subdivided at least into two podomeres, metatarsus/tarsus, basitarsus/telotarsus or tarsus 1/tarsus 2, one of which is adesmatic, and this subdivision may be related to the change from digitigrade to plantigrade stance associated with terrestrial locomotion (Størmer 1963). The terminal podomere has been given a variety of names, but apotele is here preferred (Couzijn 1976, p. 462).

The *Baltoeurypterus* walking leg V (section 4) has a definite coxa, double trochanter, knee, and therefore femur before and patella after, followed by tibia, two tarsal podomeres and an apotele. Figures 20 and 21 depict the podomeres and joints, respectively, of *Baltoeurypterus* limbs II to VI. Using limb V, a comparison with the walking legs of other chelicerates (e.g. van der Hammen 1977, table 1) shows the *Baltoeurypterus* leg is not directly comparable to any other, but most closely resembles the leg of the Cryptognomae (van der Hammen 1979, fig. 30).

7. Conclusions concerning chelicerate evolution

Manton (1977) showed that knowledge of the jointing of the limbs of arthropods provides valuable clues to their evolutionary relationships. Limb jointing has been used by van der Hammen (1977) as a major criterion for distinguishing relationships within the Chelicerata. The podomere and joint diagrams of *Baltoeurypterus* presented herein (Figs 20, 21) (the first to be prepared for an extinct arthropod) are therefore an important aid to understanding chelicerate evolution. Manton (1973a, 1977, p. 37 *et seq.*) produced a scheme contrasting the methods of feeding of, on the one hand, most Crustacea, *Limulus* and trilobites, and on the other, Uniramia and Crustacea specialised for feeding on large food particles. In the former group, all of which are primarily aquatic arthropods, food is passed forwards along the ventral body surface by serially arranged coxal gnathobases and endites which also masticate the food. A large labrum directs food into the mouth, where it is ingested by a suctorial pharynx. The primarily terrestrial Uniramia, and arthropods which feed on large food particles, transport food directly upwards from the substrate towards the mouth, which is also situated supero-posterior to a large labrum (Manton 1977, fig. 2.1). The method of transporting food from below directly up to an oral cavity suits not only benthonic and terrestrial animals feeding off the substrate, but also predators which swim or fly and can pounce upon prey from above. *Baltoeurypterus* probably captured prey from above and transferred the food upwards into the oral

cavity where it was masticated by the gnathobases of the radially-arranged coxae. For ground-dwelling arachnids which hunt prey often as large as themselves, it is advantageous to have a forwardly directed feeding apparatus.

It may be possible to derive the feeding mechanisms of some modern arachnids from the eurypterid type, by restricting feeding to the anterior limbs and locomotion to the posterior. Correlated with the development of anterior feeding apparatuses would have been the liberation of coxae from the masticatory role, and their fixation on the body as a stable base for the operations of locomotory limbs. A promotor–remotor swing occurring at joints distal to the coxa is an important characteristic of arachnids and, as shown herein, of eurypterids also. The development of a post-coxal swing would have occurred as a result of the separation of the feeding and locomotory systems, for greater efficiency in their separate operations. The coxa retains both modes of action in the xiphosurans. The eurypterids occupy an intermediate position in which all coxae bear gnathobases for feeding and a post-coxal promotor–remotor swing has developed. The radial coxal arrangement which aids stability in arachnids (Manton 1977, p. 453) had already developed in eurypterids. As the feeding apparatus moved forwards, so at first the posterior coxae, then progressively more anterior ones, become fixed. Anteriorly directed food-gathering limbs are found in the scorpion-like eurypterids, which may be representative of this trend.

Such a scheme suggests a derivation for the enlarged ventrally expanded coxae found in a number of, but not all, arachnid groups, and the post-coxal promotor–remotor swing. It does not suggest that the eurypterids were ancestral to the whole Arachnida, a grouping now considered (van der Hammen 1977) to consist of 7 classes, the inter-relationships of which are obscure. If one or more (but not all) of the arachnid groups were shown to share a common ancestor with the Eurypterida, which the above scheme suggests is quite possible, then both Merostomata and Arachnida are unnatural groups.

8. Acknowledgements
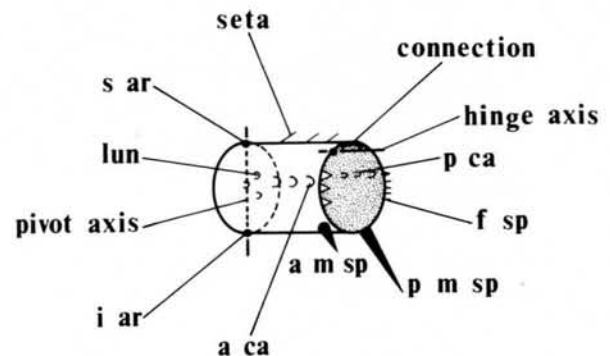
Figure 19 Hypothetical podomere of *Baltoeurypterus*; key to Figure 20.

Podomeres / Limbs	Coxa	2 / 2	3	3	4 / 4 / 5	5 / 6	6 / 7	7 / 8
		2	3	4	5	6	7	8
								9
II								
III								
IV								
V								
VI								

Figure 20 *Baltoeurypterus tetragonophthalmus.* Diagrammatic representation of the podomeres of limbs II to VI, not to scale. Each is shown in antero-lateral aspect (podomeres VI7 and VI8 are tilted slightly); key is Figure 19. Podomere numbers: top row, limb. II; middle row, limbs III and IV; bottom row, limbs V and VI.

Joints / Limbs	Body - Coxa	Coxa - 2 / Coxa - 2	2 - 3	2 - 3 / 3 - 4	3 - 4 / 3 - 4 / 4 - 5	4 - 5 / 5 - 6	5 - 6 / 6 - 7	6 - 7 / 7 - 8
		Coxa - 2	2 - 3	3 - 4	4 - 5	5 - 6	6 - 7	7 - 8
								8 - 9
II								
III								
IV								
V								
VI								

Figure 21 *Baltoeurypterus tetragonophthalmus.* Diagrammatic representation of the joints of limbs II to VI, after the convention of Manton (e.g. 1977, figs 5.15 and 10.2). The concentric lines represent overlapping podomeres, the inner line being the distal podomere; articulations shown by black spots, close podomere connections by curved lines and articulation axes by straight lines. Each joint is viewed proximally and end-on, anterior facing left and superior uppermost (except VI6–VI7 joint, supero-lateral aspect). Pivot joints are those in which the articulation axis bisects the joint, in hinges the axis is more tangential to the concentric lines.
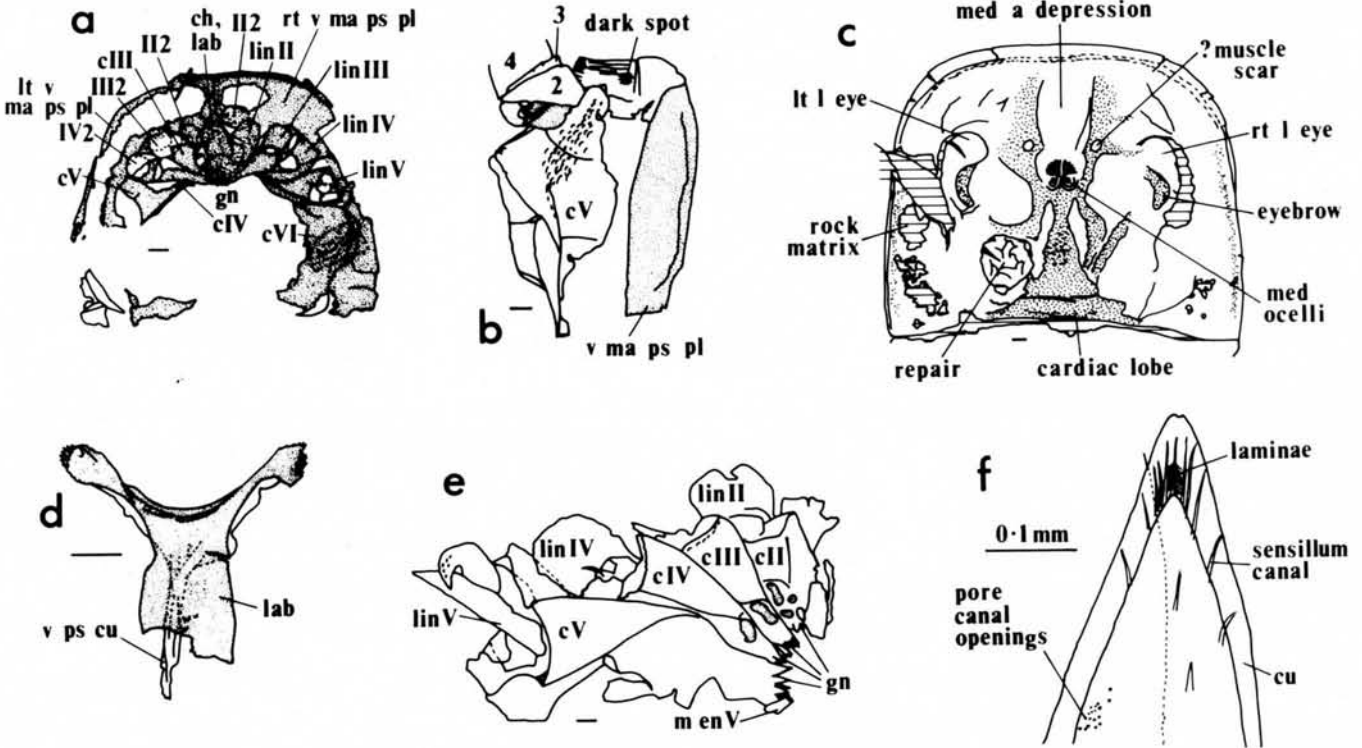
Figure 22 Explanatory drawings for Figure 23.

Figure 23 (opposite) a–c, f–o. *Baltoeurypterus tetragonophthalmus*
d, e. *Limulus polyphemus* (Xiphosura,
Recent)

a. Ar 50013b, SEM. ?Follicle with broken seta, rhomboid pits on cuticle surface; ×1050.

b. Ar 50013b, SEM. ?Sense organ or follicle with seta missing; ×1050.

c. Ar 50013b, SEM. ?Sense organ; ×1050.

d. *Limulus*, moult cuticle, SEM. Setal follicle with broken base of seta; ×263.

e. *Limulus*, moult cuticle, SEM. ?Sense organ; ×1050.

f. Ar 35307. Carapace and parts of mesosomal tergites, dorsal aspect; ×1·6 (Fig. 22c).

g. Ar 49961. Left ventral marginal plate of prosoma, posterior part, attached to parts of limb V; ×4 (Fig. 22b).

h. Ar 50140. Left ventral marginal plate of prosoma, posterior part, attached to lintel of coxa VI, and terrace lines grading to broad lunules, ventral aspect; ×3·6.

i. Ar 35320. Ventral marginal plate showing terrace lines and dark spot (X); ×1·8.

j. Ar 35330. Prosoma with carapace, metastoma, endostoma and most of coxae VI and limb rami absent, dorsal aspect, showing arrangement of coxae and ventral marginal plates; ×2·9 (Fig. 22a, adhering pieces of dorsal surface and membranes omitted).

k. Ar 50048. Coxae II to V, ventral aspect, showing radiating arrangement and comparison of coxal triangles; ×9·6 (Fig. 22e).

l. Ar 50070. Labrum attached to ventral prosomal cuticle; ×5·9 (Fig. 22d).

m. I 3406/1. Recent fungi attached to eurypterid cuticle that have survived the etching; ×28.

n. I 3406/14. Gnathobasic tooth of coxa V, with row of ?chemosensilla canals (Nebenzähnchen of Eisenack 1956), and dendritic feature (?impression of nerves); ×161.

o. I 3406/14. Gnathobasic tooth of coxa V showing cuticular structures; ×250 (Fig. 22f).
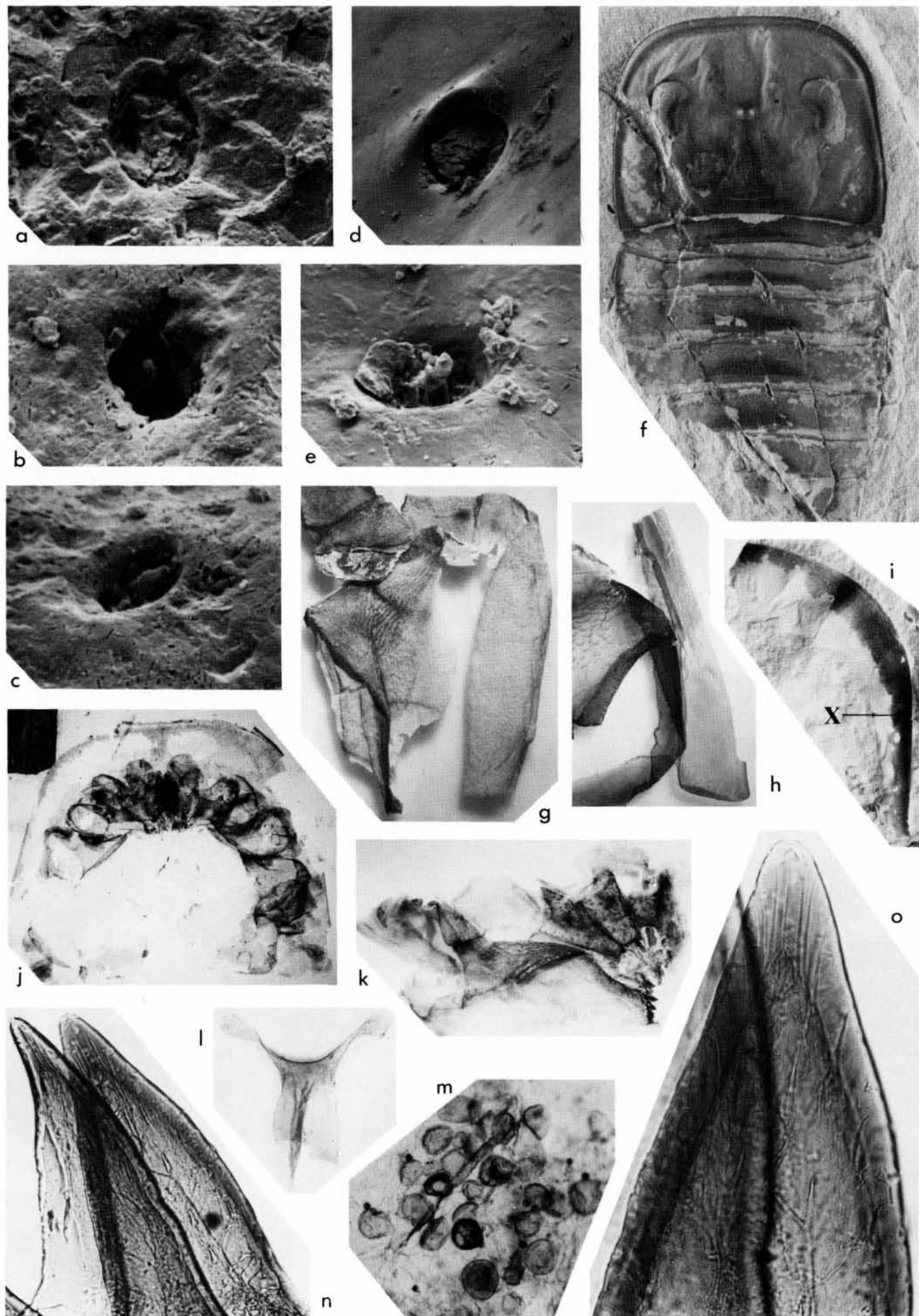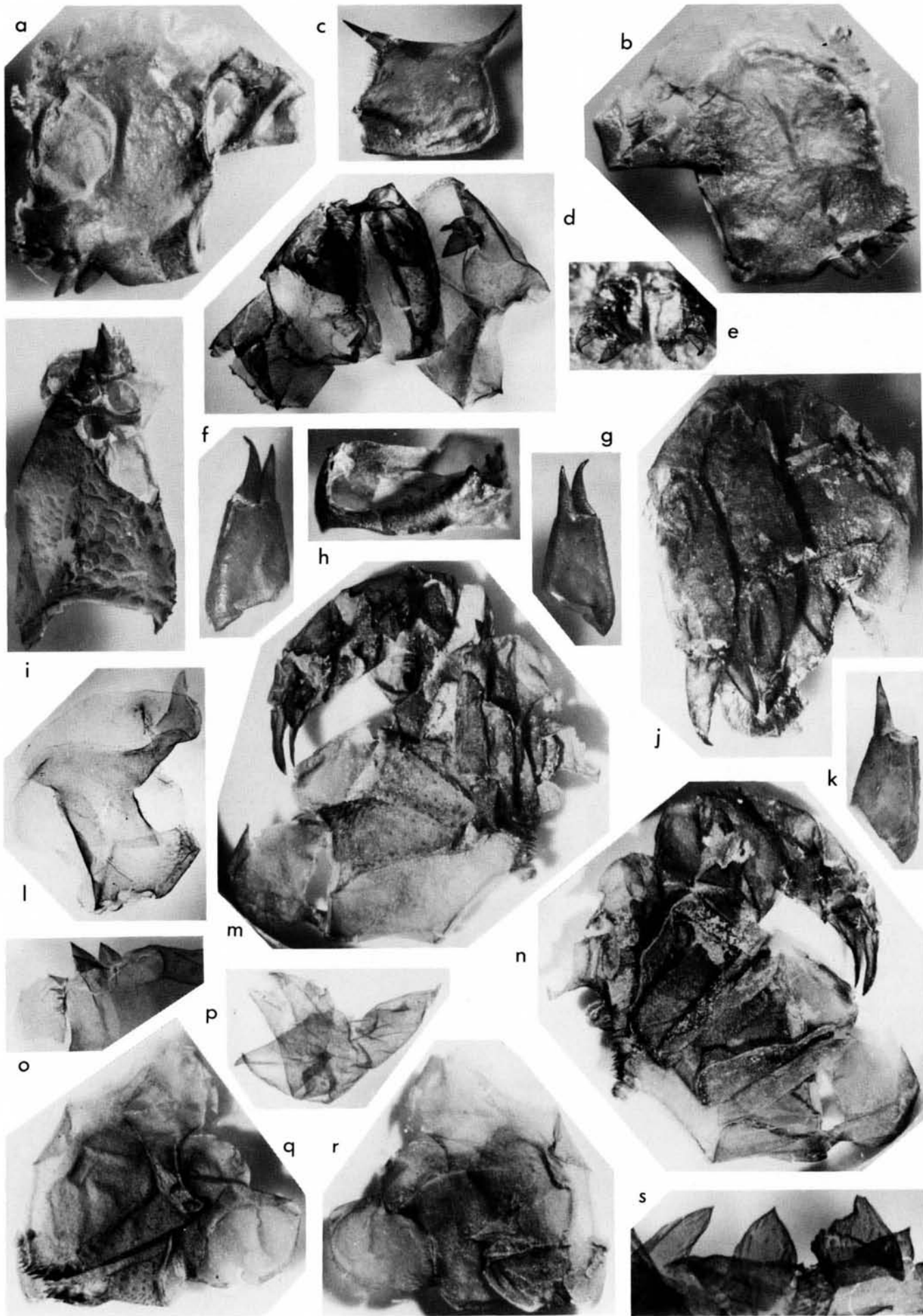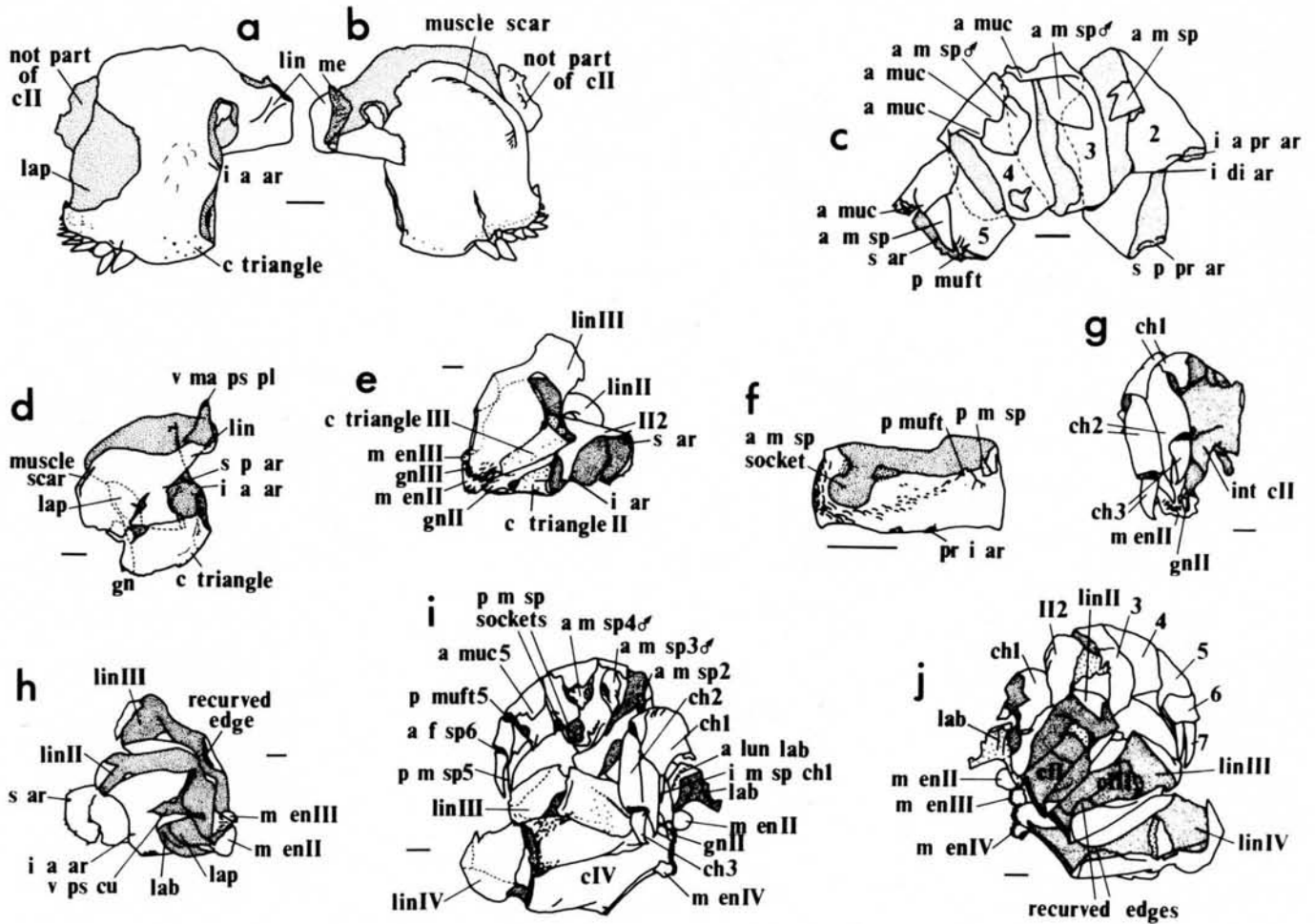
Figure 24 (opposite) *Baltoeurypterus tetragonophthalmus*

a. Ar 49916. Coxa II, anterior aspect; ×15 (Fig. 25a).

b. Ar 49916. Coxa II, posterior aspect; ×15 (Fig. 25b).

c. Ar 49967. Podomere 1 of chelicera, anterior aspect, distal joint to left with articulation and bristles, inferior to top; ×4·1.

d. Ar 50098. Podomeres 2 to 5 of limb II, male, inferior aspect; ×8·4 (Fig. 25c).

e. Ar 35344. Chelicerae *in situ*, movable fingers of chelae to inside; ×8·9.

f. Ar 49952. Podomere 2 of chelicera, posterior aspect, and podomere 3, anterior aspect (displaced), showing inferior tendon; ×9·5.

g. Ar 49952. As f, anterior aspect of podomere 2, posterior of podomere 3; ×8·5.

h. Ar 49948. Podomere II3, inferior aspect, distal to top; ×14 (Fig. 25f).

i. Ar 50029. Coxa II, ventral aspect, 4 movable teeth absent; ×12.

j. I 3406/9. Chelicerae and coxa II, ventral aspect; ×8·3 (Fig. 25g).

k. Ar 49950. Podomere 2 of chelicera, posterior aspect, showing distal articulations; ×8.9.

l. Ar 50087. Coxa II, posterior aspect; ×7·8 (Fig. 25d).

m. I 3406/10. Right coxae III, IV, limb II (male), chelicera, and labrum, ventral aspect; ×4·8 (Fig. 25i).

n. I 3406/10. As m, dorsal aspect; ×4·8 (Fig. 25j).

o. Ar 50132. Gnathobase of coxa II, showing 3 movable ventral teeth (top), fixed teeth and part of movable endite (left), with setae, bristles and follicles; ×12.

p. Ar 50163. Cheliceral chela (bottom left) in closed position showing crossed tips of fingers; ×21.

q. Ar 50022. Coxae II, III, and podomere II2, postero-ventral aspect; ×6·7 (Fig. 25e).

r. Ar 50022. As q, anterior aspect, also showing lappet and movable endite of coxa II, and labrum; ×6·7 (Fig. 25h).

s. Ar 50132. Anterior movable spines of limb II, male, podomere 2 left, podomere 3 middle and podomere 4 right: ×8·1.
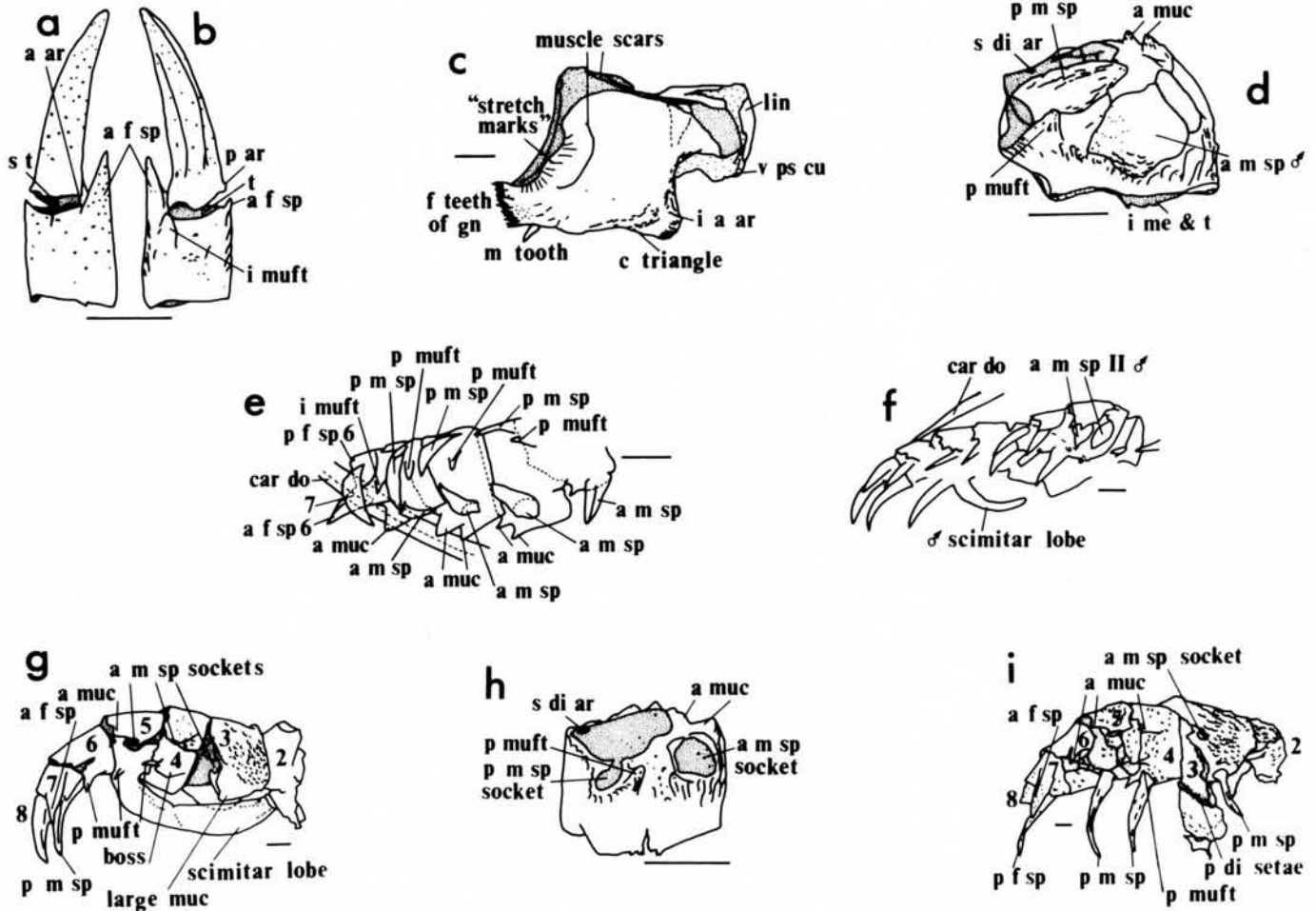
Figure 25 Explanatory drawings for Figure 24.

Figure 26 Explanatory drawings for Figure 27.

Figure 27 (opposite) *Baltoeurypterus tetragonophthalmus*

a. Ar 49949. Podomeres II6 and II7, antero-superior aspect, showing superior tendon of podomere II7 (displaced outside II6), and follicles on cuticle surface; ×18 (Fig. 26a).

b. Ar 49949. As a, postero-inferior aspect; ×18 (Fig. 26b).

c. Ar 50037. Podomeres 3 and 4 of limb III, female, inferior aspect, distal to top; ×3·2.

d. Ar 49926. Podomere III2, inferior aspect, distal to top, note superior articulation at top left, and distal spines; ×9·9.

e. Ar 49926. As d, superior aspect, distal to bottom; ×8·4.

f. Ar 50183. Podomeres 4 and 5 of limb III, male, posterior aspect, showing base of scimitar lobe arising adjacent to posterior movable spine and multifolliculated tubercle of podomere 5; ×6·2.

g. Ar 49974. Ramus of limb III, female, infero-anterior aspect; ×9·8.

h. I 3406/17. Podomeres 6 to 8 of limb III, inferior aspect, posterior to right; ×7·3.

i. Ar 49941. Podomere II4, male, superior aspect, distal to top; ×13.

j. Ar 49941. Podomere II4, male, inferior aspect, distal to top; ×16 (Fig. 26d).

k. Ar 49939. Podomeres II6 and II7, inferior aspect, posterior to left, showing large multifolliculated tubercle; ×14.

l. Ar 49939. As k, superior aspect; ×14.

m. Ar 50027. Podomere III4, male inferior aspect, anterior movable spine to left, distal part of podomere III3 attached (below)

showing large inferior mucro; ×5.

n. Ar 49931. Coxa III, posterior aspect, 2 movable teeth of gnathobase absent; ×7·2.

o. Ar 49931. Coxa III, anterior aspect; ×7·2 (Fig. 26c).

p. Ar 49928. Podomeres 2 and 3 of limb III, female, posterior aspect, distal to top, inferior to left (movable spines missing); ×11.

q. Ar 49927. Podomere II2, inferior aspect, distal to top, anterior (movable spine absent) to left; ×8·2.

r. Ar 49927. Podomere II2, superior aspect, distal to top, anterior to right; ×8·2.

s. Ar 50072. Gnathobase of coxa III, posterior aspect, showing movable teeth with setal follicles, fixed teeth, and bristles; ×12.

t. Ar 50158. Limb II, female, inferior aspect; ×14 (Fig. 26e).

u. Ar 50150. Podomeres 5 to 8 of limb III, female, inferior aspect, posterior to top; ×11.

v. Ar 49943. Podomere III6, postero-inferior aspect, distal to top; ×13.

w. I 3406/1. Limbs II and III, male, infero-anterior aspect; ×6·8 (Fig. 26f).

x. Ar 50061. Podomeres 3 and 4 of limb III, female, inferior aspect, distal to top, anterior to right, note symmetric lunules grading into asymmetric; ×4·2.

y. I 3406/11. Ramus of limb III, male, infero-anterior aspect; ×5·5 (Fig. 26g).

z. Ar 49930. Podomere II5, inferior aspect, distal to top; ×15 (Fig. 26h).

aa. Ar 50056. Podomeres 2 to 8 of limb III, female, infero-anterior aspect; ×2·0 (Fig. 26i).
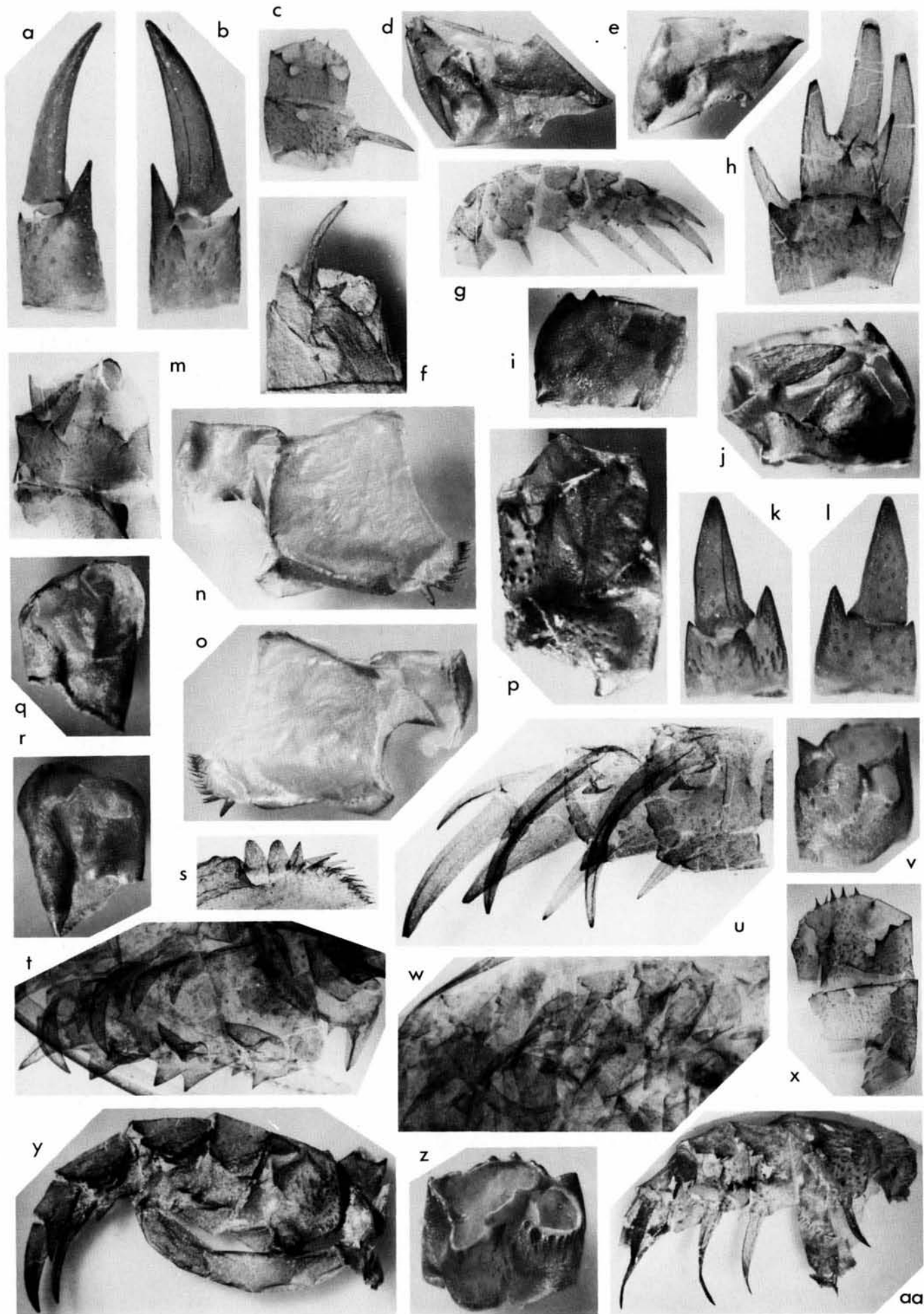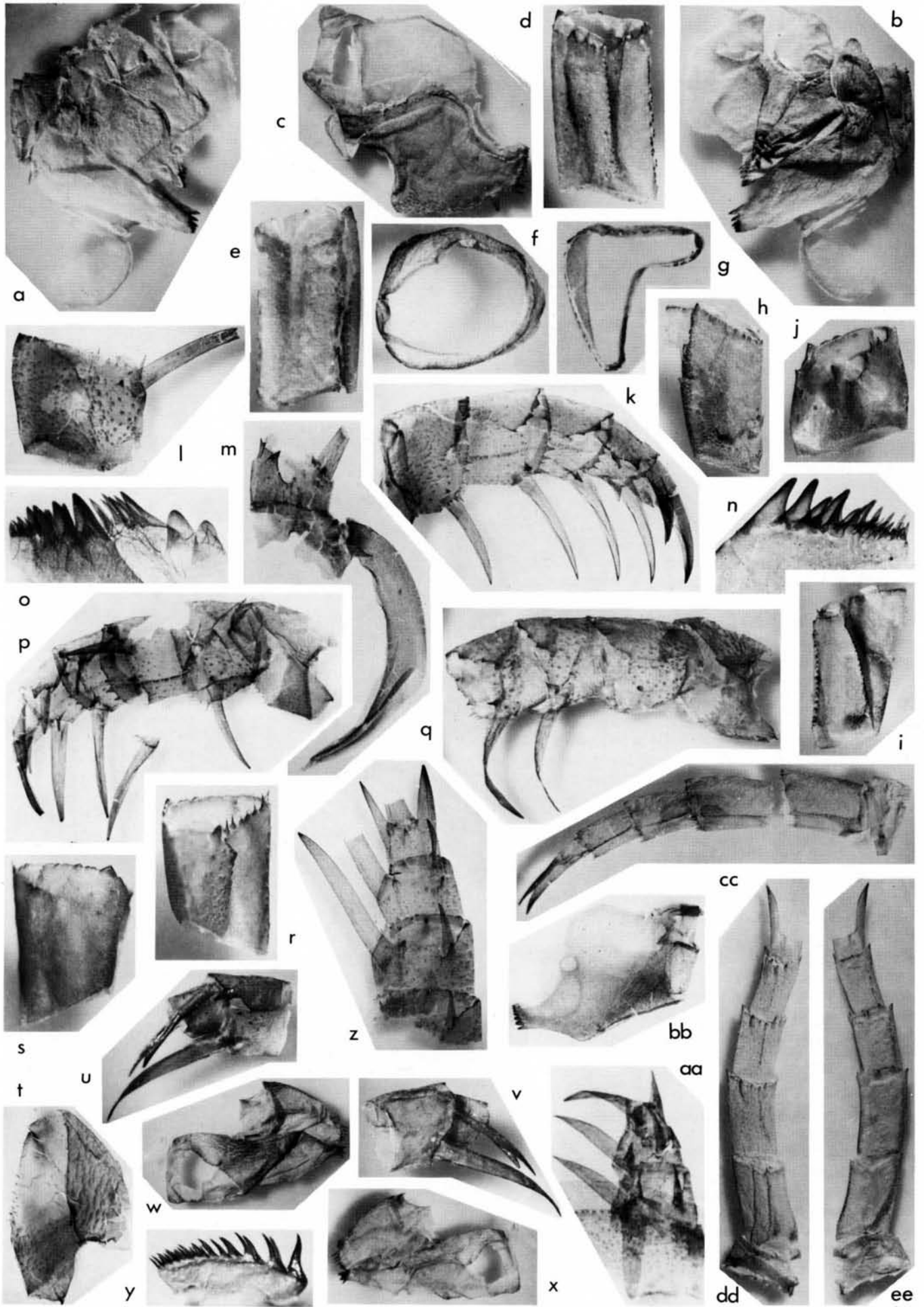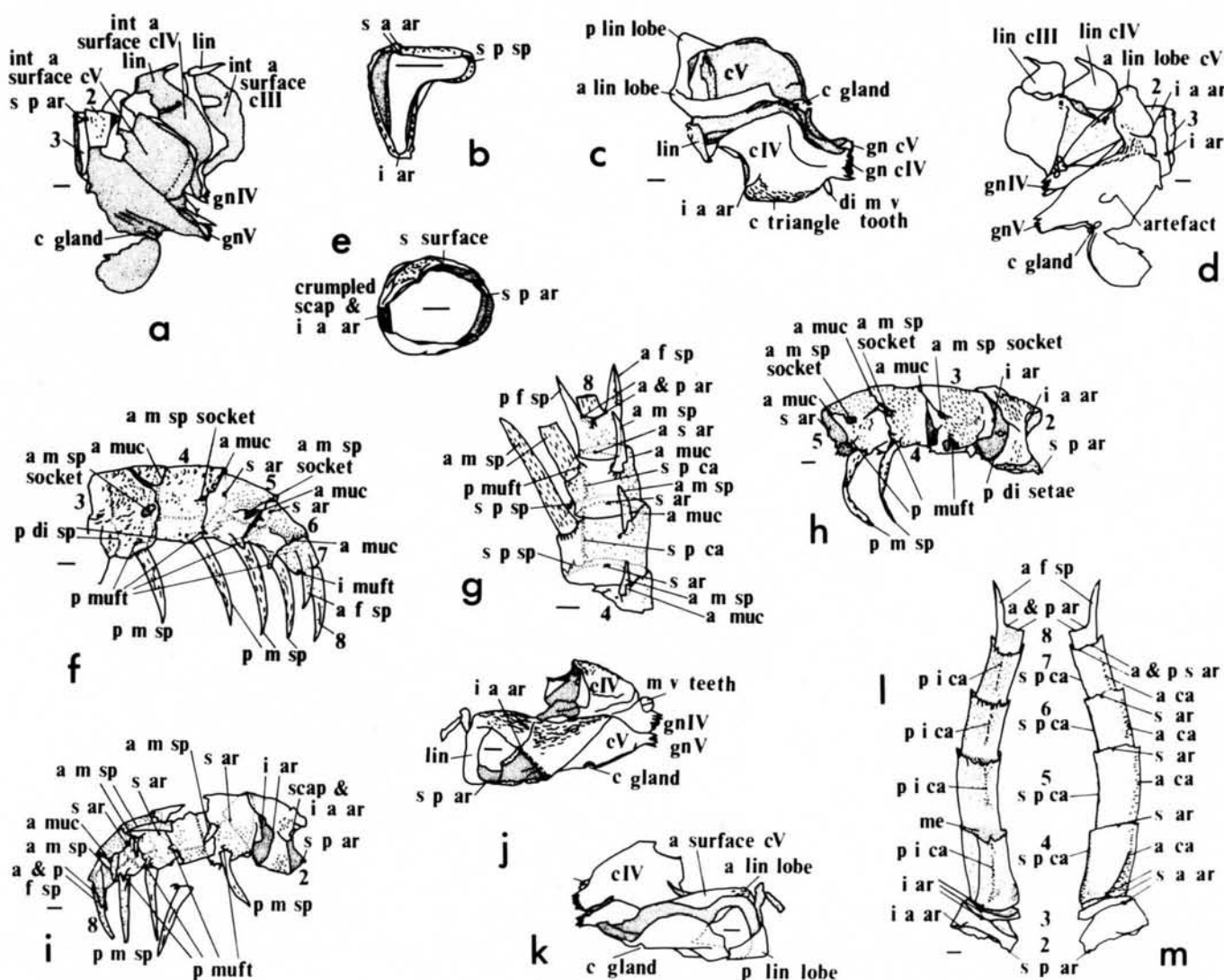
Figure 28 (opposite) *Baltoeurypterus tetragonophthalmus*

a. Ar 50023 Coxae III, IV and V, with podomeres V2 and V3, dorsal aspect; ×5·7 (Fig. 29a).

b. Ar 50023. As a, ventral aspect; ×5·7 (Fig. 29d).

c. Ar 49979. Coxae IV (front) and V (behind, top), anterior aspect; ×3·9 (Fig. 29c).

d. Ar 49935. Podomere V5, inferior aspect, distal to top, anterior to left, showing infero- and supero-posterior carinae, mucrones and spines around distal joint; ×8·1.

e. Ar 49935. Podomere V5, superior aspect, distal to top, anterior to right; ×8·1.

f. Ar 50040. Podomere V2, proximal aspect, superior to top; ×9·1 (Fig. 29e).

g. Ar 49945. Podomere V3, distal aspect, superior to top; ×11 (Fig. 29b).

h. Ar 49936. Podomere V4, superior aspect, distal to top, anterior to left; ×5·6.

i. Ar 49936. Podomere V4, inferior aspect, distal to top, anterior to right; ×6·5.

j. Podomere IV4, postero-inferior aspect, distal to top; ×9.4.

k. I 3406/12. Ramus of limb IV, antero-inferior aspect; ×4·0 (Fig. 29f).

l. Ar 50053. Podomere IV3, postero-superior aspect, distal to top; ×4·2.

m. Ar 50024. Parts of podomeres 5 and 6 of limb III, male, inferior aspect, scimitar lobe of posterior surface of podomere 5 shows minute, short setae; ×4·8.

n. Ar 49919. Gnathobase of coxa V, posterior aspect; ×24.

o. I 3406/12. Gnathobases of coxa IV (right), including movable ventral teeth, and coxa V (left), posterior-aspect, with setae and bristles; ×9·9.

p. Ar 50106. Ramus of limb IV, antero-inferior aspect; ×2·2 (Fig. 29i).

q. Ar 50047. Podomeres 2 to 5 of limb IV, antero-inferior aspect; ×4·4 (Fig. 29h).

r. Ar 49940. Podomere IV3, postero-inferior aspect, distal to top; ×9·0.

s. Ar 49940. Podomere IV3, antero-superior aspect, distal to top; ×9·0.

t. Ar 50052. Podomere IV2, antero-inferior aspect, distal to top left, showing articulations, distal spines and superior setae; ×4·3.

u. Ar 50045. Podomeres 5 and 6 of limb IV, infero-anterior aspect, distal to left; ×5·1.

v. Ar 50045. As u, postero-superior aspect; ×5·1.

w. Ar 50021. Coxae IV and V, ventral aspect, anterior to top; ×3·0 (Fig. 29j).

x. Ar 50021. Coxae IV and V, dorsal aspect, anterior to top; ×3·0 (Fig. 29k).

y. Ar 50028. Gnathobasic fixed teeth of coxa IV, anterior aspect; ×8·8.

z. Ar 50011. Podomeres 4 (part), 5, 6, 7 and 8 (part) of limb IV, inferior aspect, anterior aspect, anterior to right; ×4·8 (Fig. 29g).

aa. Ar 49978. Carapace rim overlying podomeres 5 to 8 of limb III, juvenile male, superior aspect, anterior to right, showing immature scimitar lobe arising adjacent to posterior movable spine of podomere 5 and pointing to bottom of picture; ×8·4.

bb. Ar 50004. Coxa V, posterior aspect, showing coxal gland opening, anterior surface (with muscle scar) showing through posterior surface; ×4·6.

cc. I 3406/31. Ramus of limb V, supero-posterior aspect; ×3·2.

dd. Ar 50013a. Ramus of limb V, podomere 9 and posterior fixed spine of podomere 8 absent (Ar 50013b), inferior aspect; ×3·2 (Fig. 29l).

ee. Ar 50013a. As dd, superior aspect; ×3·2 (Fig. 29m).

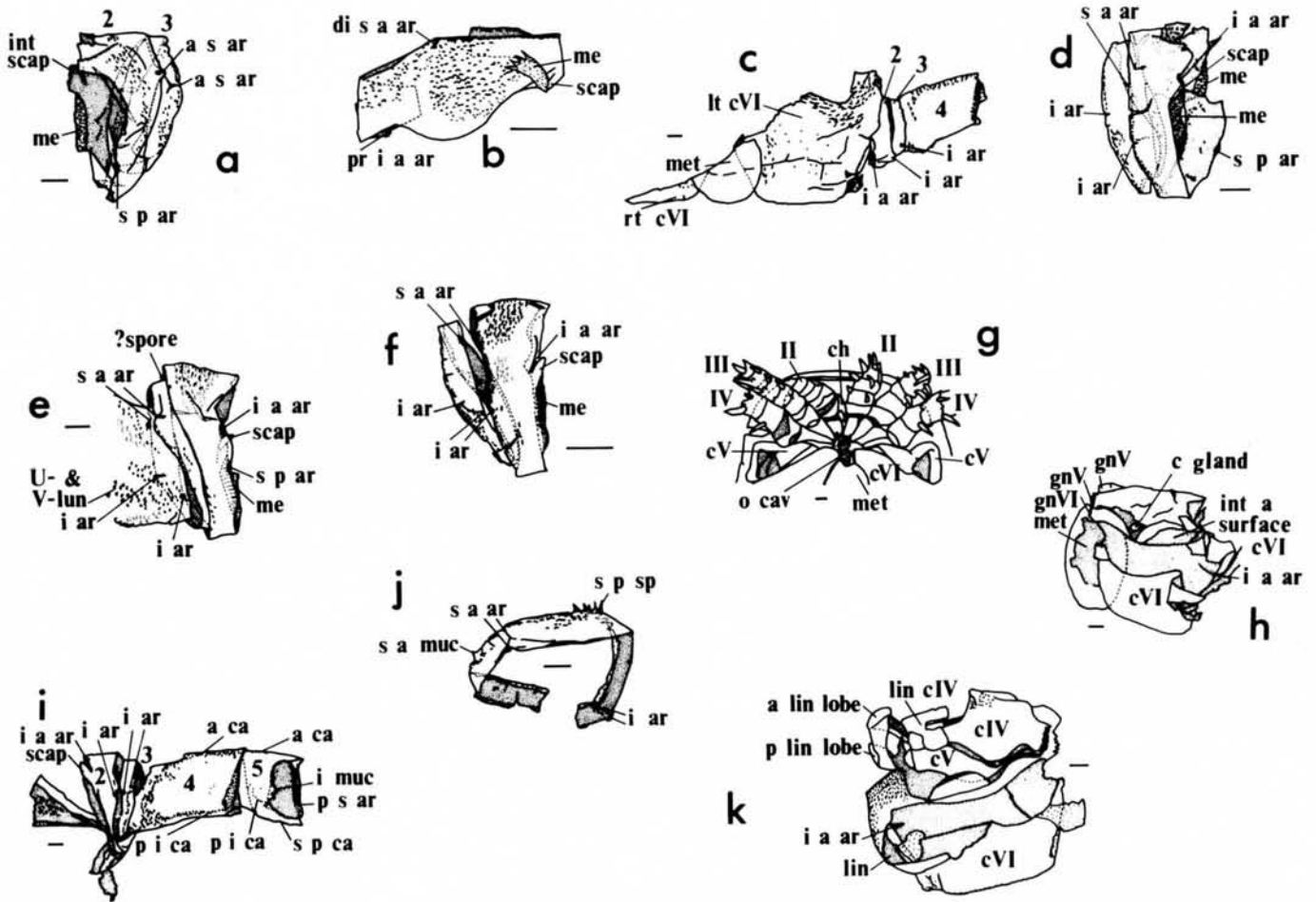**Figure 29** Explanatory drawings of Figure 28.

**Figure 30** Explanatory drawings for Figure 31.
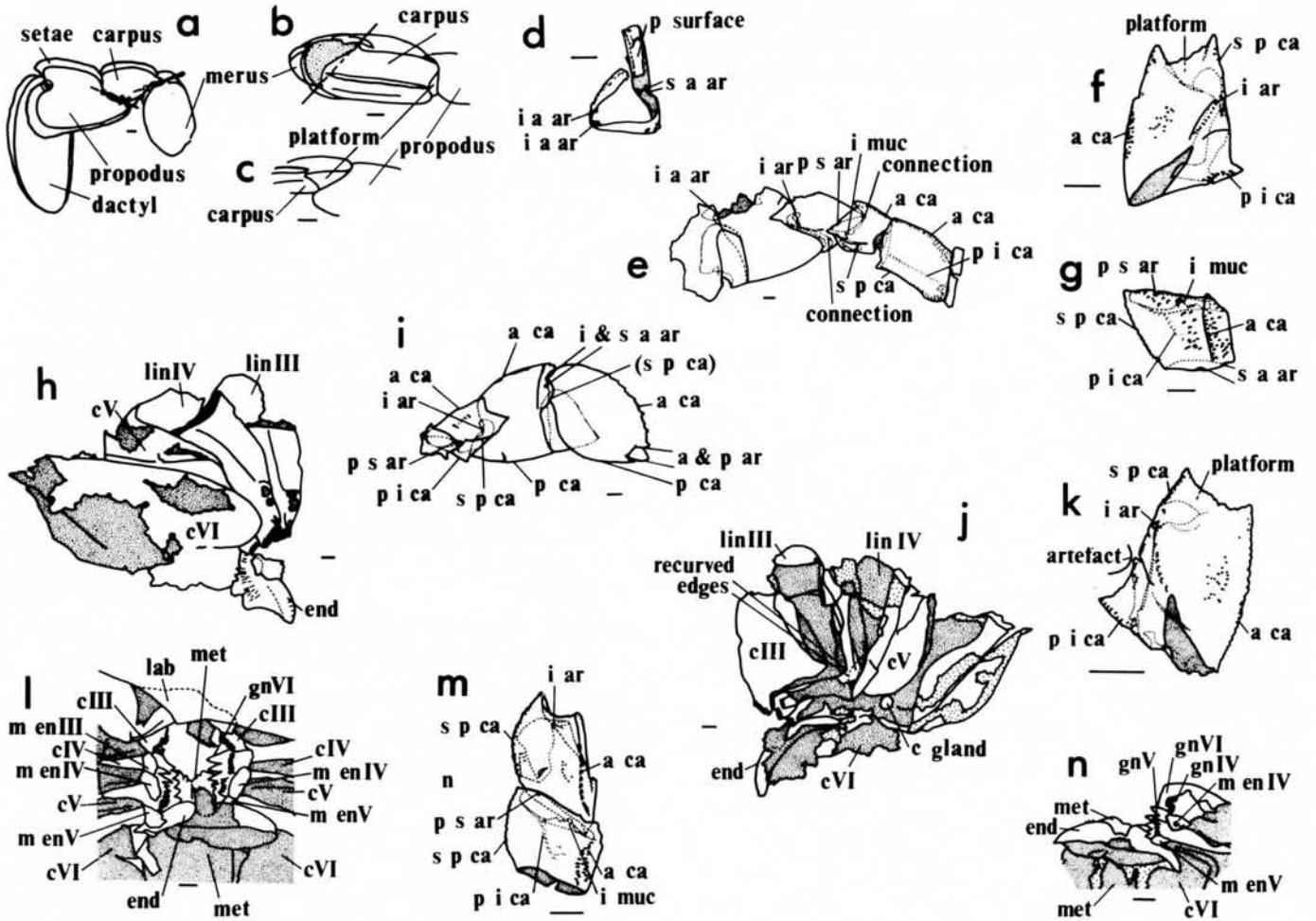
Figure 31 (opposite) *Baltoeurypterus tetragonophthalmus.*

a. Ar 50146. Podomeres VI2 and VI3, superior aspect, shows striated membrane (tendon bases in arthrodial membrane) at left; ×7·7 (Fig. 30a).

b. Ar 49947. Podomere V2, superior aspect; ×13 (Fig. 30b).

c. Ar 50123. Podomeres VI2 and VI3, inferior aspect; ×6·2 (Fig. 30d).

d. Ar 50177b. Coxa and podomeres 2 to 4 limb VI, etc., ventral aspect; ×2·6 (Fig. 30c).

e. Ar 50137. Podomeres V8 and V9, inferior aspect, anterior to left; ×10.

f. Ar 50120. Podomeres 2, 3 and 4 (part) of limb VI, superior aspect; ×7·2 (Fig. 30e).

g. Ar 49955. Podomeres VI2 and VI3, inferior aspect, scaphoid process prominent on right; ×29 (Fig. 30f).

h. I 3406/2. Anterior part of prosoma, ventral aspect; ×2·7 (Fig. 30g).

i. Ar 50108. Distal tip of podomere V9 showing follicles and internal black body; ×65.

j. Ar 50051. Podomere V2; ×6·0 (Fig. 30j).

k. Ar 50172. Coxae V (top) and VI and metastoma, dorsal aspect; ×2·6 (Fig. 30h).

l. I 3406/19. Podomeres 7 to 9 of limb V, superior aspect, anterior to right; ×5·3.

m. Ar 50062. Podomeres V5 (anterior at right) and V6 (anterior at left), showing distal mucrones, articulations and follicle distribution; ×3·6.

n. Ar 49925. Podomere V6, superior aspect, distal to top, anterior to left; ×7·1.

o. Ar 49925. Podomere V6, inferior aspect, distal to top, anterior to right; ×7·1.

p. Ar 50020. Coxa VI, attached to metastoma on right, and ventral marginal plate (part) on left, to which is also attached coxa V (part) with podomeres 2 to 4 of limb V, dorsal aspect; ×3·3.

q. Ar 49955. Podomere VI4, superior aspect, distal to left; ×7·9.

r. Ar 50049. Large tooth of gnathobase VI showing papulose surface; ×13.

s. Ar 50138. Podomere V5, anterior aspect, distal to right, anterior to top; ×4·7.

t. Ar 50001. Podomere V9, inferior aspect, distal end (top) showing abrasion; ×7·3.

u. Ar 50046. Gnathobasic teeth of coxa VI; ×17.

v. Ar 34713. Gnathobase VI, mesial aspect, ventral to top, gnathobase II in front; ×11.

w. Ar 34713. Gnathobase VI, ventral aspect, gnathobase II on right; ×8·7.

x. Ar 50166. Podomeres 2 to 5 of limb VI, inferior aspect, anterior to top; ×3·5. (Fig. 30i).

y. Ar 50049. Coxa VI, ventral aspect, showing surface sculpture; ×1·7.

z. Ar 49951. Coxa IV, V and VI, dorsal aspect; ×3·3 (Fig. 30k).

aa. Ar 49951. Coxae IV, V and VI, ventral aspect; ×3·3.
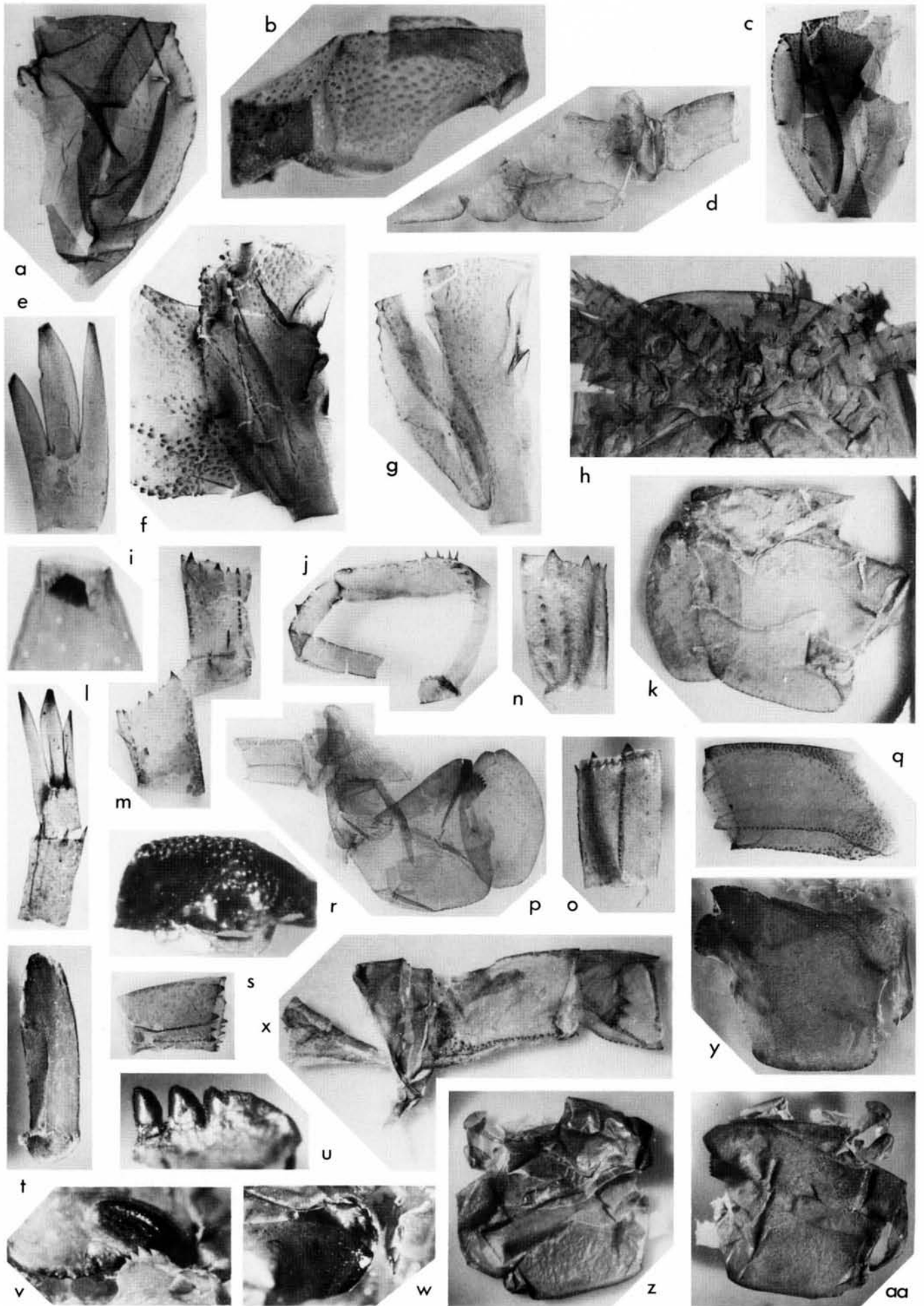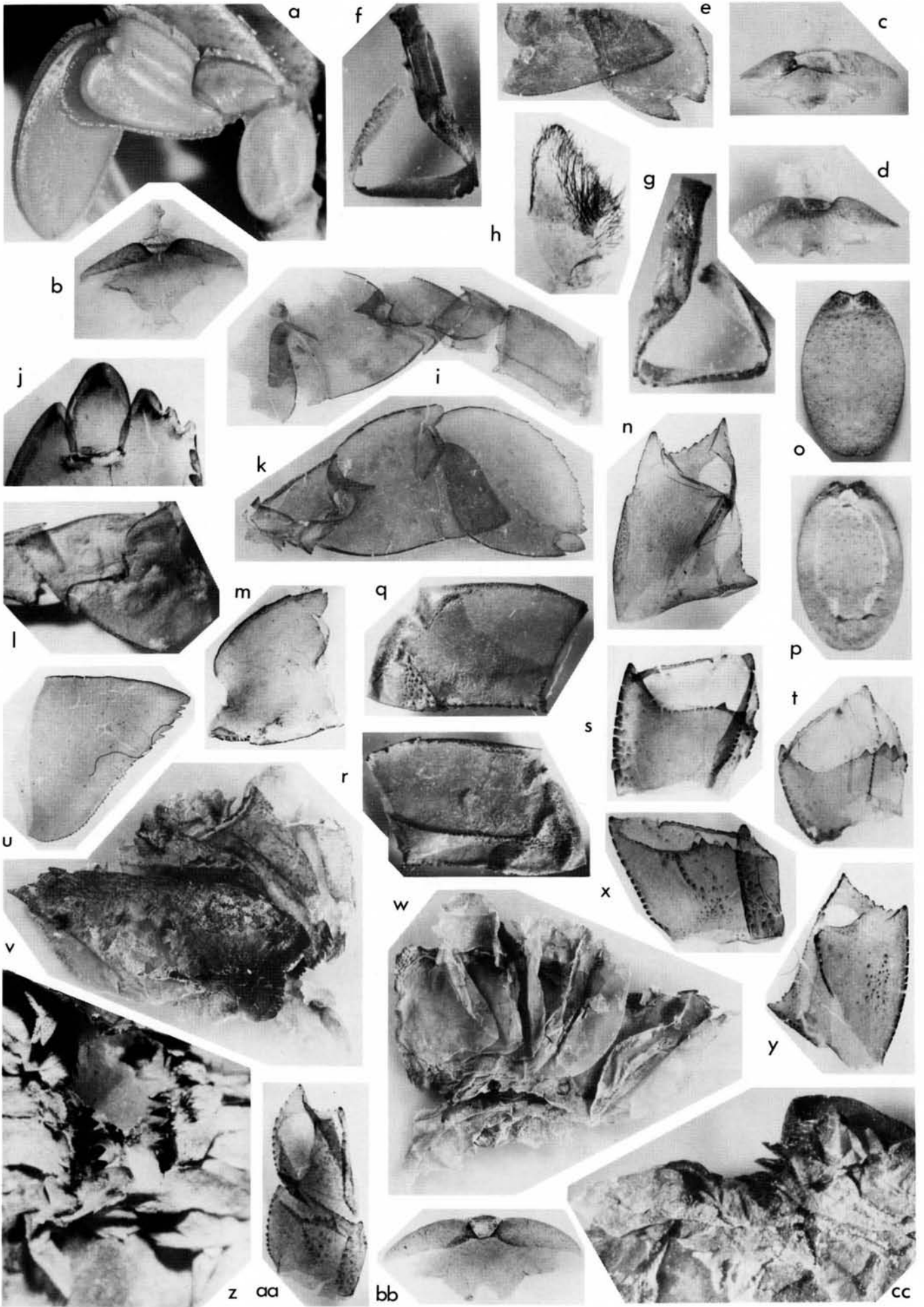
Figure 32 (opposite) a. *Macropipus depurator* (Crustacea, Recent)
b–cc. *Baltoeurypterus tetragonophthalmus*

a. *Macropipus*. Left 5th pereiopod, ischium (part) to dactyl (left), superior aspect; ×2·2 (Fig. 33a, showing articulations (solid and open circles, close podomere connection shown by a X) and articulation axes; b, merus–carpus joint viewed distally, carpus–propodus joint in anterior aspect; c, carpus–propodus joint viewed distally.)

b. I 3406/21. Endostoma, ventral aspect, anterior to top; ×4·9.

c. Ar 49944. Endostoma, dorsal aspect, anterior to top; ×7·4.

d. Ar 49944. Endostoma, ventral aspect, anterior to top; ×7·4.

e. Ar 49937. Posterior parts of podomeres 7, lobe 7a and 8 of limb VI, inferior aspect, distal to right; ×2·5.

f. Ar 49929. Podomere V13, proximal aspect, superior to right; ×8·0. (Fig. 33d).

g. Ar 49929. Podomere V13, distal aspect, superior to left; ×8·8.

h. I 3406/15. Movable endite of ?coxa V, basal joint at bottom, mesial to right; ×22.

i. Ar 50113. Podomeres 2 to 8 (part) of limb VI, superior aspect; ×2·3 (Fig. 33e).

j. Ar 49970. Podomere VI9 *in situ* on VI8, inferior aspect, posterior to left; ×6·4.

k. I 3406/18. Podomeres 5 (part) to 9 of limb VI, superior aspect; ×3·6 (Fig. 33i).

l. I 3406/2. Podomere VI6 attached to VI5 (left) and VI7 (right), inferior aspect, anterior to top; ×5·0.

m. Ar 49913. Podomere VI7, superior aspect, anterior to top, distal to right; ×5·0.

n. Ar 49924. Podomere VI6, superior aspect, anterior to left,

distal to top; ×8·2 (Fig. 33f).

o. I 3406/20. Mestastoma, ventral aspect, anterior to top; ×3·3.

p. I 3406/20. Mestastoma, dorsal aspect, anterior to top; ×3·3.

q. Ar 49946. Podomere VI4, inferior aspect, anterior to top, distal to right; ×5·6.

r. Ar 49946. Podomere VI4, superior aspect, anterior to top, distal to left; ×5·6.

s. Ar 50159. Podomere VI6, inferior aspect, anterior to left, distal to top; ×6·2.

t. Ar 49999. Podomere VI5, superior aspect, anterior to left, distal to top; ×3·1.

u. Ar 50180. Lobe 7a, superior aspect, posterior to top, distal to right; ×6·2.

v. Ar 50179e. Right coxae III to VI (part), and endostoma, ventral aspect; ×2·8 (Fig. 33h).

w. Ar 50179e. As v, dorsal aspect; ×2·8 (Fig. 33j).

x. Ex E9/45. Podomere VI5, superior aspect, anterior to right, distal to top; ×8·1 (Fig. 33g).

y. Ex E9/20. Podomere VI6, superior aspect, anterior to right, distal to top; ×9·4 (Fig. 33k).

z. Ar 35341. Oral cavity, dorsal aspect; ×7·8 (Fig. 33l).

aa. Ar 50129. Podomeres VI5 and VI6, inferior aspect, anterior to left, distal to top; ×6·0 (Fig. 33m).

bb. Ar 50079. Endostoma, inferior aspect, anterior to top; ×5·8.

cc. Ar 50169. Organs around posterior part of oral cavity, dorsal aspect, anterior to top; ×11 (Fig. 33n).

Figure 33 Explanatory drawings for Figure 32.

tenure of a Natural Environment Research Council studentship at Darwin College, Cambridge, and completed at the Department of Geology, Goldsmiths' College, University of London.

9. Explanation of figures

a	anterior, antero-
ar	articulation(s)
c	coxa(e) (l)
ca	carina(e) (l)
car	carapace
cav	cavity
ch	chelicera(e)
cl	closer muscle(s)
cu	cuticle
d	dorsal
dep	depressor muscle(s)
di	distal
do	doublure
en	endite(s)
end	endostoma
ent	endosternite
ex	extensor muscle(s)
f	fixed
fl	flexor muscle(s)
gn	gnathobase, gnathobasic
H	hinge joint(s)
i	inferior, infero-
int	interior
l	lateral
lab	labrum
lap	lappet
lev	levator muscle(s)
lin	lintel(s)
lt	left
lun	lunule(s)
m	movable
ma	marginal
me	membrane(s)
med	median
met	metastoma
muc	mucro(nes)
muft	multifolliculated tubercle(s)
o	oral
op	opener muscle(s)
P	pivot joint(s)
p	posterior, postero-
pl	plate
pr	proximal
ps	prosomal
ptr	protractor muscle(s)
rt	right
rtr	retractor muscle(s)
s	superior, supero-
scap	scaphoid process
sp	spine
t	tendon
v	ventral
I to VI	limb numbers
1 to 9	podomere numbers

Solid lines: outline of externally visible parts
Dashed lines: parts showing through from behind
Fine stipple: interior parts (except membrane)
Dense coarse stipple: arthrodial membrane (exterior)
Sparse coarse stipple: arthrodial membrane (interior)
Scale bars represent 1 mm unless stated otherwise.

10. References

Andrews, H. E., Brower, J. C., Gould, S. J. & Reyment, R. A. 1974. Growth and variation in *Eurypterus remipes* DeKay. BULL GEOL INST UNIV UPSALA **4**, 81–114.

Barber, S. B. 1956. Chemoreception and proprioception in *Limulus*. J EXP ZOOL **131**, 51–74.

Barbour, E. H. 1914. Carboniferous eurypterids of Nebraska. AM J SCI **38**, 507–10.

Barr, D. & Smith, B. P. 1979. The contribution of setal blades to effective swimming in the aquatic mite *Limnochares americana* (Acari: Prostigmata: Limnocharidae). ZOOL J LINN SOC **65**, 55–69.

Briggs, D. E. G., Rolfe, W. D. I. & Brannan, J. 1979. A giant myriapod trail from the Namurian of Arran, Scotland. PALAEONTOLOGY **22**, 273–91.

Bristowe, W. S. 1958. *The World of Spiders*. London: Collins.

Bruton, D. L. 1981. The Middle Cambrian arthropod *Sidneyia*, Burgess Shale, British Columbia. PHILOS TRANS R SOC LONDON B, in press.

Clark, B. D. & Bemis, W. 1979. Kinematics of swimming of penguins at the Detroit Zoo. J ZOOL LONDON **188**, 411–28.

Clarke, J. M. & Ruedemann, R. 1912. The Eurypterida of New York. MEM NEW YORK STATE MUS NAT HIST **14**, vol. I pp. 1–439, vol. II plates.

Clarkson, E. N. K. 1975. The evolution of the eye in trilobites. FOSSILS AND STRATA **4**, 7–31.

Couzijn, H. W. C. 1976. Functional anatomy of the walking-legs of Scorpionida with remarks on terminology and homologization of leg segments. NETH J ZOOL **26**, 453–501.

Dalingwater, J. E. 1973. The cuticle of a eurypterid. LETHAIA **6**, 179–86.

Dalingwater, J. E. 1975. Further observations on eurypterid cuticles. FOSSILS AND STRATA **4**, 271–9.

Dalingwater, J. E. 1980. SEM observations on the cuticles of some chelicerates. 8th INT ARACHNOL CONGR VIENNA **1980**, 285–9.

DeKay, J. E. 1825. Observations on a fossil crustaceous animal of the order Branchiopoda. ANN LYCEUM NAT HIST **1**, 375–7.

Dennell, R. 1960. Integument and exoskeleton. *In* Waterman, T. H. (ed.) *The Physiology of Crustacea*, vol. 1, 449–72. New York: Academic Press.

Depitout, A. 1962. Étude des gigantostracés siluriens du Sahara central. PUBL CENT RECH SAHARIENNES GEOL **2**, 1–141.

Edel, R. K. & Winn, H. E. 1978. Observations on underwater locomotion and flipper movement of the humpback whale *Megaptera novaeangliae*. MAR BIOL BERLIN **48**, 279–87.

Eichwald, E. von 1854. Die Grauwackenschichten von Liev- und Esthland. BULL SOC NAT MOSCOU **27**, 3–111.

Eichwald, E. von 1860. *Lethaea Rossica*, vol. 1. Stuttgart: Schweizerbart.

Eisenack, A. 1956. Beobachtungen an Fragmenten von Eurypteriden-Panzern. NEUES JAHRB GEOL PALAEONTOL ABH **104**, 119–28.

English, A. W. 1976. Limb movements and locomotor function in the California sea lion (*Zalophus californianus*). J ZOOL LONDON **178**, 341–64.

Evans, M. E. G. 1977. Locomotion in the Coleoptera Adephaga, especially Carabidae. J ZOOL LONDON **181**, 189–226.

Firstman, B. 1973. The relationship of the chelicerate arterial system to the evolution of the endosternite. J ARACHNOL **1**, 1–54.

Fischer de Waldheim, G. 1839. Notice sur un crustacé fossile du genre *Eurypterus* de Podolie. BULL SOC NAT MOSCOU **11**, 125–8.

Fisher, D. C. 1975. Swimming and burrowing in *Limulus* and *Mesolimulus*. FOSSILS AND STRATA **4**, 281–90.

Fisher, D. C. 1979. Evidence for subaerial activity of *Euproops danae* (Merostomata, Xiphosurida). *In* Nitecki, M. H. (ed.) *Mazon Creek Fossils*, 379–447. New York: Academic Press.

Fortey, R. A. & Clarkson, E. N. K. 1976. The function of the glabellar 'tubercle' in *Nileus* and other trilobites. LETHAIA **9**, 101–6.

Gnatzy, W. & Tautz, J. 1977. Sensitivity of an insect mechanoreceptor during moulting. PHYSIOL ENTOMOL **2**, 279–88.

Gray, J. 1968. *Animal Locomotion*. London: Weidenfeld & Nicholson.

Hall, J. 1859. *Palaeontology of New York*, Vol. 3 (In *Natural History of New York* Part 4) part 1, 382–419; part 2, plates 80–84A. Albany: New York State Museum.

Hammen, L. van der 1977. A new classification of Chelicerata. ZOOL MEDED LEIDEN **51**, 307–19.

Hammen, L. van der 1979. Comparative studies on Chelicerata I. The Cryptognomae (Ricinulei, Architarbi and Anactinotrichida). ZOOL VERH **174**, 1–62.

Hanken, N.-M. & Størmer, L. 1975. The trail of a large Silurian eurypterid. FOSSILS AND STRATA **4**, 255–70.

Hansen, H. J. 1925. *Studies on Arthropoda II. On the Comparative Morphology of the Appendages in the Arthropoda. A. Crustacea.* Copenhagen: Gyldendalske Boghandel.

Hansen, H. J. 1930. *Studies on the Arthropoda III. On the Comparative Morphology of the Appendages in the Arthropoda. B. Crustacea (Supplement), Insecta, Myriapoda and Arachnida.* Copenhagen: Gyldendalske Boghandel.

Hartnoll, R. G. 1971. The occurrence and significance of swimming in the Brachyura. ANIM BEHAV **19**, 34–50.

Haupt, J. & Coineau, Y. 1978. Moulting and morphogenesis of sensilla in a prostigmatic mite (Acari, Actinotrichida, Actinedida: Caeculidae). 1. Mechanoreceptive bristles. CELL TISSUE RES **186**, 63–79.

Hede, J. E. 1929. Berggrunden (Silursystemet). *In* Munthe, H., Hede, J. E. & Lundqvist, G. Beskrivning till kartbladet Katthammarsvik. SVER GEOL UNDERS ser. Aa **170**, 14–57.

Holm, G. 1896. Über eine neue Bearbeitung des *Eurypterus fischeri* Eichw. BULL ACAD SCI ST PETERSBOURG **4**, 369–72.

Holm, G. 1898. Über die Organisation des *Eurypterus fischeri* Eichw. MEM ACAD SCI ST PETERSBOURG **8**, 1–57.

Holm, G. 1899. Palaeontologiska notiser: 13. Om den yttre anatomien hos *Eurypterus fischeri.* GEOL FOEREN STOCKHOLM FOERH **21**, 83–128.

Hoyle, G. 1976. Arthropod walking. *In* Herman, R. M., Grillner, S., Stein, P. S. G. & Stuart, D. G. (eds) *Neural Control of Locomotion.* ADV BEHAV BIOL **18**, 137–79, New York: Plenum Press.

Hughes, C. P. 1975. Redescription of *Burgessia bella* from the Middle Cambrian Burgess Shale, British Columbia. FOSSILS AND STRATA **4**, 415–35.

Hughes, G. M. 1958. The co-ordination of insect movements. III. Swimming in *Dytiscus, Hydrophilus*, and a dragonfly nymph. J EXP BIOL **35**, 567–83.

Hughes, G. M. & Mill, P. J. 1974. Locomotion: terrestrial. *In* Rockstein, M. (ed.) *The Physiology of Insecta*, 2nd edn, vol. III, 335–79. New York: Academic Press.

Kaestner, A. 1968. *Invertebrate Zoology II — Arthropod relatives, Chelicerata, Myriapoda* (translated and adapted from the German by H. W. Levi & L. R. Levi) 2nd edn. New York: Interscience.

Kaljo, D. 1970. *Silur Estonii.* Tallin: Institut Geologii Akademii Nauk Estonickoi CCP.

Kennedy, T. S. 1945. Observations on the mass migration of desert locust hoppers. TRANS R ENTOMOL SOC LONDON **95**, 247–62.

Kjellesvig-Waering, E. N. 1979. Eurypterids. *In* Jaanusson, V., Laufeld, S. & Skoglund, R. (eds). Lower Wenlock faunal and floral dynamics — Vattenfallet section, Gotland. SVER GEOL UNDERS AFH C **762**, 57–64.

Kühl, H. 1933. Die Fortbewegung der Schwimmkrabben mit Bezug auf die Plastizität des Nervensystems. Z VGL PHYSIOL **19**, 489–521.

Lankester, E. R., Benham, W. B. S. & Beck, E. J. 1885. On the muscular and endoskeletal systems of *Limulus* and *Scorpio*; with some notes on the anatomy and generic characters of scorpions. TRANS ZOOL SOC LONDON **11**, 311–84.

Lauck, D. R. 1959. Locomotion of *Lethocerus* (Hemiptera: Belostomatidae). ANN ENTOMOL SOC AM **52**, 93–9.

Laurie, M. 1893. The anatomy and relations of the Eurypteridae. TRANS R SOC EDINBURGH **37**, 509–28.

Levi-Setti, R. 1975. *Trilobites: A Photographic Atlas.* Chicago: University of Chicago Press.

Lochhead, J. H. 1961. Locomotion. *In* Waterman, T. H. (ed.) *The Physiology of Crustacea*, vol. II, 313–64. New York: Academic Press.

Manten, A. A. 1971. *Silurian Reefs of Gotland.* Developments in Sedimentology 13. Amsterdam: Elsevier.

Manton, S. M. 1952. The evolution of arthropodan locomotory mechanisms. Part 2. General introduction to the locomotory mechanisms of the Arthropoda. J LINN SOC (ZOOL) **42**, 93–117.

Manton, S. M. 1958. Hydrostatic pressure and leg extension in arthropods, with special reference to arachnids. ANN MAG NAT HIST **1**, 161–82.

Manton, S. M. 1964. Mandibular mechanisms and the evolution of arthropods. PHILOS TRANS R SOC LONDON B **247**, 1–183.

Manton, S. M. 1965. The evolution of arthropodan locomotory mechanisms. Part 8. Functional requirements and body design in Chilopoda, together with a comparative account of their skeleto-muscular systems and an appendix on a comparison between burrowing forces of annelids and chilopods and its bearing upon the evolution of the arthropodan haemocoel. J LINN SOC (ZOOL) **45**, 251–484.

Manton, S. M. 1972. The evolution of arthropodan locomotory mechanisms. Part 10. Locomotory habits, morphology and evolution of the hexapod classes. ZOOL J LINN SOC **51**, 203–400.

Manton, S. M. 1973a. Arthropod phylogeny — a modern synthesis. J ZOOL LONDON **171**, 111–30.

Manton, S. M. 1973b. The evolution of arthropodan locomotory mechanisms. Part 11. Habits, morphology and evolution of the Uniramia (Onychophora, Myriapoda, Hexapoda) and comparisons with the Arachnida, together with a functional review of uniramian musculature. ZOOL J LINN SOC **53**, 257–375.

Manton, S. M. 1977. *The Arthropoda: Habits, Functional Morphology, and Evolution.* Oxford: Oxford University Press.

Miller, J. 1975. Structure and function of trilobite terrace lines. FOSSILS AND STRATA **4**, 155–78.

Miller, J. 1976. The sensory fields and life mode of *Phacops rana* (Green, 1832) (Trilobita). TRANS R SOC EDINBURGH **69**, 337–67.

Miller, P. L. 1972. Swimming in mantids. J ENTOMOL LONDON **46**, 91–7.

Milne, L. & Milne, M. 1967. *The Crab that Crawled out of the Past.* London: Bell.

Mitchill, S. L. 1818. An account of the impressions of a fish in the rocks of Oneida county, New York. AM MON MAG CRIT REV **3**, 291.

Mutvei, H. 1977. SEM studies of arthropod exoskeletons. 2. Horseshoe crab *Limulus polyphemus* (L.) in comparison with extinct eurypterids and recent scorpions. ZOOL SCR **6**, 203–13.

Nachtigall, W. 1960. Über Kinematik, Dynamik und Energetik des Schwimmens einheimischer Dytisciden. Z VGL PHYSIOL **43**, 48–118.

Nachtigall, W. 1962. Funktionelle Morphologie, Kinematik und Hydromechanik des Ruderapparates von *Gyrinus*. Z VGL PHYSIOL **45**, 193–226.

Nachtigall, W. 1974. Locomotion: mechanics and hydrodynamics of swimming in aquatic insects. *In* Rockstein, M. (ed.) *The Physiology of Insecta*, 2nd edn, vol. III, 382–432. New York: Academic Press.

Nieszkowski, J. 1858. *De Euryptero Remipede.* (dissertation). Dorpat: Gläser.

Nieszkowski, J. 1859. Der *Eurypterus remipes* aus den obersilurischen Schichten der Insel Oesel. ARCH NATURKD LIV-EST- KURLANDS **2**, 299–344.

Patten, W. 1894. On the morphology and physiology of the brain and sense organs of *Limulus*. Q J MICROSC SCI **35**, 1–96.

Petrunkevitch, A. 1955. Arachnida. *In* Moore, R. C. (ed.) *Treatise on Invertebrate Paleontology.* P. Arthropoda 2, P42-P162. Lawrence, Kansas: University of Kansas & Geological Society of America.

Robinson, J. A. 1975. The locomotion of plesiosaurs. NEUES JAHRB GEOL PALAEONTOL ABH **149**, 286–332.

Rosenheim, O. 1905. Chitin in the carapace of *Pterygotus osiliensis*, from the Silurian rocks of Oesel. PROC R SOC LONDON B **76**, 398–400.

Savory, T. H. 1964. *Arachnida.* London: Academic Press.

Schenke, G. 1963. Untersuchungen zum Bau und zur Funktion der Schwimmenextremitäten von *Corixa punctata* Illig. ENTOMOL BER **1**, 83–92.

Schenke, G. 1965a. Die Ruderbewegungen von *Corixa punctata* Illig. (Cryptocerata). INT REV GESTAMTEN HYDROBIOL **50**, 73–84.

Schenke, G. 1965b. Schwimmgeschwindigkeit, Schlagfrequenz und Steuern von *Corixa punctata* Illig. ZOOL ANZ **176**, 5–12.

Schenke, G. 1965c. Zu einigen morphologischen Voraussetzungen des Schwimmens von *Corixa punctata* Illig. 1807 (Hemiptera, Heteroptera). WISS Z PAEDAGOG HOCHSCH POTSDAM **9**, 399–408.

Schenke, G. 1965d. Schwimmhaarsystem und Rudern von *Notonecta glauca*. Z MORPHOL OEKOL TIERE **55**, 631–40.

Schmidt, F. 1883. Die Crustaceenfauna der Eurypterenschichten von Rootziküll auf Oesel — Miscellanea silurica III. MEM ACAD SCI ST PETERSBOURG **31**, 28–85.

Schrenk, A. 1854. Uebersicht des oberen silurischen Schichtensystems Liv- und Esthlands, vornähmlich ihrer Inselgruppe. ARCH NATURKD LIV- EST- KURLANDS **1**, 1–112.

Shelton, R. G. J. & Laverack, M. S. 1968. Observations on a redescribed crustacean cuticular sense organ. COMP BIOCHEM PHYSIOL **25**, 1049–59.

Smith, B. P. & Barr, D. 1977. Swimming by the water mite *Limnochares americana* Lundblad (Acari, Parasitengona, Limnocharidae). CAN J ZOOL **55**, 2050–9.

Spirito, C. P. 1972. An analysis of the swimming behavior of the portunid crab *Callinectes sapidus.* MAR BEHAV PHYSIOL **1**,

261–76.

Stockton, W. L. & Cowen, R. 1976. Stereoscopic vision in one eye: paleophysiology of the schizochroal eye of trilobites. PALEOBIOLOGY 2, 304–15.

Størmer, L. 1934. Merostomata from the Downtonian sandstone of Ringerike, Norway. SKR NOR VIDENSK-AKAD MAT-NATURVIDENSK KL 1933 10, 1–125.

Størmer, L. 1936. Eurypteriden aus den Rheinischen Unterdevon. ABH PREUSS GEOL LANDESANST 175, 1–74.

Størmer, L. 1938. *Eurypterus fischeri* in Ludlow beds (9d) at Ringerike. NOR GEOL TIDSKR 18, 69–70.

Størmer, L. 1944. On the relationships and phylogeny of fossil and Recent Arachnomorpha. (A comparative study on Arachnida, Xiphosura, Eurypterida, Trilobita, and other fossil Arthropoda). SKR NOR VIDENSK-AKAD MAT-NATURVIDENSK KL 1944 5, 1–158.

Størmer, L. 1955. Merostomata. *In* Moore, R. C. (ed.) *Treatise on Invertebrate Paleontology*. P. Arthropoda 2, P1–P41. Lawrence, Kansas: University of Kansas & Geological Society of America.

Størmer, L. 1963. *Gigantoscorpio willsi*, a new scorpion from the Lower Carboniferous of Scotland and its associated preying microorganisms. SKR NOR VIDENSK-AKAD MAT-NATURVIDENSK KL 1963 8, 1–171.

Størmer, L. 1972. Arthropods from the Lower Devonian (Lower Emsian) of Alken an der Mosel, Germany. Part 2: Xiphosura. SENCKENBERGIANA LETHAEA 53, 1–29.

Størmer, L. 1973. Arthropods from the Lower Devonian (Lower Emsian) of Alken an der Mosel, Germany. Part 3: Eurypterida, Hughmilleriidae. SENCKENBERGIANA LETHAEA 54, 119–205.

Størmer, L. 1974. Arthropods from the Lower Devonian (Lower Emsian) of Alken an der Mosel, Germany. Part 4: Eurypterida, Drepanopteridae, and other groups. SENCKENBERGIANA LETHAEA 54, 359–451.

Størmer, L. 1976. Arthropods from the Lower Devonian (Lower Emsian) of Alken an der Mosel, Germany. Part 5: Myriapoda and additional forms, with general remarks on fauna and problems regarding invasion of land by arthropods. SENCKENBERGIANA LETHAEA 57, 87–183.

Størmer, L. 1980. Sculpture and microstructure of the exoskeleton in chasmopinid and phacopid trilobites. PALAEONTOLOGY 23, 237–71.

Størmer, L. & Kjellesvig-Waering, E. N. 1969. Sexual dimorphism in eurypterids. *In* Westermann, G. E. G. (ed.) *Sexual Dimorphism in Fossil Metazoa and Taxonomic Implications*. International Union of Geological Sciences Ser. A, No. 1, 201–14.

Stuttgart: Schweizerbart.

Tarasoff, F. J., Bisaillon, A., Pierard, J. & Whitt, A. P. 1972. Locomotory patterns and external morphology of the river otter, sea otter and harp seal. CAN J ZOOL 50, 915–31.

Tobien, H. 1937. Über Sinneshaare bei *Pterygotus* (*Erettopterus*) *osiliensis* Schmidt aus dem Obersilur von Oesel. PALAEONTOL Z 19, 254–66.

Vachon, M. 1945. Remarques sur les appendices du prosoma des Limules at leur arthrogenèse. ARCH ZOOL EXP GEN 84, 271–300.

Văscăutanu, T. 1932. Formatiunile Siluriene din Malul Romanesc al Nistrului (Contributiuni al Cunoasterea Paleozoicului din Basinul Moldo-podolic). ANU INST GEOL ROM 15, 425–663.

Versluys, J. & Demoll, R. 1923. Das *Limulus*-Problem. Die Verwandtschaftsbeziehungen der Merostomen und Arachnoiden unter sich und mit anderen Arthropoden. ERGEB FORTSCHR ZOOL 5, 67–388.

Walker, W. F. 1971. Swimming in sea turtles of the family Cheloniidae. COPEIA 1971, 229–33.

Ward, D. V. 1969. Leg extension in *Limulus*. BIOL BULL MAR BIOL LAB WOODS HOLE 136, 288–300.

Warner, G. F. 1977. *The Biology of Crabs*. London: Elek Science.

Waterston, C. D. 1964. Observations on pterygotid eurypterids. TRANS R SOC EDINBURGH 66, 9–33.

Waterston, C. D. 1979. Problems of functional morphology and classification in stylonuroid eurypterids (Chelicerata, Merostomata), with observations on the Scottish Silurian Stylonuroidea. TRANS R SOC EDINBURGH 70, 251–322.

Whittington, H. B. 1975. Trilobites with appendages from the Burgess Shale, Middle Cambrian, British Columbia. FOSSILS AND STRATA 4, 97–136.

Whittington, H. B. 1980. Exoskeleton, moult stage, appendage morphology, and habits of the Middle Cambrian trilobite *Olenoides serratus*. PALAEONTOLOGY 23, 171–204.

Wills, L. J. 1965. A supplement to Gerhard Holm's "Über die Organisation des *Eurypterus fischeri* Eichw." with special reference to the organs of sight, respiration and reproduction. ARK ZOOL 18, 93–145.

Wyse, G. A. & Dwyer, N. K. 1973. The neuromuscular basis of coxal feeding and locomotory movements in *Limulus*. BIOL BULL MAR BIOL LAB WOODS HOLE 144, 567–79.

Zug, G. R. 1971. Buoyancy, locomotion, morphology of the pelvic girdle and hindlimb and systematics of cryptodiran turtles. MISC PUBL MUS ZOOL UNIV MICHIGAN 142, 1–98.

PAUL A. SELDEN, Department of Extra-Mural Studies, University of Manchester, Manchester M13 9PL, England.